BOEING

Solar Power Satellite System Definition Study

Volume IV
Phase I, Final Report
Silicon Solar Cell Annealing Tests
D180-25037-4

NASA CR-
160373

BOEING
GENERAL ELECTRIC
GRUMMAN
Arthur D Little Inc
TRW

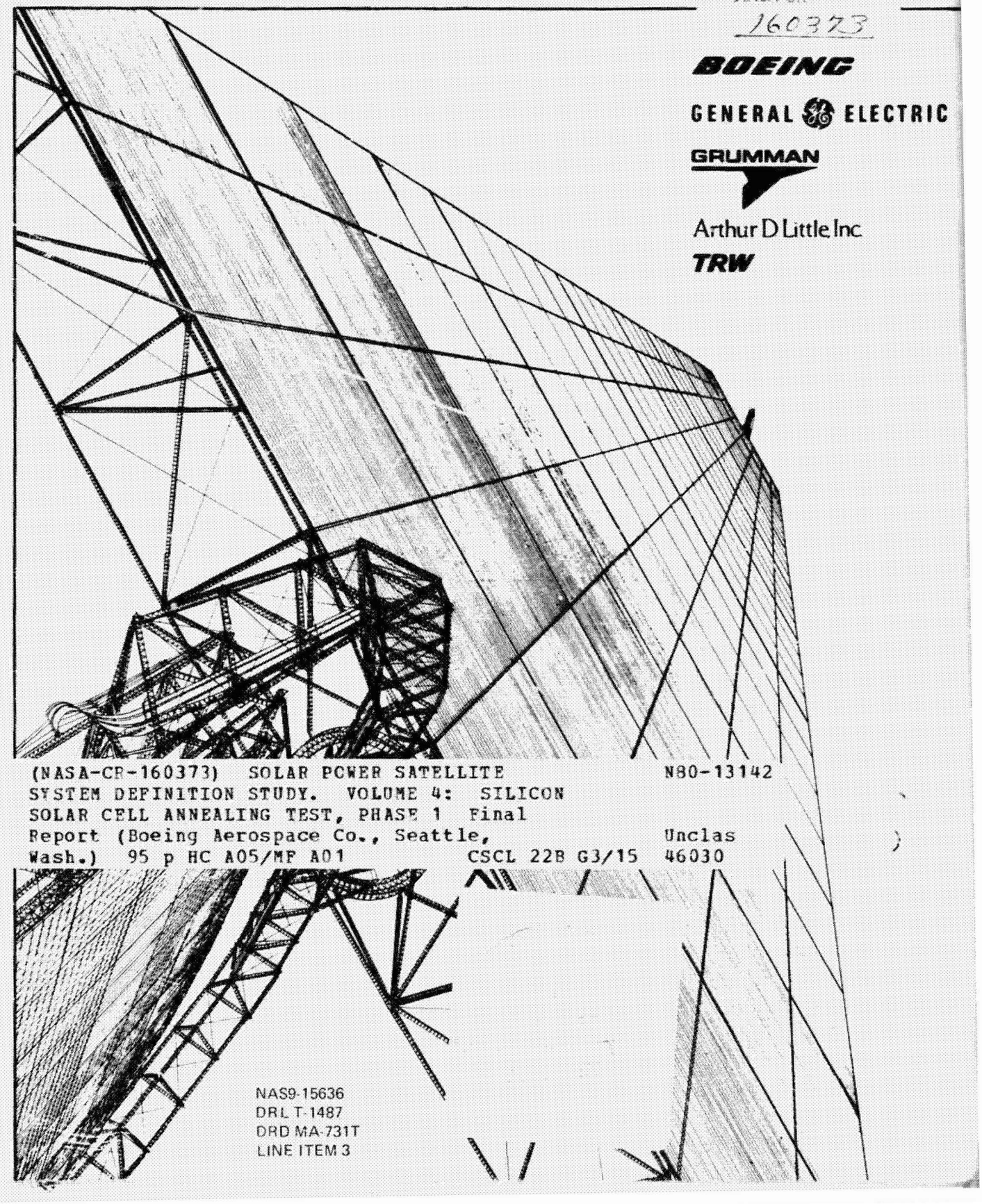

(NASA-CR-160373) SOLAR POWER SATELLITE SYSTEM DEFINITION STUDY. VOLUME 4: SILICON SOLAR CELL ANNEALING TEST, PHASE 1 Final Report (Boeing Aerospace Co., Seattle, Wash.) 95 p HC A05/MF A01 CSCL 22B G3/15

N80-13142

Unclas 46030

NAS9-15636
DRL T-1487
DRD MA-731T
LINE ITEM 3

Solar Power Satellite
System Definition Study
Conducted for the NASA Johnson Space Center
Under Contract NAS9-15636

Volume IV
PHASE I, FINAL REPORT
Silicon Solar Cell Annealing Test
D180-25037-4

April 1979

Prepared By: Frank Walker
Frank Walker

Supervised By: Sidney W. Silverman
S. W. Silverman

Approved By: G R Woodcock
G. R. Woodcock
Study Manager

Boeing Aerospace Company
Ballistic Missiles and Space Division
P.O. Box 3999
Seattle, Washington 98124

TABLE OF CONTENTS

1.0 ABSTRACT

Annealing of the solar blanket on an SPS will require a technique tailored to that purpose, as well as a blanket design compatible with annealing temperatures. Thermal bulk annealing of radiation damage in silicon has been repeatedly demonstrated in the laboratory. Attention has been given to laser directed-energy annealing under this contract. Initial tests of laser annealing of thin solar cells with glass covers were dedicated to measuring thermal response of solar cells to laser energy density. Resulting energy requirements are less than earlier estimates by about a factor of 5 and have been reflected in definition of the reference laser annealing system.

A test program was conducted to further explore the laser annealing of glass-encapsulated 50-micron solar cells but a suitable method of glassing was not found. Ten cells were coated with 75 microns of glass by Schott in Germany using electron-beam evaporation of the glass. The coatings were of poor quality, e.g., full of bubbles, and contained much frozen-in strain. When subjected to annealing temperatures, the coated cells curled up like potato chips and the glass fractured. Attempts at RF sputtering at Boeing yielded glass deposition rates too low to be usable. Ion sputtering was tried on a few cells at Ion Tech. Good quality coatings were produced, but the cells were damaged in handling. Some damaged cells were subjected to annealing temperatures and did not exhibit the mechanical failures of the Schott-coated cells. Ion sputtering merits further investigation, as does electrostatic bonding of glass microsheet.

Laser annealing tests were conducted on ten 50-micron cells. Two were control cells that were not irradiated. These showed no loss in output due to exposure to the laser. Two cells were broken in handling. Six cells were successfully tested. All cells tested without breakage showed some recovery. One cell was subjected to two cycles and showed recovery on both cycles. Cells that were moderately degraded appeared to recover more completely than those more severly degraded. Exposure times ranged from two to ten seconds at 500°C. There was some indication that longer exposure was beneficial.

2.0 RATIONALE

The front surface cover glass of a solar cell must be capable of withstanding the various environmental conditions to which the solar array is exposed. To be compatible with both the space environment and thermal annealing techniques, the cover must meet the following criteria:

1. The front surface cover must pass solar inolation in the spectral range compatible with the spectral response of the solar cell.

2. The front surface cover must resist loss of transmissivity due to color center formation caused by charged particle irradiation.

3. The front surface cover and silicon solar cell face must be closely matched, optically and thermally, such that spectral reflectance at the interface is minimized and thermal expansion at the interface from -150°C to +600°C, is not destructive to the cell structure or the cover glass.

Cerium-doped borosilicate glass meets the specified requirements for a front surface cover, provided the glass can be bonded to the solar cell in such a way as to prevent damage caused by high temperature exposure or thermal expansion mismatch between the glass and silicon. Thermal expansion of cerium-doped borosilicate glasses currently available does not match the thermal expansion of silicon closely enough to be integrally compatible from low temperature through annealing temperatures (500°C).

In past experiments (1), 250 μm-thick silicon solar cells with electrostatically bonded 250 μm-thick front surface covers of Corning 7070 glass have been successfully annealed. Thermal expansion characteristics of Corning 7070 borosilicate glass are closely matched to those of silicon such that this glass, integrally bonded to silicon, can survive temperature extremes from room temperature through annealing temperatures (500°C). In these tests it was shown that a silicon solar cell with an integral glass cover can withstand annealing temperatures without degrading the solar cell performance.

These previous results indicate that an annealable, integral glass cover for a 50 μm-thick solar cell is feasible. The experimental work described in this report was designed to further develop the high-temperature, low-mass cover concept, and to verify that a thin cell and thin cover glass can be joined and annealed similar to a thicker cell and thicker

glass. The rationale for evolving the thin glass/thin solar cell stack to be annealable is that space solar arrays are tending to become larger as the spacecraft's electrical loads show increases in the future. That, plus the longer life, lower weight requirement for large arrays, forces the technology to pursue achievement of a lightweight solar cell stack, with annealing capability, in order to minimize solar array area.

Since the problem of joining glass to a solar cell without adhesive is difficult, various methods of effecting the joining were explored. Among the newer possibilities are the use of a laser beam, and bonding by electrostatics.

3.0 OBJECTIVE

The objective of this test was to demonstrate the feasibility of 1) bonding an integral glass cover to a 50 μm-thick solar cell and 2) laser annealing of a 50 μm-thick solar cell with integral glass cover. Associated topics of investigation were charged particle irradiation damage of the 50 μm-thick silicon cell, structural tolerance of the 50 μm-thick cell to high temperatures (500°C and above) and annealing characteristics of 50 μm-thick solar cells.

4.0 STATEMENT OF WORK

The contract task was performed by completing the following items:

1. Establish initial test parameters for deposition of laser energy into the radiation damaged region of the silicon.

2. Test laser effects on uncovered test cells and analyze the results to determine if thermal stresses cause observable damage to the silicon cell. Adjust the test parameters to optimize thermal annealing and minimize structural damage to the cell.

3. Apply laser pulses to solar-cell-and-cover assemblies to conform the ability of the covered cells to withstand the thermal stresses of laser annealing.

4. Irradiate 7 glass-covered cells with 1 MeV electrons to a fluence level of 2×10^{15} electrons/cm^2 and irradiate 3 glass-covered solar cells with 11 MeV proton irradiation to a fluence level of 3×10^{12} protons/cm^2.

5. Laser anneal the 10 specimens, measuring performance before and after.

6. Perform repeated annealing on four of the 10 solar cell specimens. The number of repeat cycles will be determined.

7. Write a report describing the work and summarizing the results.

5.0 TEST SAMPLE DESCRIPTION

5.1 SOLAR CELLS

MANUFACTURER	THICKNESS (μm)	CELL DIMENSIONS (cm)	SURFACE FINISH	BASE RESISTIVITY	JUNCTION DEPTH	A. R. COATING	BACK SURFACE FIELD	ELECTRICAL CONTACTS	MEASURED MEAN EFF. (%)
SOLAREX	50	2 x 2	Chemical Etch	2Ωcm	2-3μm	Ta_2O_5	Compensated Back Surface Field	Ti-Pd-Ag Chevron	10.22
O.C.L.I.	50	2 x 2	Chemical Etch	2Ωcm	2-3μm	OCLI Multi-layer Coating	Back Surface Field	Ti-Pd-Ag Grid	10.28

5.2 GLASSES

MANUFACTURER	THERMAL EXPANSION 20-300°C ($\times 10^{-7}$°C)	EMISSIVITY (+0.01)	SPECIFIC HEAT $\left(\frac{cal.}{g\text{-}^{o}C}\right)$	VISCOSITY DATA: STRAIN POINT (°C)	VISCOSITY DATA: (10^{13} POISE) ANNEALING POINT (°C)	VISCOSITY DATA: ($10^{7.6}$ POISE) SOFTENING POINT (°C)	VISCOSITY DATA: (10^{4} POISE) WORKING POINT (°C)	DENSITY (g/cm^3)	DIELECTRIC CONST.	REFRACTIVE INDEX (λ=0.58μm)
SCHOTT 8329 Glass	27.5	0.89@20μm 0.91@50μm	0.218	562	--	--	--	2.201	--	1.4689
CORNING 7070 Glass	32.0	--	--	455	495	--	1070	2.13	4.1	1.469

Figure 1; Test Sample Description

6.0 TECHNICAL APPROACH

6.1 INTEGRAL GLASS COVER DEVELOPMENT

Traditionally, glass covers have been bonded to the solar cell using adhesives. At annealing temperatures (400-500°C) these adhesives degrade. In seeking a non-adhesive integral bond between glass and solar cell, electrostatic bonding, ion sputtering, and electron beam evaporation were considered. At the time of this report it was believed that Corning 7070 borosilicate glass is most suitable as an integral cover for silicon as the thermal expansion of both materials is closely matched. Because Corning 7070 glass was not available in thin sheets (50-75μm thick), electrostatic coverglass bonding could not be investigated. The procedures of ion beam sputtering and electrom beam evaporation were both used to create thin (50-75μm) integral glass covers on 50 μm-thick cells.

Once the thin cells were provided with integral glass covers, the covered cells were subjected to thermal tests to determine the structural properties at annealing temperatures.

6.2 LASER ANNEALING TESTS

Each thin cell, once provided with an integral glass cover, was charged particle irradiated to simulate damage received in a space environment. These radiation damaged cells were then to be annealed using a CO_2 laser as the annealing energy source. At this point, laser annealing could be analyzed to improve annealing effectiveness using a laser.

7.0 TEST RESULTS

7.1 INTEGRAL GLASS COVER

In the first stage of this testing program 50 μm-thick solar cells were provided with integral glass covers. Fifteen solar cell samples were coated with 46 to 78 μm of Schott 8329 glass by means of an electron beam evaporation process. These cells were to be the primary glass-covered test specimens for laser annealing studies to be conducted in a later portion of the test sequence. In a separate procedure four cell samples were coated with 50 μm of Corning 7070 glass. This glass coating procedure employed an ion beam sputtering process.

7.2 EARLIER TESTS

Pre-test analysis of 50 μm-thick, glass-covered solar cell annealing was based on earlier thin-cell annealing studies and on a thermodynamic model of a 50 μm-thick silicon solar cell with a 50 μm-thick borosilicate glass cover. Previous studies conducted under subcontract to Boeing, by SPIRE Corporation, shows annealing effects (Figure 2) of an unglassed, 200 to 300 μm-thick, violet cell after pulsed laser irradiation. In this test series, electron beams were also tried on unglassed cells with similar results. A second series of tests was conducted with the intent of ascertaining the feasibility of annealing cells with electrostatic-bonded glass covers. It was decided to concentrate on laser annealing, since there was concern that the electron beam would not penetrate the glass cover and would heat the glass excessively. SPIRE attempted to bond 250 μm glass coverslips to 50 μm silicon solar cells using their electrostatic technique. These attempts were unsuccessful, resulting in cell breakage in every case. Consequently, annealing tests were conducted using conventional (200 μm to 300 μm) silicon cells with 250 μm covers. Initial laser tests were conducted using a Nd-YaG laser with a pulse duration of roughly 1 msec. These laser pulses heated the cell preferentially and resulted in cell breakage.

At this point, SPIRE resorted to a CO_2 laser with a much longer pulse (2 seconds) of lower intensity. The CO_2 laser energy (1.6 m) was absorbed entirely in the glass, preferentially heating the glass which then heated the cell by conduction. It was observed that depsoiting the laser energy in the glass rather than in the solar cell reduced cell breakage. The phenomenon is under continuing investigation. The same effect could be obtained with the electron beam, but the electron charge poses potential problems. Charge accumulation in the glass may cause dielectric breakdown; also the electron beam path might be influenced by electric or magnetic fields around the target, thus posing issues as to its practical application on an SPS. CO_2 laser annealing tests were conducted on a 250 m-thick solar cell with a 250 m-thick ESB cover glass (Figure 3), indicating good annealing results after electron irradiation degradation. In these tests the front surface cover glass (Figure 4) reached sufficient temperature to cause the glass to melt, but the solar cell was not damaged and the solar cell-to-glass cover bond was unbroken. The laser spot size was smaller than the cell; a total of five laser pulses was used in each case. The locations where the laser pulses impinged on the solar cells are clearly discernible in Figure 4. These tests had the cells mounted on heat sinks and employed an energy intensity of 64 watts/cm^2. Thus the tests were not a good simulation of annealing an array in space, where both sides of the array will reject heat only by radiation.

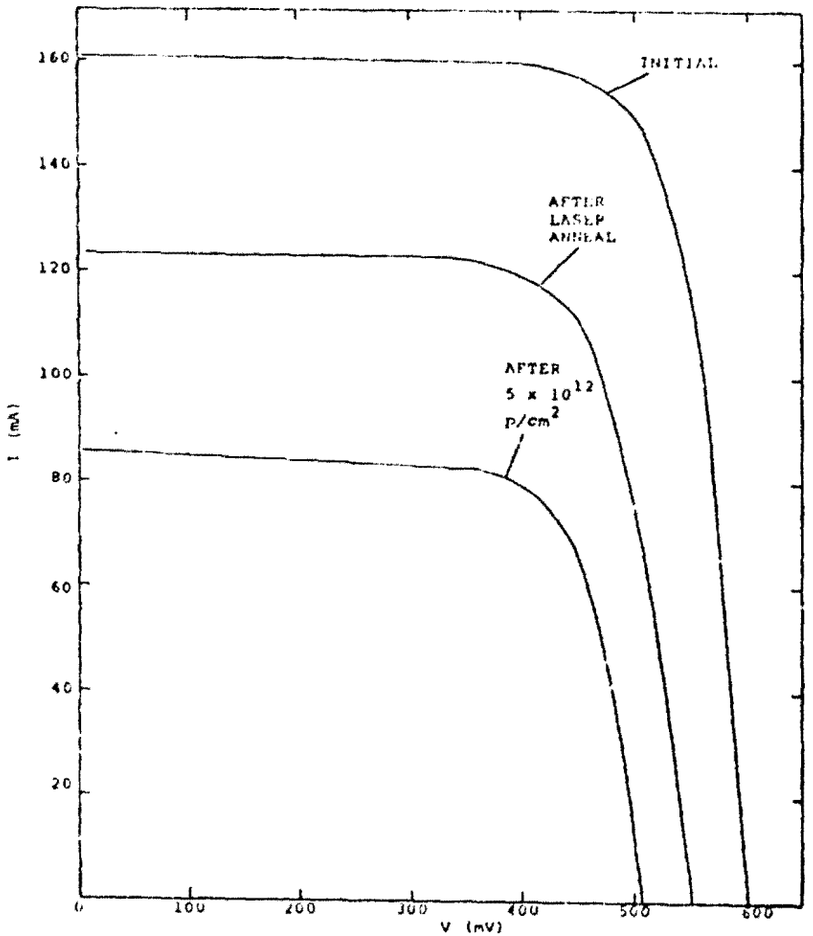

Figure 2; The Effect of Pulsed Laser Anneal on Violet Cell 12E

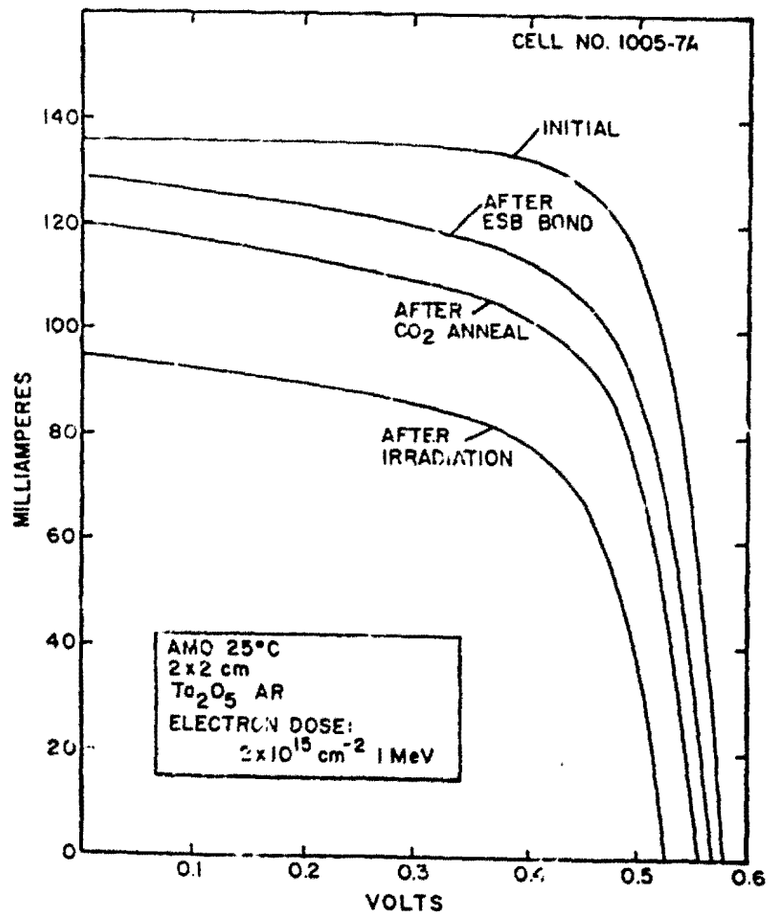

Figure 3; I-V Characteristics of Cells with ESB 7070 Coverglass After Electron Irradiation and After CO_2 Laser Anneal

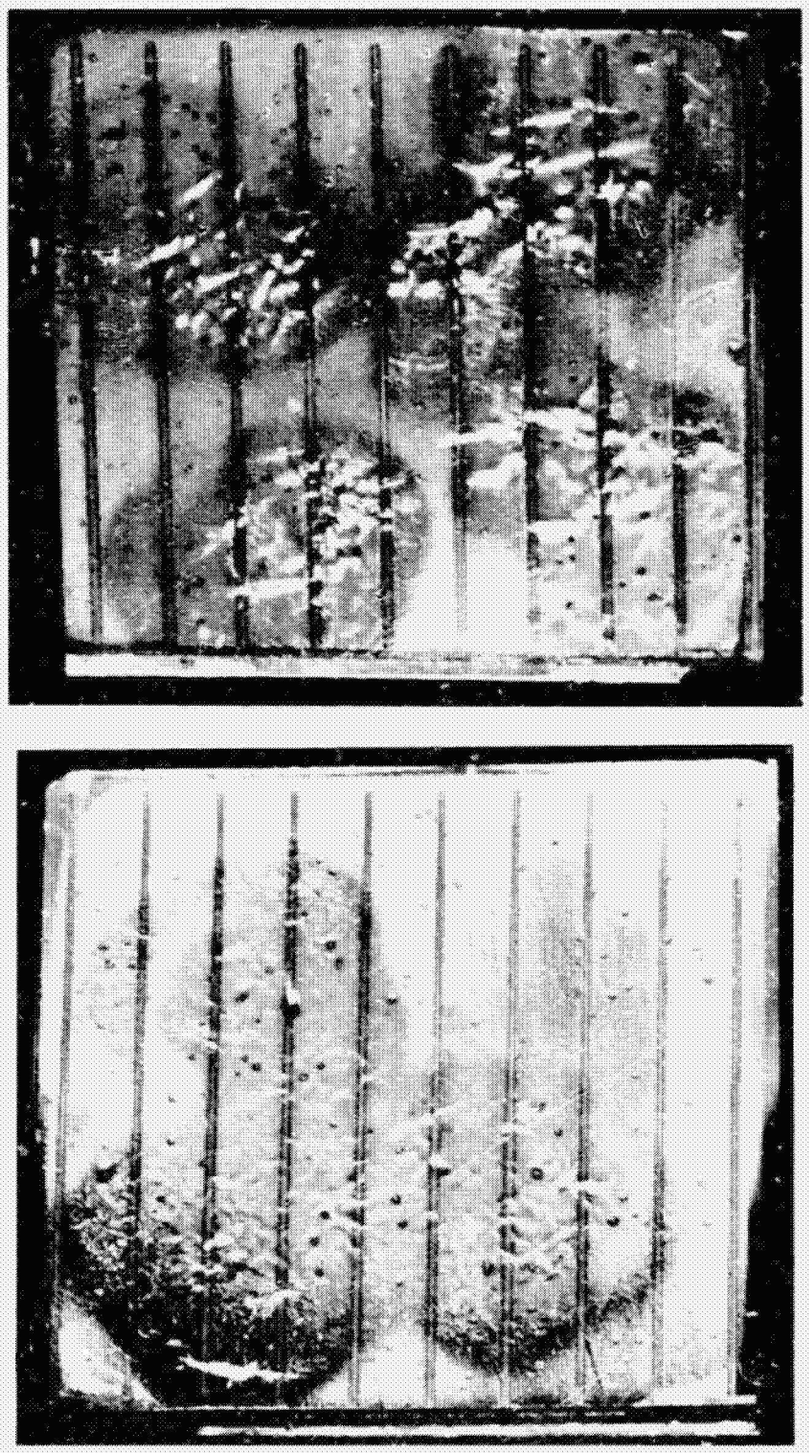

Figure 4: Laser Damage Incurred During Early Laser Annealing Tests of 250μm Silicon Solar Cell With 250μm ESB Coverglass

A steady-state thermodynamic analysis of the 50 μm-thick solar cell with 50 μm-thick glass cover reveals the theoretical energy density required to maintain temperatures in the region of from 200°C to 500°C (Figure 5), and the time required to attain 500°C for different energy densities ranging from 10 to 40 watts/cm^2 (Figure 6).

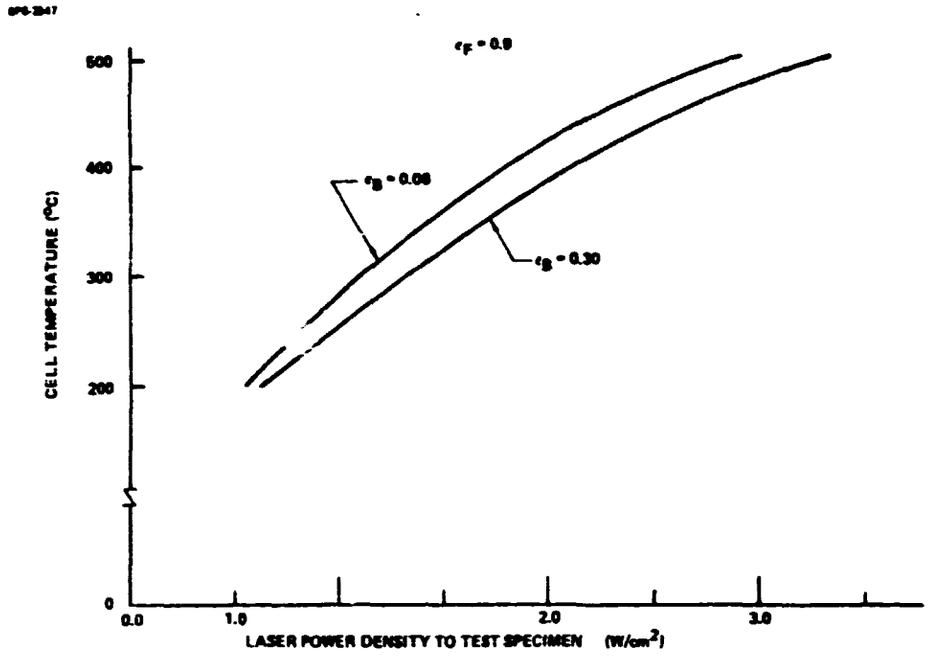

Figure 5; Steady State Temperature Resulting From Different Energy Densities in a 50-μm-Thick Solar Cell With 50-μm-Thick Integral Glass Cover

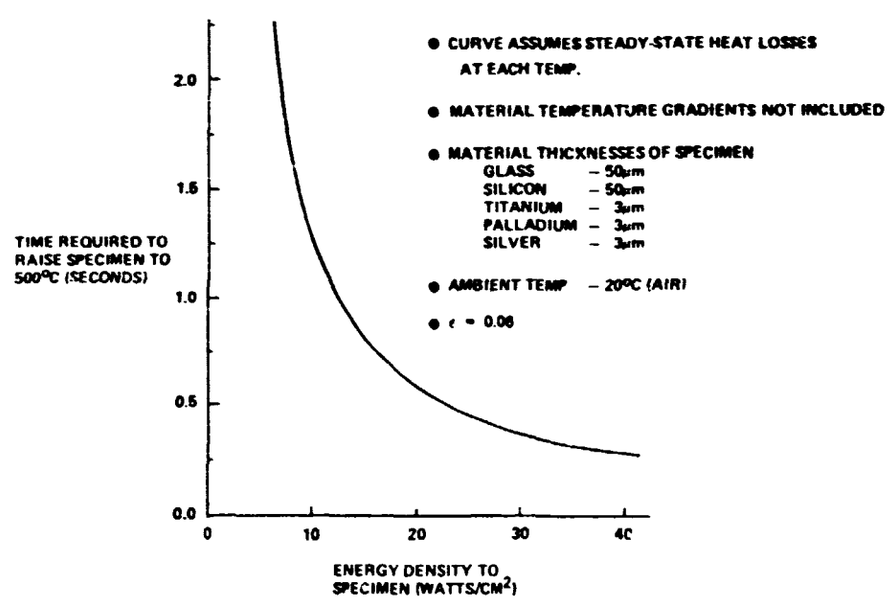

Figure 6; Time to Temperatore (500°C) Curve For Different Energy Densities In A 50-μm-Thick Silicon Solar Cell With 50-μm-Thick Integral Glass Cover

7.3 LASER ANNEALING TEST SET-UP

This procedure describes the test set-up and test sequence used at the Boeing Metrology Laboratory (BML) for heating solar cells with pulses of CO_2 laser radiation.

7.3.1 Laser Test Set-Up Description

Figure 7 shows schematically the test set-up. A CO_2 laser capable of greater than 150 watts CW was used as the laser source. A mechanical shutter was used which utilizes two knife edge shutter leafs and a light emitting diode - photo cell to generate a pulse of laser radiation and an electrical timing pulse respectively. The electrical pulse was measured with a counter to determine the exact laser beam pulse length. With the shutter held open, a sampling mirror was placed in the beam to deflect the beam into the reference power transducer which was used to measure the total raw beam power as a reference.

A zinc selenide lens with a 5.0 inch focal length was used to spread the beam. Distance C in Figure 7 was adjusted to give the required power density at the test plane.

The beam travels through a motor-driven mirror arrangement which was computer controlled and can be used for aligning and centering the beam and for scanning the beam across the aperture plate (2 mm aperture) to provide power density profile maps of the beam.

The laser test facility is pictorially illustrated in Figures 8 through 12. Figure 8 shows the coherent optics, Everlase 150 laser with the test set-up on the work table above the laser cabinet. Figures 9 and 10 show the target site with power meter to measure beam uniformity. Figures 11 and 12 show the test cell and control cell for thermal measurement. Note that the cells are thermally insulated from the fire brick target area by ceramic pillars.

An HP 3052A automated data acquisition and control system is used to collect all the outputs from:

1. The reference transducer.
2. The standard transducer behind the aperature plate.
3. The thermocouple.
4. The shutter timing signal.

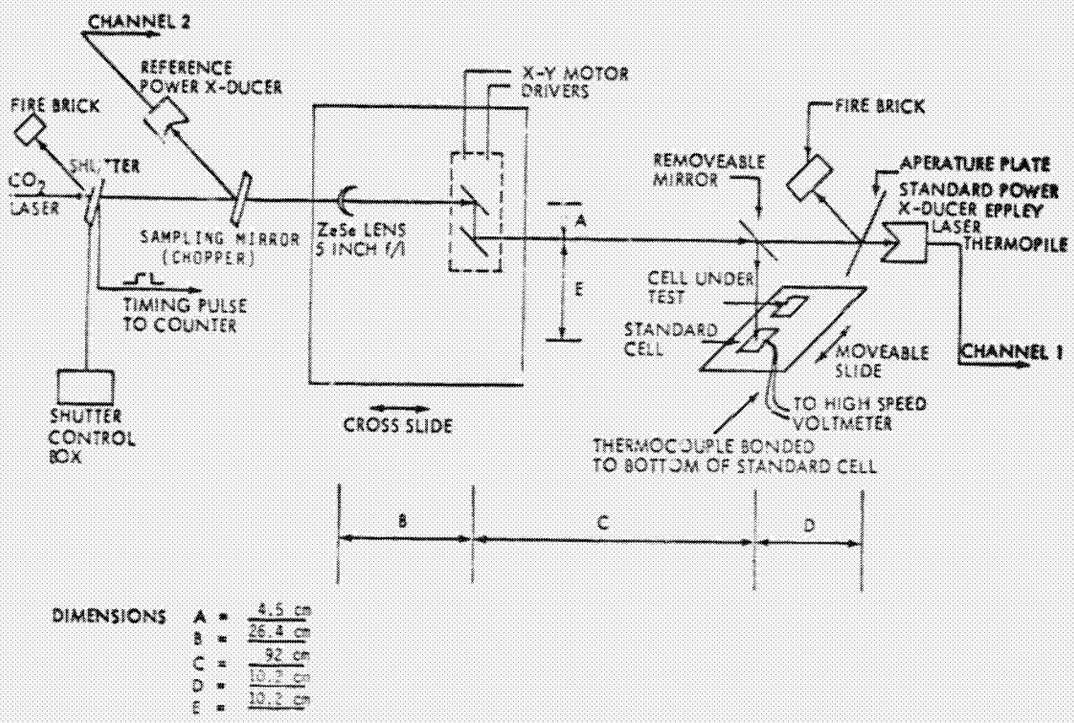

Figure 7; Laser Annealing of Solar Cells — Test Schematic

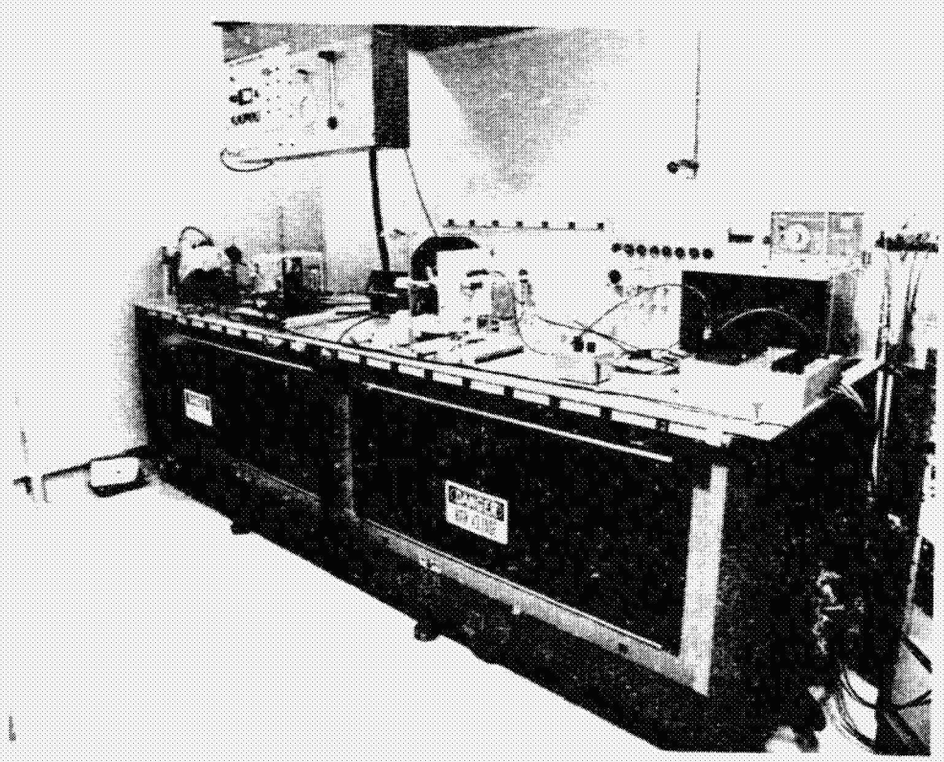

Figure 8; Laser Annealing Test Setup With Coherant Optics Everlase 150 CO_2 Laser

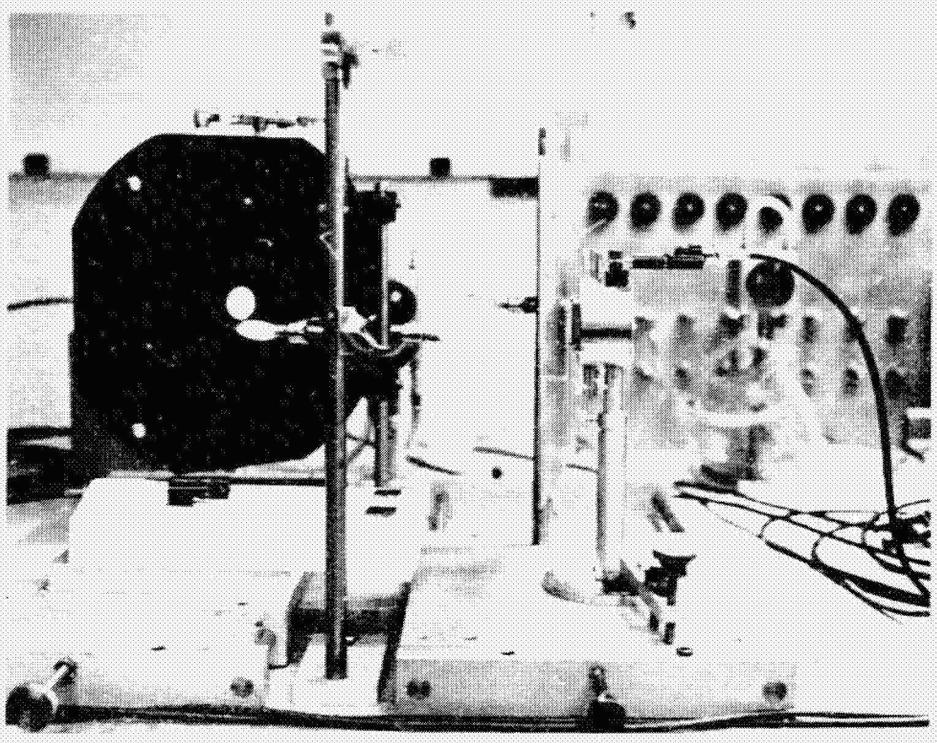

Figure 9

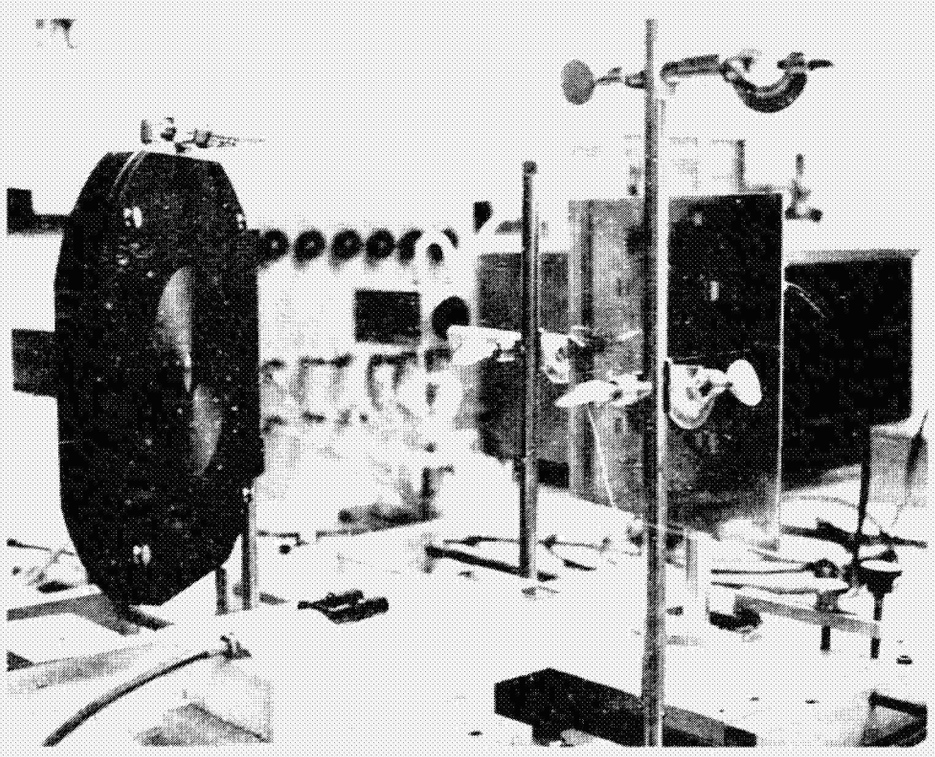

Figure 10

These Views Show the Laser Target Area with Control Cell, Test Cell and Power Meter to Monitor Beam Uniformity.

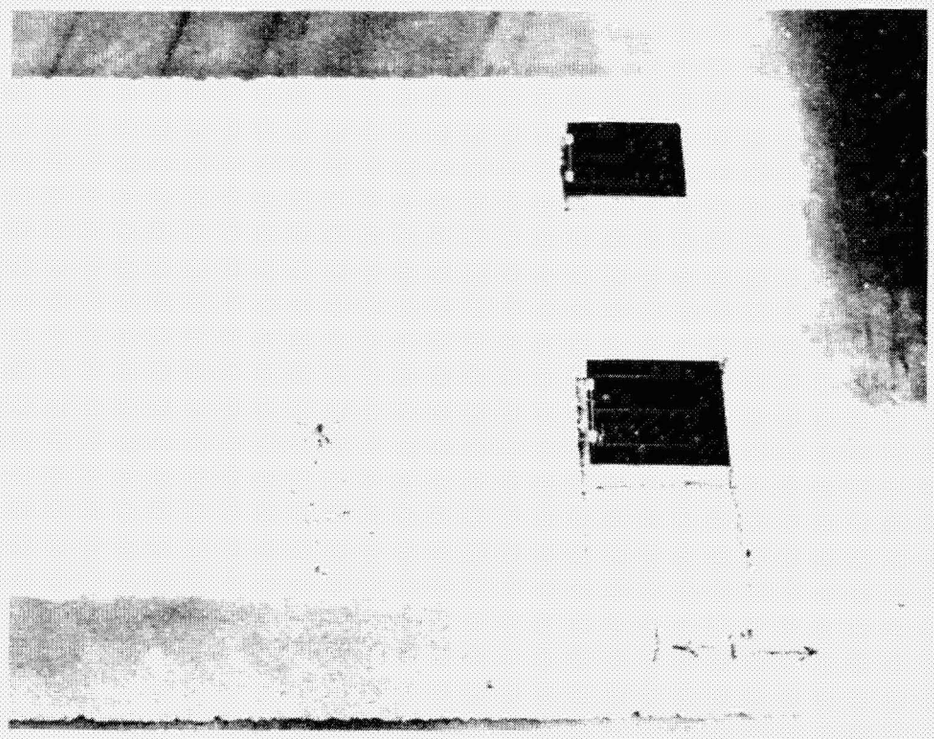

Figure 11; This View Of The Laser Target Site Shows Control Cell, Test Cell And Fire Brick Which Can Be Moved On A Track To Place The Appropriate Cell In The Laser Beam.

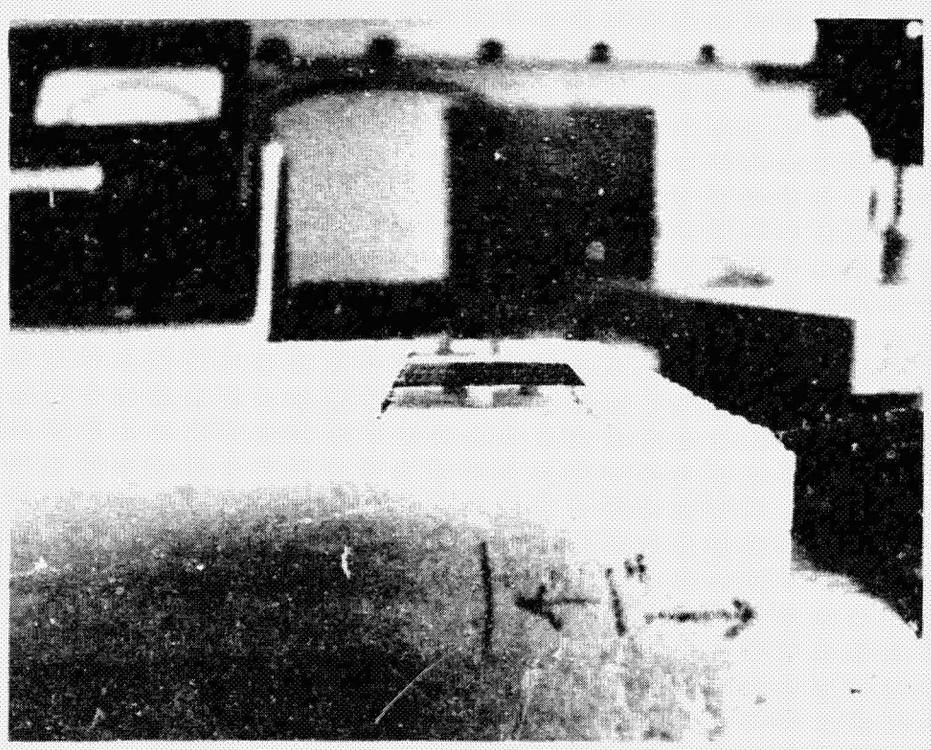

Figure 12; This View Shows The Ceramic Piliars Used To Thermally Isolate The Test Cell From The Fire Brick Target Base.

The system was also used to control the X-Y mirror scanner and provided beam profile tables (Figure 13) and plots (Figure 14). A temperature versus time plot was also provided for the thermocouple on the test cell (Figure 15).

7.3.2 Laser Test Sequence

Figure 16 shows a sample data sheet for recording run #, peak power density, pulse length and temperature rise for the standard cell. Several runs were made on the standard cell to determine the repeatability both before and after the test cell is irradiated as shown in Figure 17.

12-06-76 12:37:06
NORMALIZED POWER DENSITY MAP FOR:
CO2 EXPANDED
3.00 cm SCAN DIA.
LASER ARNEAL 167 WATTS TOTAL

Y \ X-POSITION	-5	-4	-3	-2	-1	0	1	2	3	4	5
5	0.072	0.076	0.068	0.112	0.166	0.188	0.195	0.182	0.151	0.107	0.061
4	0.044	0.083	0.127	0.173	0.236	0.257	0.254	0.249	0.217	0.169	0.112
3	0.063	0.124	0.202	0.282	0.366	0.416	0.411	0.358	0.317	0.252	0.175
2	0.127	0.197	0.311	0.429	0.565	0.599	0.615	0.544	0.406	0.314	0.228
1	0.151	0.265	0.431	0.537	0.796	0.307	0.715	0.595	0.523	0.400	0.262
0	0.211	0.372	0.596	0.790	0.382	0.382	0.903	0.825	0.621	0.436	0.269
-1	0.249	0.437	0.643	0.809	0.590	0.973	1.000	0.851	0.609	0.387	0.233
-2	0.250	0.424	0.617	0.745	0.662	0.976	0.955	0.786	0.588	0.367	0.204
-3	0.215	0.342	0.493	0.635	0.710	0.781	0.797	0.645	0.457	0.308	0.181
-4	0.162	0.234	0.352	0.441	0.504	0.516	0.489	0.451	0.323	0.190	0.107
-5	0.097	0.158	0.220	0.275	0.327	0.360	0.328	0.250	0.169	0.100	0.046

BEAM SPLITTER RATIO(INCIDENT/TRANSMITTED) = 10.0000
MAX POWER DENSITY(W/O BEAM SPLITTER) = 42.14 W/CM^2
AVG REF PWR(WATTS) = 129.986
+ -2.55% - -3.60%
LIMIT FOR REFERENCE REPEATABILITY: 1.00 %
WAIT TIME BETWEEN READINGS 6.0 sec

Figure 13; Numerical CO_2 Laser Beam Profile Matrix

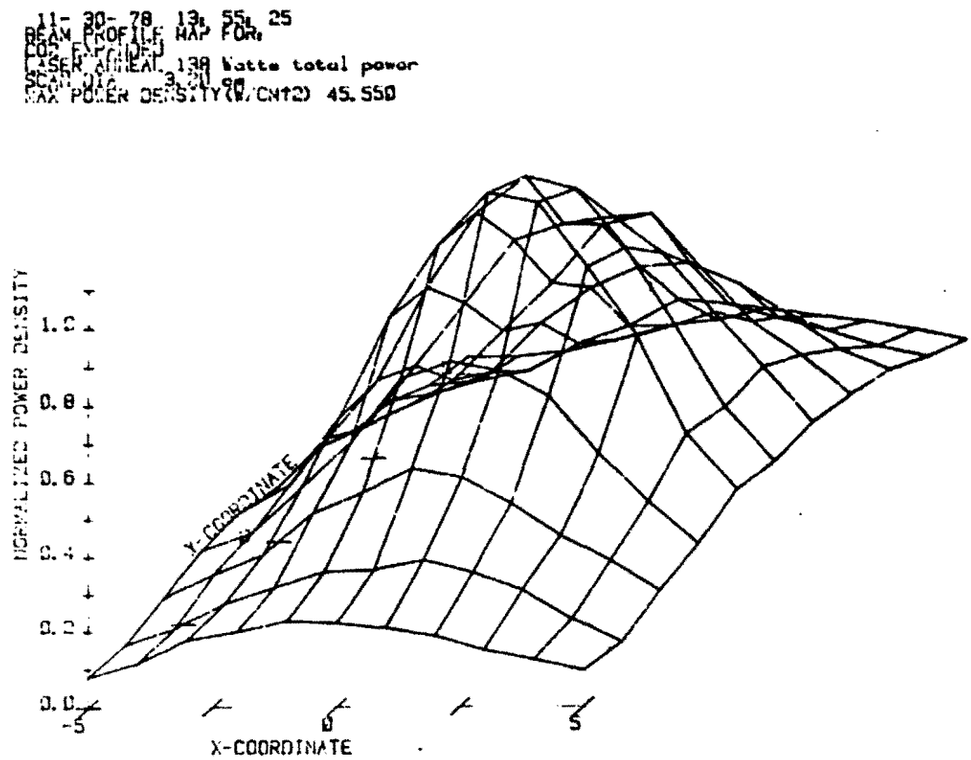

Figure 14; CO_2 Laser Beam Profile Map

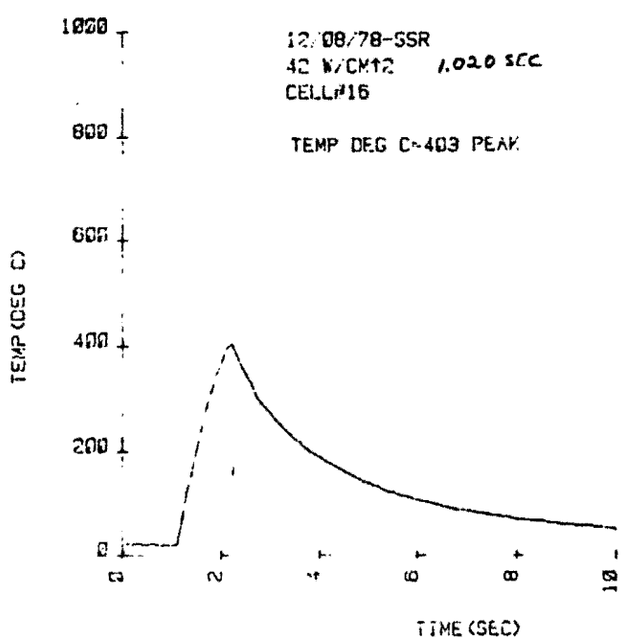

Figure 15; Temperature Vs. Time Plot For Laser Annealing Test

LASER ANNEAL OF SOLAR CELL

Date: _____

By: _____

Cell Description:

Run #	Peak Pwr Density W/cm²	MAP #	Pulse (sec)	Temp Rise (°C) T/C # 1	T/C # 2	Infra Scope mV	°C	Ref Pwr (watts)

Figure 16: Sample Data Sheet For Recording Laser Anneal Test Data

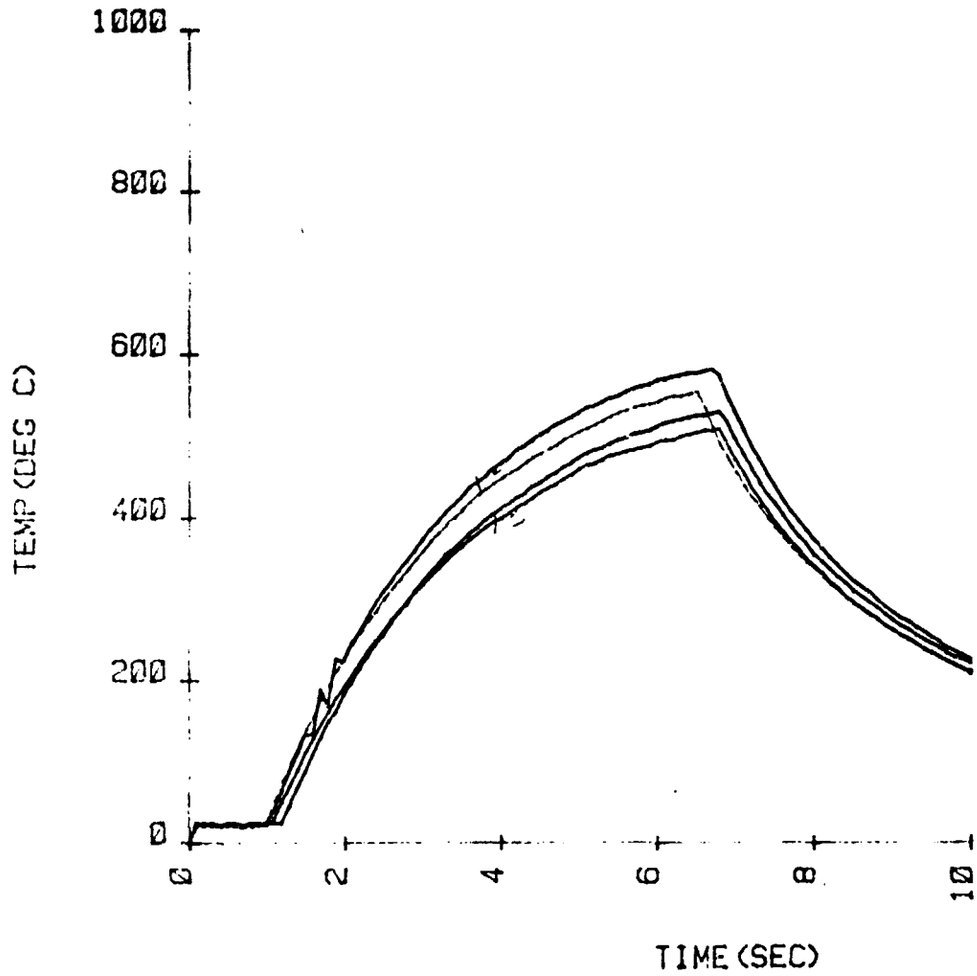

Figure 17; Repeated Time Vs. Temp. Plots To Determine Test Repeatibility

7.4 EVALUATION OF E-BEAM EVAPORATED INTEGRAL GLASS COVER

Fifteen, 50 μm-thick solar cells were covered with 46 to 78 μm of Schott 8329 borosilicate glass by means of an electron-beam evaporation process. This work was done at the Schott Glass Facility in Mainz, Germany. The process was able to deposit up to 100 μm/hr. of the 8329 glass. Corning 7070 glass or the Schott equivalent 8248 glass was preferable for this application as a close thermal expansion match to silicon is required due to thermal extremes experienced during annealing (400-500°C). Schott was unable to obtain either Corning 7070 or Schott 8248 in the proper form for their E-beam sputtering process so Schott 8329 glass was used to provide the deposition process compatibility with 50 μm-thick solar cells.

Figures 18, 19, and 20 show magnifications of the resultant 8329 glass deposition. The photos were taken at the glass edge where the cell surface was masked to prevent glass deposition over the electrical contact pads. Note the high bubble content in the deposited glass. It is believed that this is a result of the deposition rate and may be inherent to the E-beam evaporation process.

Figures 21 through 26 show electrical parameter degradation due to the glass deposition process. The Solarex solar cells had an average 9.15% power reduction after the integral glass cover was applied, while the OCLI cells showed a 12.31% reduction in output power. The decrease in solar cell performance may be due to cell damage incurred during the E-beam deposition process or it may be attributable to the quality of the glass cover and its bubble content.

Upon subjecting these glass covered test cells to annealing temperatures, the 8329 glass was found to fracture at temperatures above 200°C. This indicates either an unexpectedly high thermal mismatch between the solar cell and integral glass cover or deposition process induced stresses in the 8329 glass. Figures 27 and 28 show glass covered solar cells after being raised to 500°C by CO_2 laser exposure. These cells exhibit glass fracture and deformation of the cell and cover structure. The 50 μm-thick cell shown in Figure 29 was heated from room temperature to 300°C over a period of 45 minutes in an oven. Figure 29 shows the glass beginning to fracture in long, smooth breaks. The portion of the cell that is missing and the smaller fractures in the corner of the solar cell are the result of handling of the solar cell. Figure 30 shows a glass covered 50 μm-thick solar cell after an 18 watt C.W. laser exposure that raised the temperature of the cell to 200°C. In this test, glass fractures first became apparent after 3 seconds at a cell temperature of

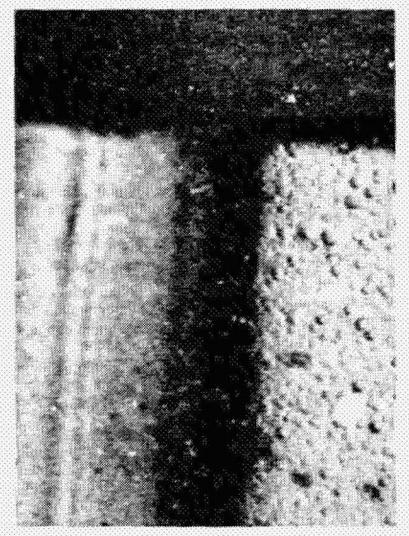

Figure 18; 75 μm of Borosilicate Glass Electron Beam Sputtered onto an O.C.L.I. Manufactured 50-μm-thick Solar Cell. Picture is Focused on the Glass. Note Bubble Content in Glass.

Figure 19; Same Specimen as in Figure 18 with the Photograph Focused on the Unglassed Silicon. Note the Color Lines as the Glass becomes Thin. (1-2 μm)

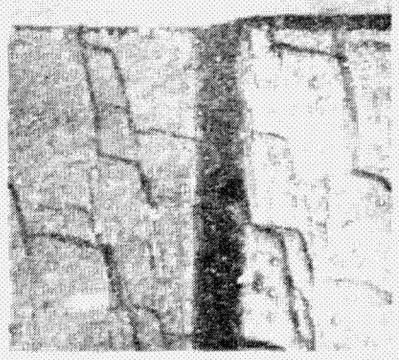

Figure 20; 50 μm of Borosilicate Glass Electron Beam Sputtered onto a Solarex 50-μm-thick Silicon Solar Cell. Note Surface Texture of Solarex Cell and Bubble Content in Glass on the Right.

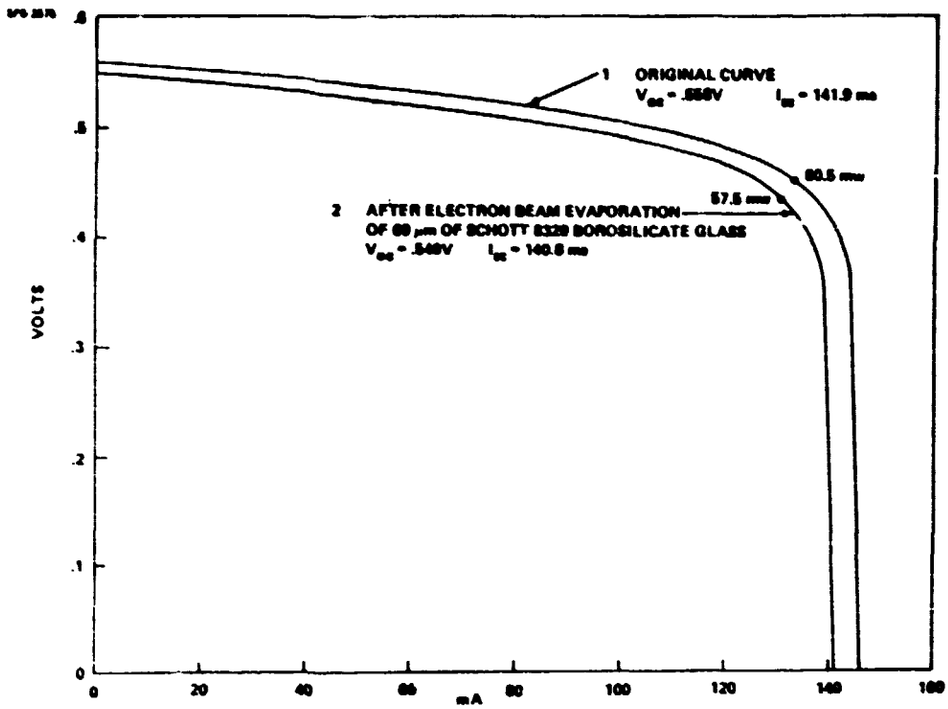

Figure 21; Glass Covered Solar Cell Characteristics, Solarex Cell No. 3

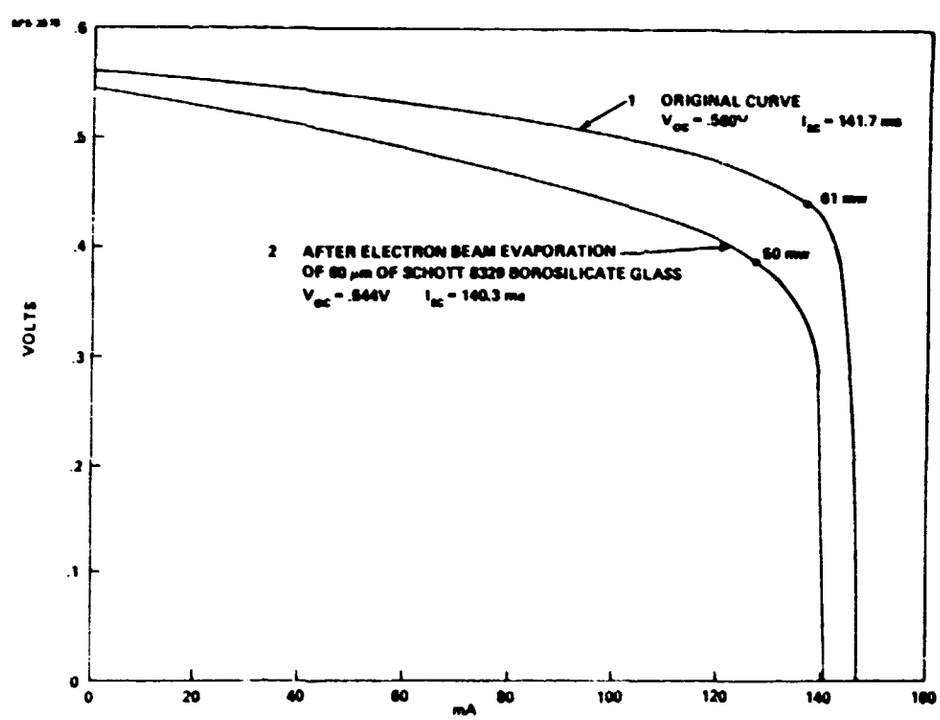

Figure 22; Glass Covered Solar Cell Characteristics, Solarex Cell No. 4

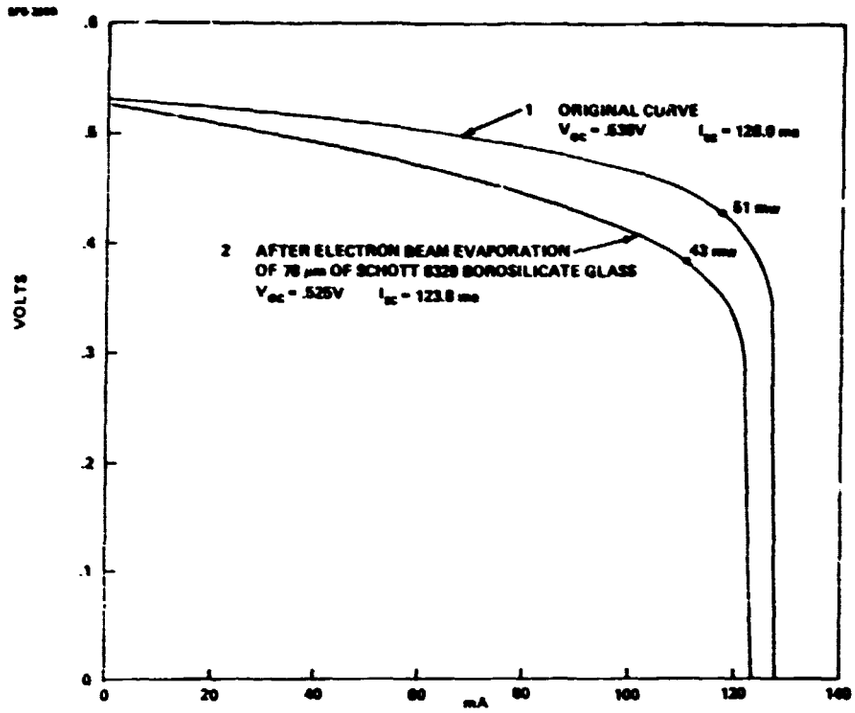

Figure 23; Glass Covered Solar Cell Characteristics, Solarex Cell No. 8

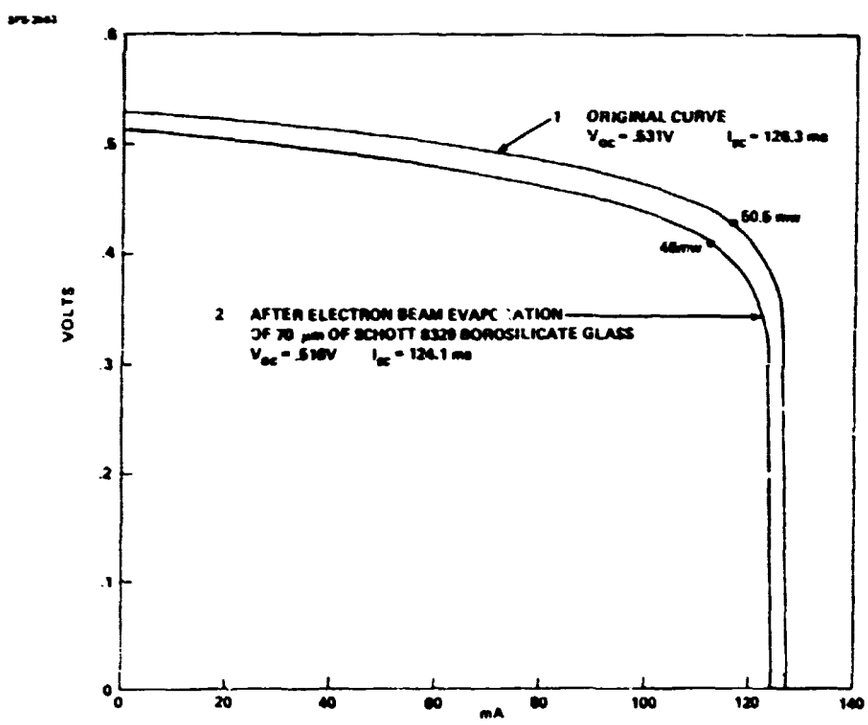

Figure 24; Glass Covered Solar Cell Characteristics, Solarex Cell No. 11

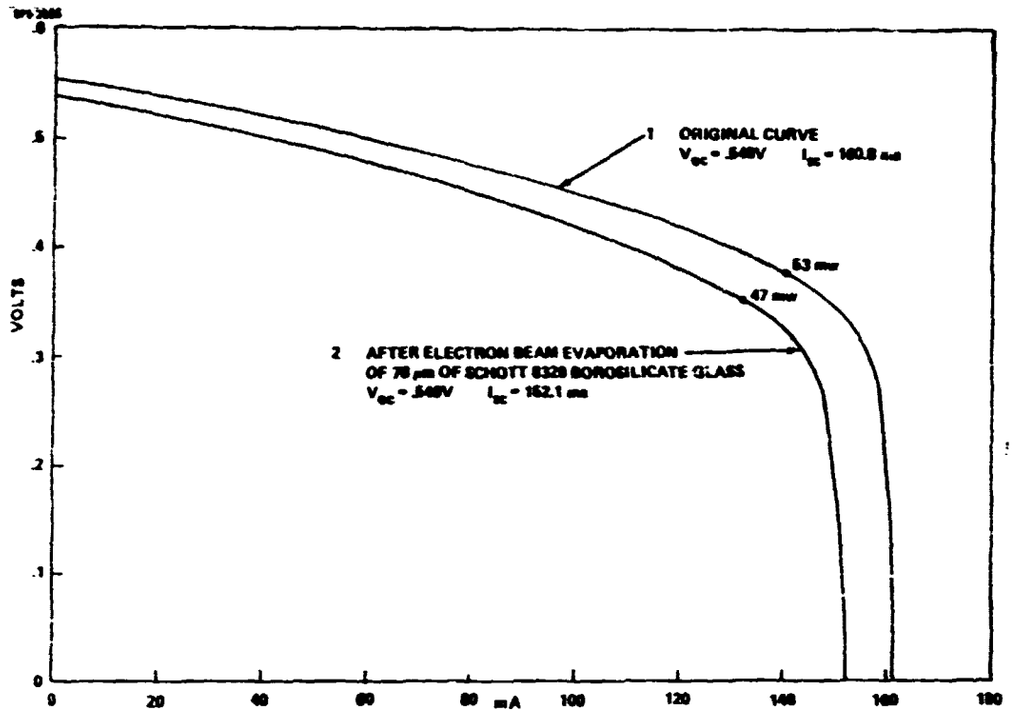

Figure 25; Glass Covered Solar Cell Characteristics, O.C.L.I. Cell No. 21

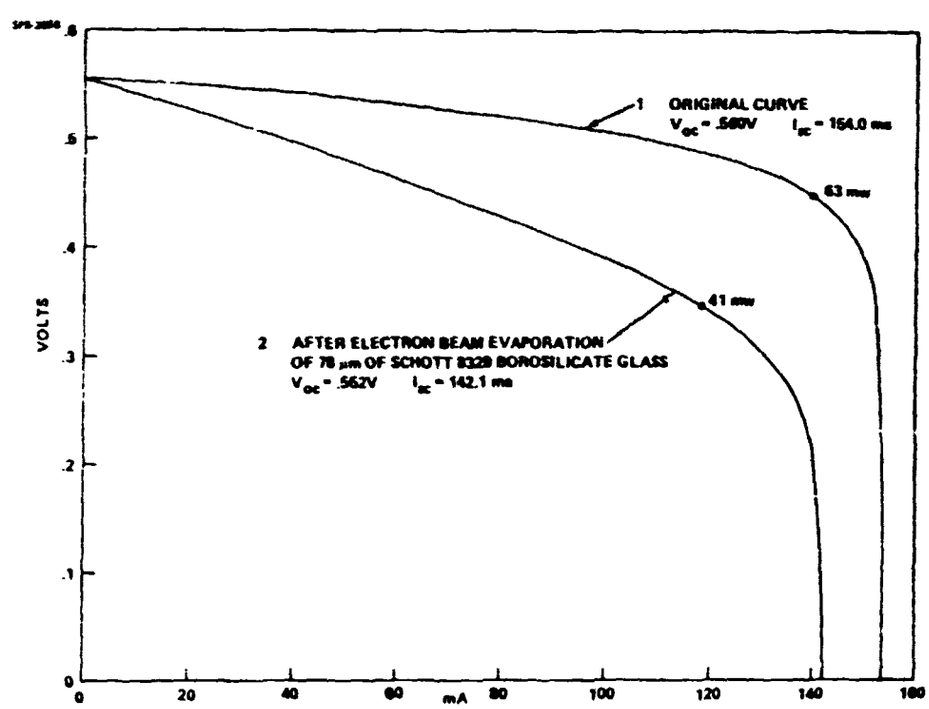

Figure 26; Glass Covered Solar Cell Characteristics, O.C.L.I. Cell No. 23

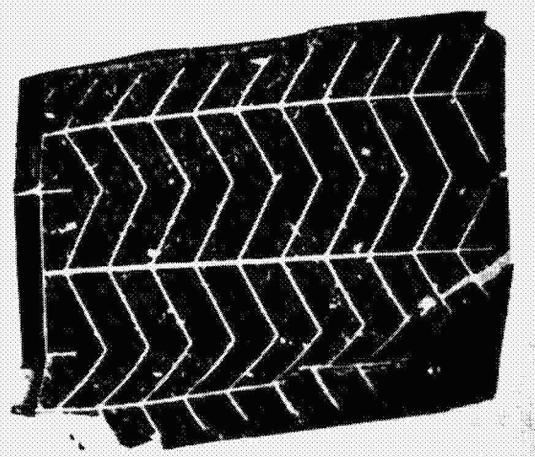

Figure 27; Solarex 50-μm-Thick Solar Cell With 70-μm-Thick Schott 8329 Glass Cover After 5.45 Sec. Laser Exposure Raising Cell Temp. to 500°C.

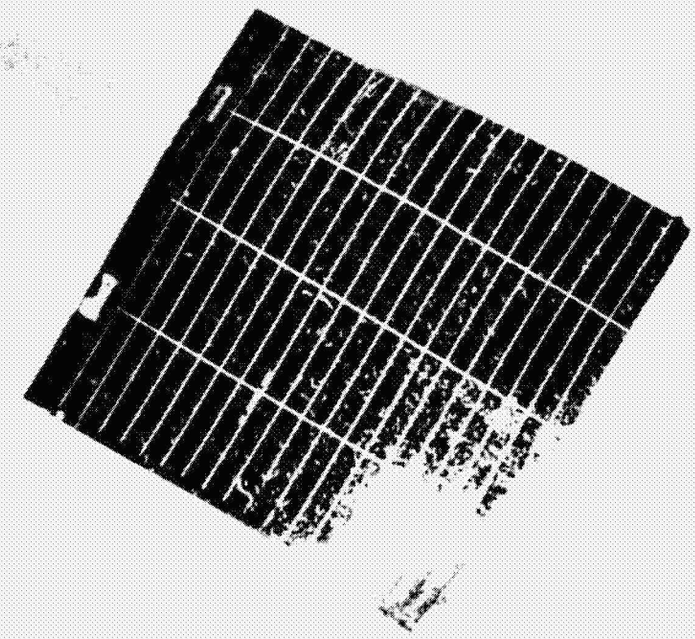

Figure 28; O.C.L.I. 50-μm-Thick Solar Cell With 60-μm-Thick Schott 8329 Glass Cover After 6.56 Sec. Laser Exposure Raising Cell Temperature to 500°C.

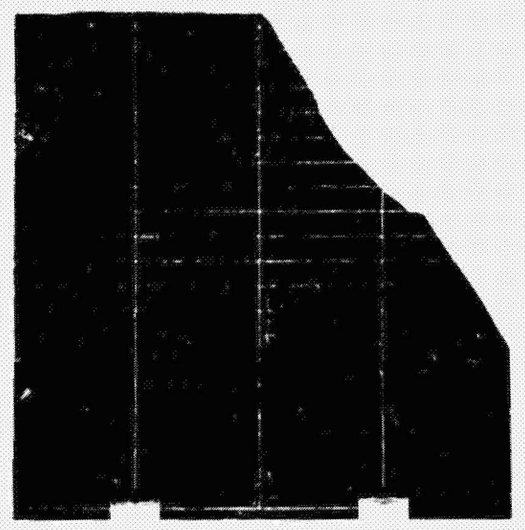

Figure 29; O.C.L.I. 50-μm-Thick Solar Cell With 78-μm-Thick Schott 8329 Glass Cover After Being Heated To 300°C In An Oven.

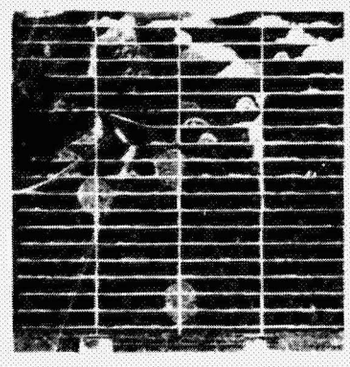

Figure 30; O.C.L.I. 50-μm-Thick Solar Cell With 78-μm-Thick Schott 8329 Glass Cover After 18 Watt C.W. Laser Exposure Raising Cell Temperature to 200°C. (Metal Grid Deformations Are Manufacturing Defects) Fractures First Appeared After 3 Sec. At A Temperature Of 150°C.

150°C. The electrical grid deformations shown are manufacturing defects as these cells were intended primarily for mechanical testing. Figures 31 and 32 show solar cell fragments with integral glass cover that was thermally tested in an oven. Figures 33 through 38 are magnified views of the glass covered solar cells showing details of cover glass fractures, solar cell surface texture,and A.R. coating shear as the glass separated from the solar cell.

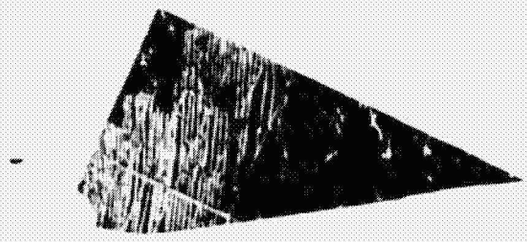

Figure 31; O.C.L.I. 50-μm-Thick Solar Cell Fragment With 70-μm-Thick Schott 8329 Glass Cover After Being Heated To 500°C In An Oven. Fractures First Appeared At 438°C.

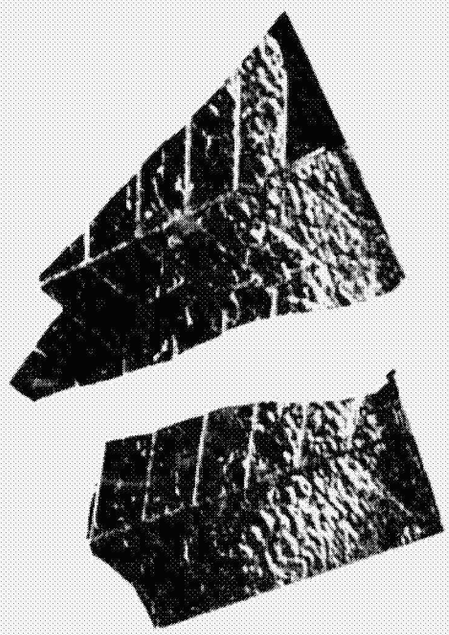

Figure 32; Solarex 50-μm-Thick Solar Cell Fragments With 70-μm-Thick Schott 8329 Glass Cover After Being Heated To 500°C In An Oven. Textured Effect On Cell Surface Is Due To Manufacturing Etch Process.

Figure 33; The Two Views Above Are 200X Magnification Of The Test Cell Described In Figure 24. Note Glass Separation From Silicon As The Light Areas In The Photos.

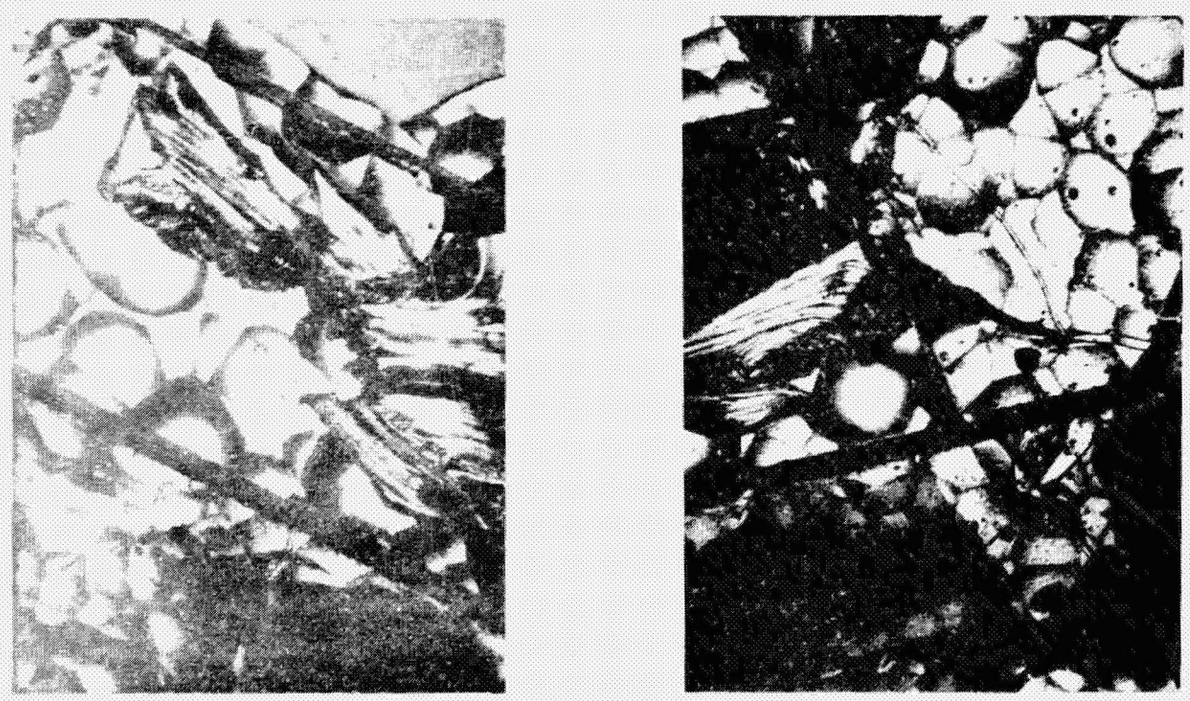

Figure 34; The Two Views Above Are 200X Magnifications Of The Test Cell Described In Figure 25. Note The Pillowed Texture Of The Solarex Cell And The Fracture Orientation Of The Glass.

200x SCALE

0.001 IN. PER DIVISION

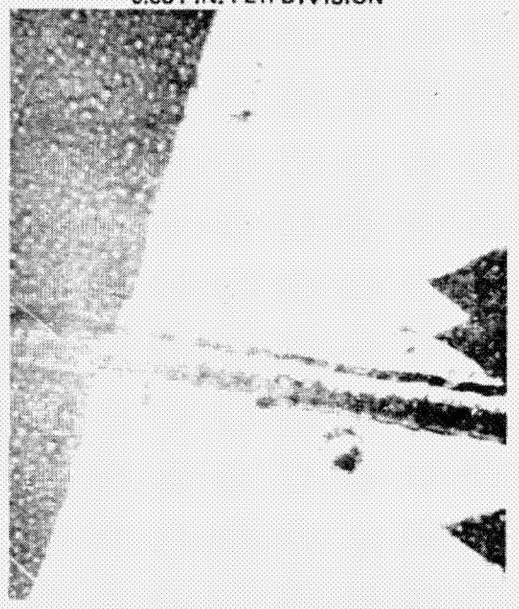

Figure 35; This View is a 200x Magnification of the Test Cell Described in Figure 22

30x SCALE

0.001 IN. PER DIVISION

Figure 36; This View is a 30x Magnification of the Test Cell Described in Figure 22

Figure 37; This View is a 30x Magnification of Glass Fracture on the Test Cell Described in Figure 24

Figure 38; This View is a 30x Magnification of Glass Fracture on the Test Cell Described in Figure 23

7.5 EVALUATION OF ION-BEAM SPUTTERED INTEGRAL GLASS COVER

Four, 50 μm-thick silicon solar cells were covered with 50 μm of Corning 7070 borosilicate glass by means of an ion beam sputtering process. This work was done by M.O.E. Systems Inc. of Fort Collins, Colorado. These tests established a 2 μm/hr. deposition rate; considerably slower than the E-Beam evaporation process. The initial deposition tests resulted in bending and cracking of the solar cells during the process. This cell damage is attributed to long term heating of the solar cell causing the cell to deform. The 50 μm-thick glass coating, as seen in Figure 39, has good optical qualities and no apparent bubbles due to deposition as in the E-beam process. Figures 40 and 41 show two Corning 7070 glass covered solar cell fragments that were heated to above 700°C by CO_2 laser irradiation. Evidence of large, discrete bubble formation is visible, but no glass fracture or cell-and-glass deformation was observed. The large bubbles that formed at high temperatures (600°C-800°C) are believed to be due to outgassing of the AR coating between the solar cell and glass cover.

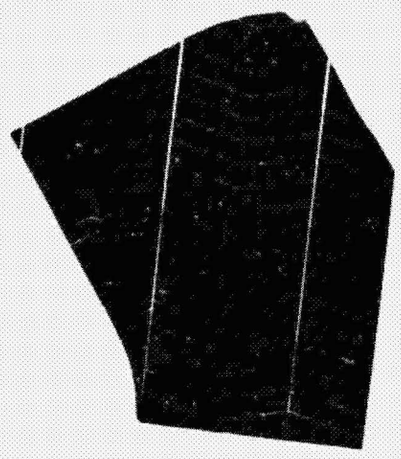

Figure 39; *Solarex 50-μm-Thick Solar Cell With Ion-Beam Sputtered, 50-μm-Thick, Corning 7070 Glass Cover Heated to Over 700°C.*

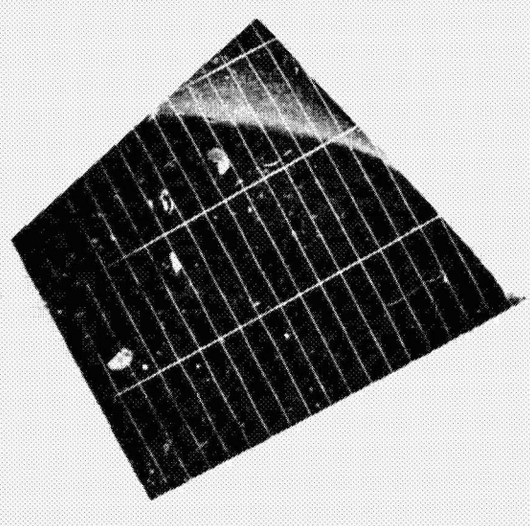

Figure 40; *O.C.L.I. 50-μm-Thick Solar Cell With Ion-Beam Sputtered, 50-μm-Thick, Corning 7070 Glass Cover After Being Laser Heated to Over 700°C.*

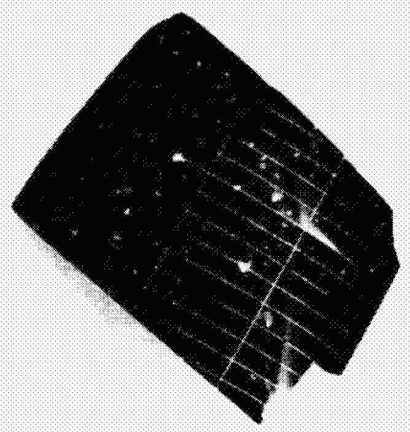

Figure 41; *O.C.L.I. 50-μm-Thick Solar Cell With Ion-Beam Sputtered, 50-μm-Thick, Corning 7070 Glass Cover After Being Laser Heated To Over 700°C.*

7.6 EVALUATION OF ELECTRICAL DEGRADATION IN UNGLASSED SOLAR CELLS DUE TO LASER EXPOSURE

Before formal laser annealing tests began, mechanical 50 μm-thick solar cell test specimens were subjected to various laser intensities and exposure durations to determine the mechanical effects of thermal shock during laser irradiation. Unglassed,50 μm-thick solar cells were found to deform in a unpredeterminable fashion above 300°C where subjected to a laser beam of uniformity similar to that shown in Figure 14. Upon measuring electrical characteristics (Figures 42 and 43) of test cells after a 5 second, 100 watt CO_2 laser exposure that raised the cell temperature to 500°C, no reduction in the solar cell's electrical characteristics was apparent within measurement variation tolerances.

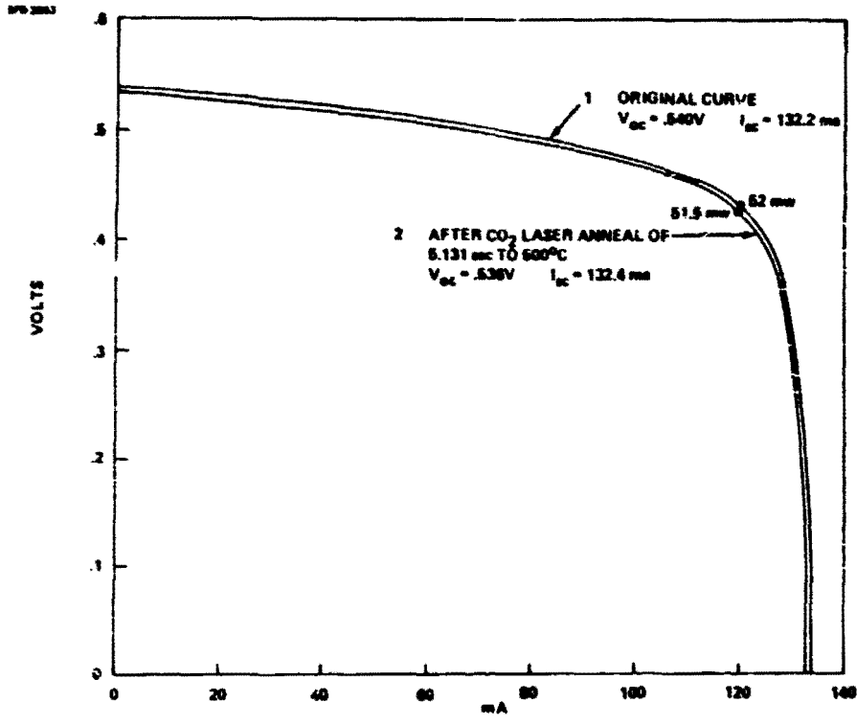

Figure 42; CO_2 Laser Annealed Solar Cell Without Coverglass, Solarex Cell No. 44

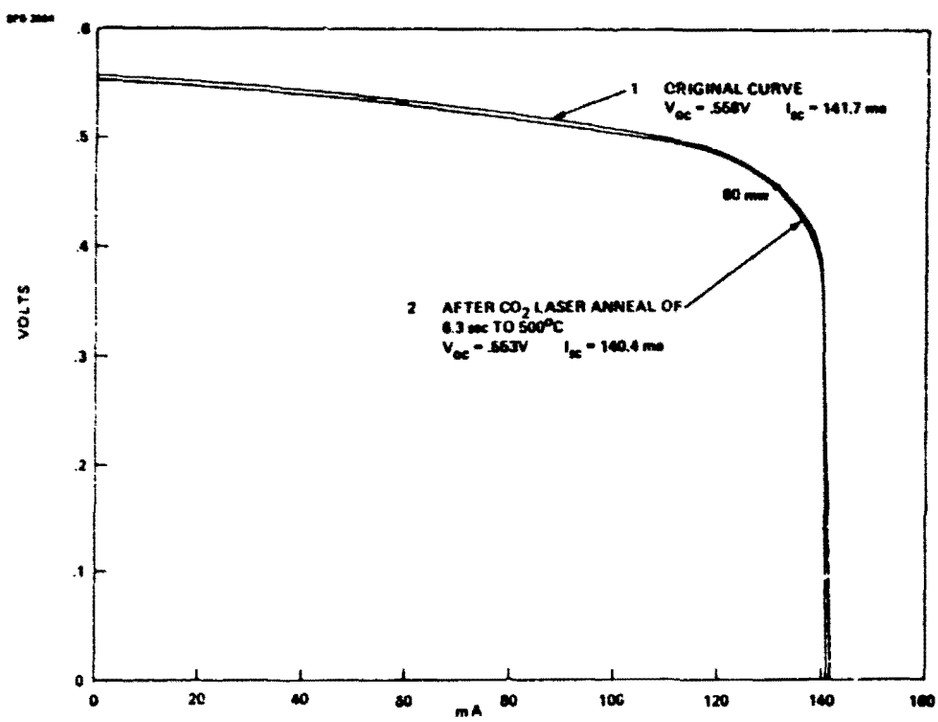

Figure 43; CO_2 Laser Annealed Solar Cell Without Coverglass, Solarex Cell No. 45

7.7 EVALUATION OF LASER-ANNEAL OF IRRADIATION DAMAGED 50 μm-THICK SOLAR CELLS

Integral glass covered solar cells provided during this test program have been found to be intolerant of annealing test temperatures or were damaged as in the case of the Corning 7070 glass covered cells. To further this testing program, unglassed 50 μm-thick solar cells were tested for annealability using a 150 watt CO_2 laser.

Figure 44 shows typical recovery characteristics of a 50 μm-thick solar cell after first being charged-particle irradiated and then laser annealed. Figure 45 shows the laser exposure (two pulses) used to anneal the cells described in Figure 44.

Figures 46 through 52 illustrate laser annealing of charged-particle irradiated Solarex and O.C.L.I. 50 μm-thick solar cells. Each cell was to be irradiated with 1.9 MeV protons to a fluence of 1×10^{12} protons/cm^2, however cells 18, 19, 31 and 32 did not receive full irradiation fluence due to malfunction of the proton source during the irradiation portion of the test sequence. Cells #18 and 32 had reduced outputs after the laser anneal portion of the test due to cell damage. Cell #18 was broken and 25% of the cell was lost. Cell #31 curled during laser exposure to such an extent that accurate electrical measurement under solar simulations conditions was not possible.

Figure 53 illustrates repeated laser annealing under the same test conditions as applied to those solar cells depicted in Figures 46 through 52. Figure 54 is a summary of output power variations after each step of the annealing test sequence for all cells except cells #18 and 32 which were damaged during laser exposure. Electrical characteristics for the annealing test sequence control cells are shown in Appendix B.

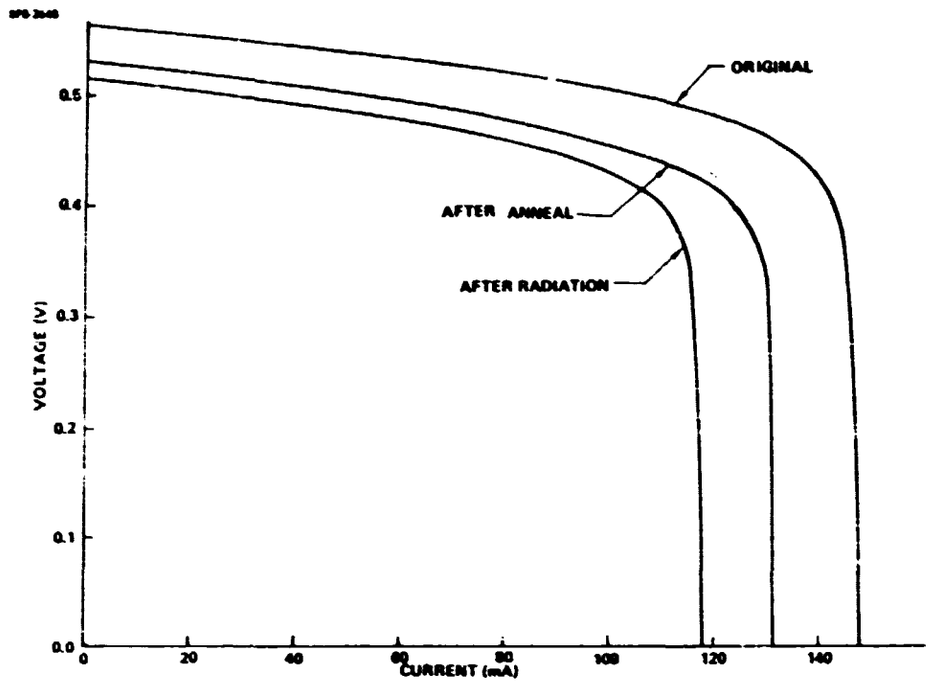

Figure 44; I-V Characteristic of 50 μm, Unglassed Solar Cell After Proton Irradiation and After CO_2 Laser Anneal.

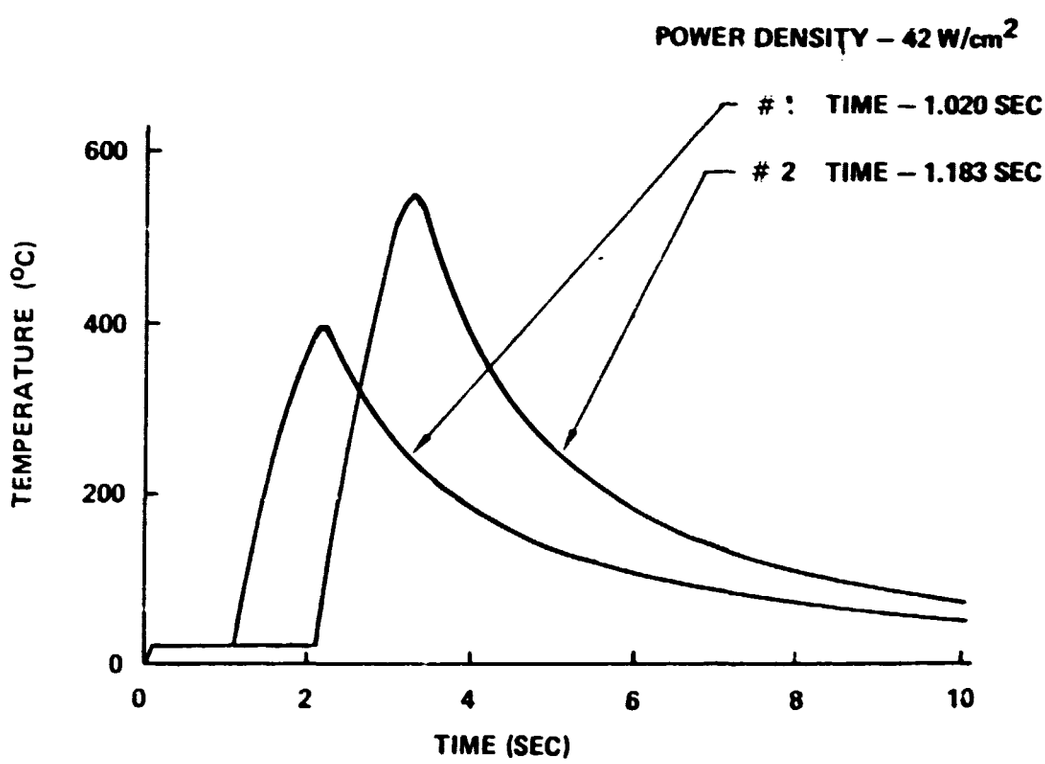

Figure 45; Temperature vs. Time Plot for Laser Annealing Test of Proton Irradiated 50 μm Silicon Solar Cell Without Coverglass.

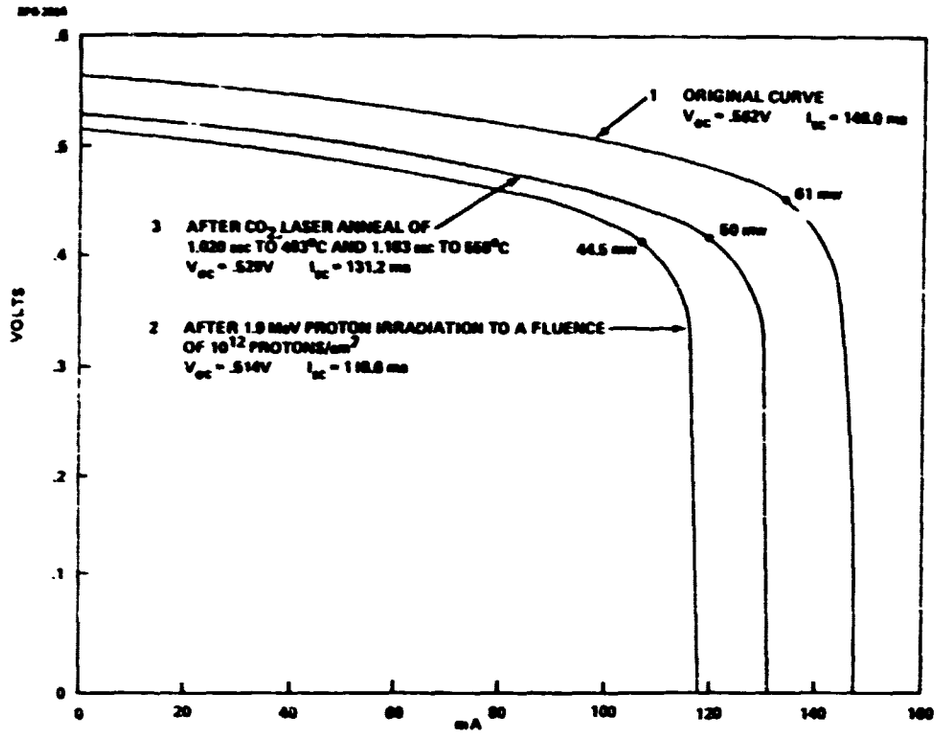

Figure 46; CO_2 Laser Annealed Solar Cell Without Coverglass, Solarex Cell No. 16

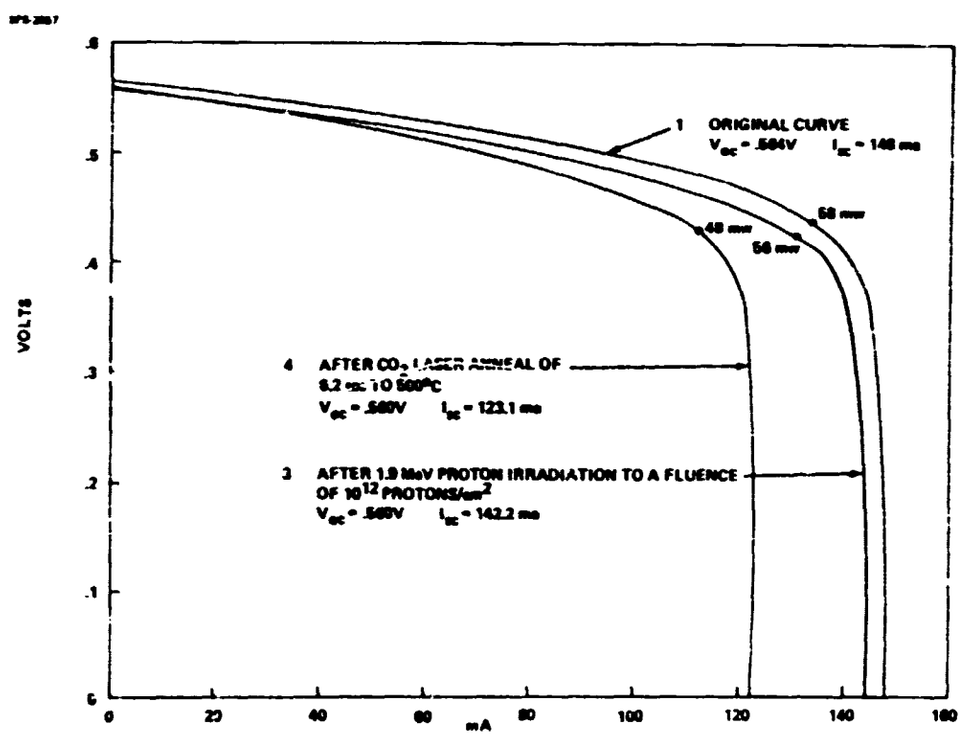

Figure 47; CO_2 Laser Annealed Solar Cell Without Coverglass, Solarex Cell No. 18

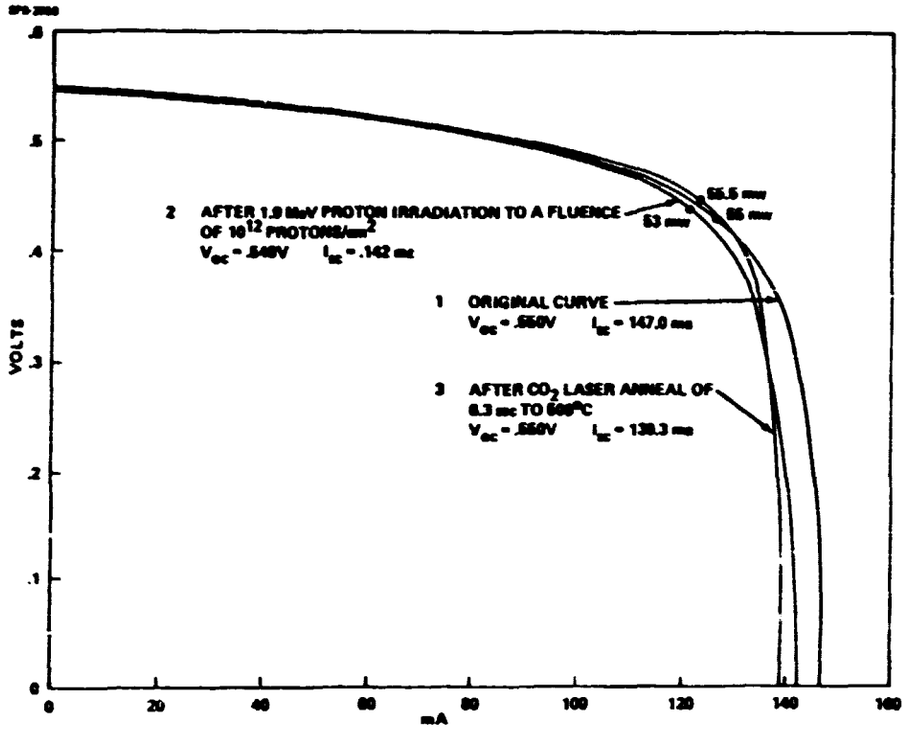

Figure 48; CO_2 Laser Annealed Solar Cell Without Coverglass, Solarex Cell No. 19

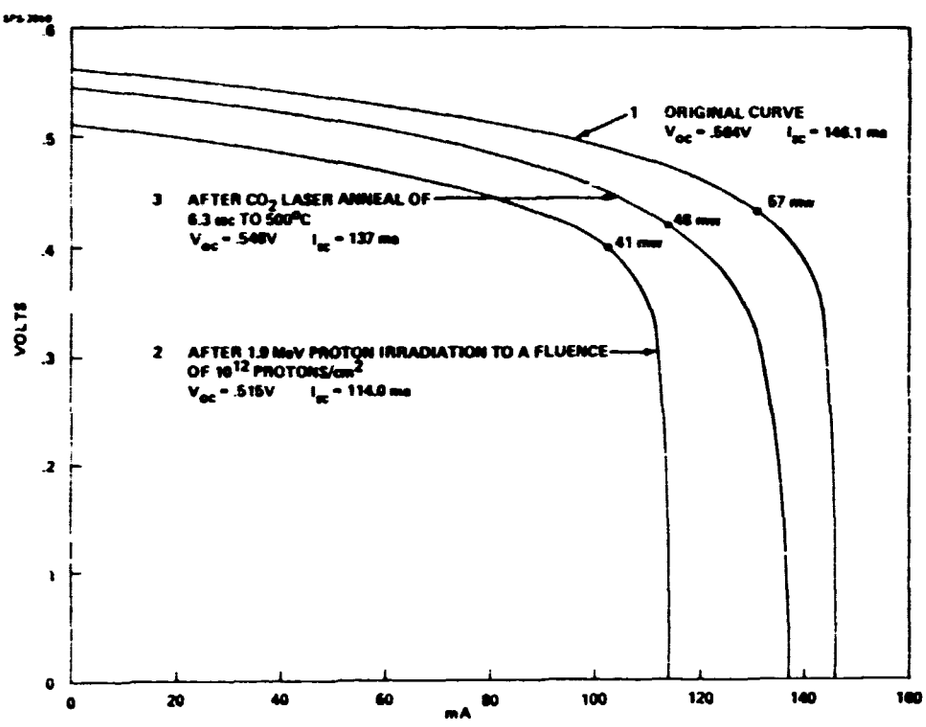

Figure 49; CO_2 Laser Annealed Solar Cell Without Coverglass, Solarex Cell No. 20

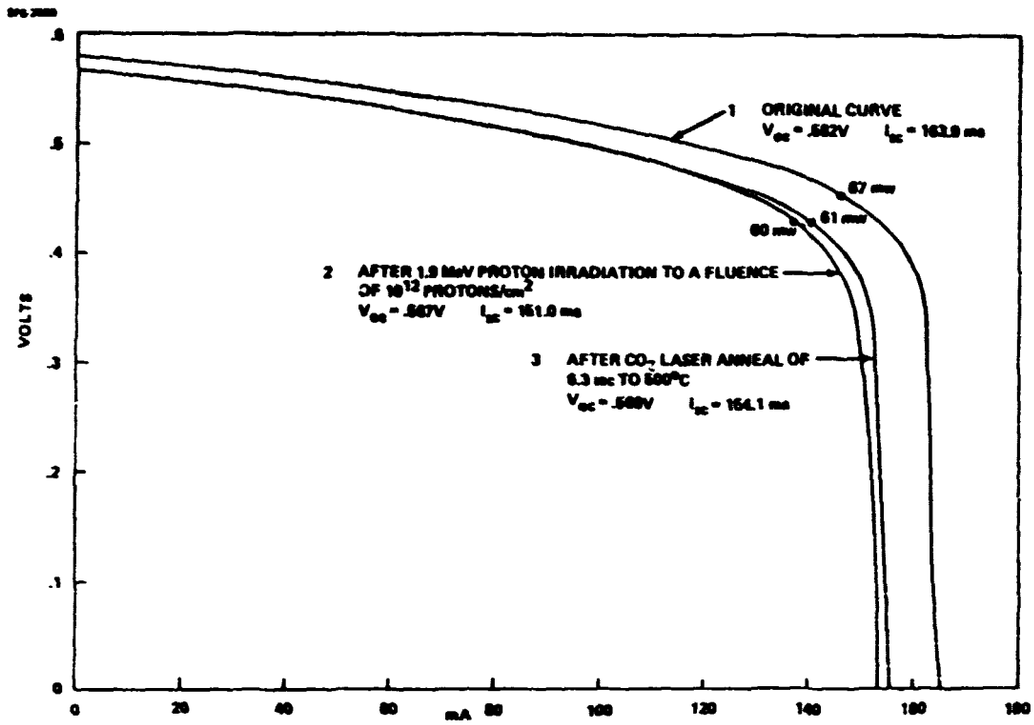

Figure 50; CO_2 Laser Annealed Solar Cell Without Coverglass, O.C.L.I. Cell No. 31

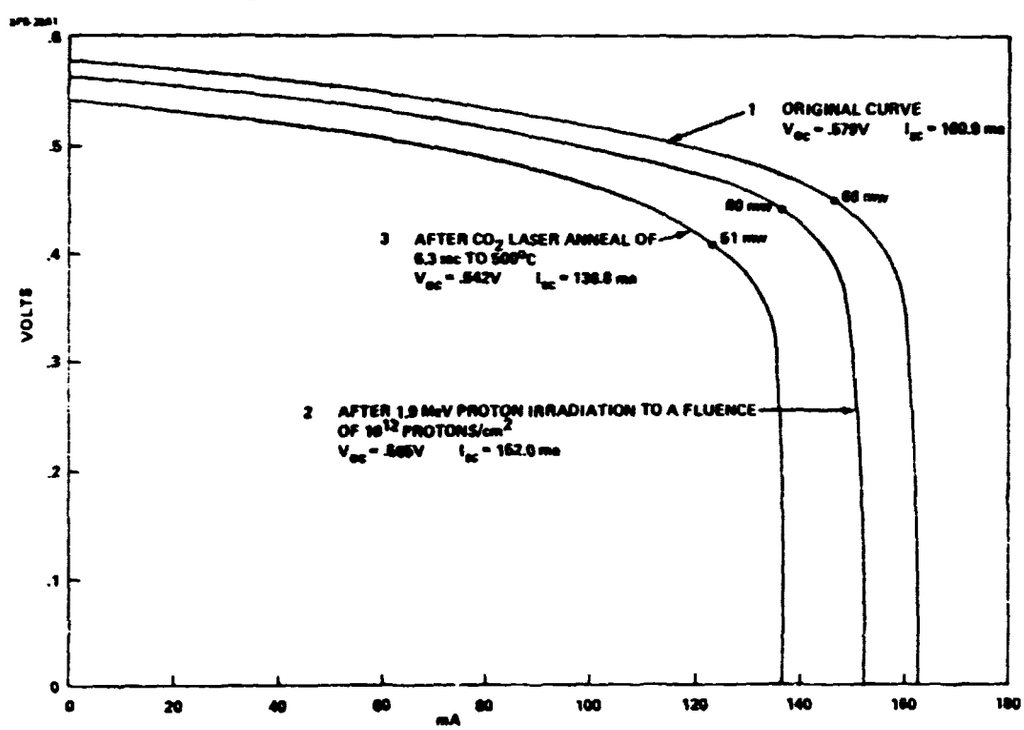

Figure 51; CO_2 Laser Annealed Solar Cell Without Coverglass, O.C.L.I. Cell No. 32

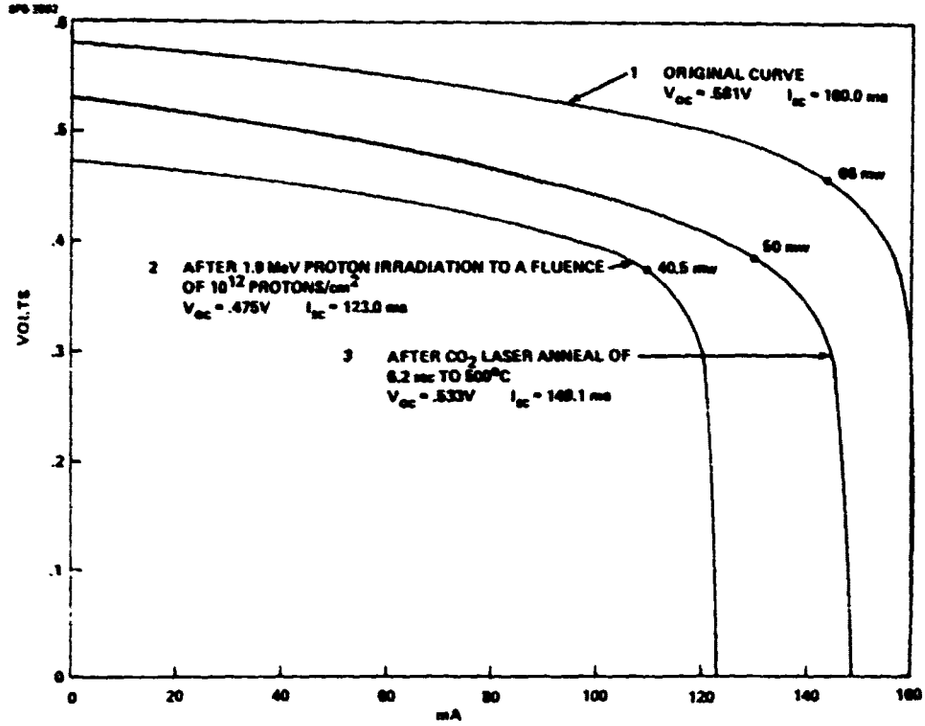

Figure 52; CO_2 Laser Annealed Solar Cell Without Coverglass, O.C.L.I. Cell No. 33

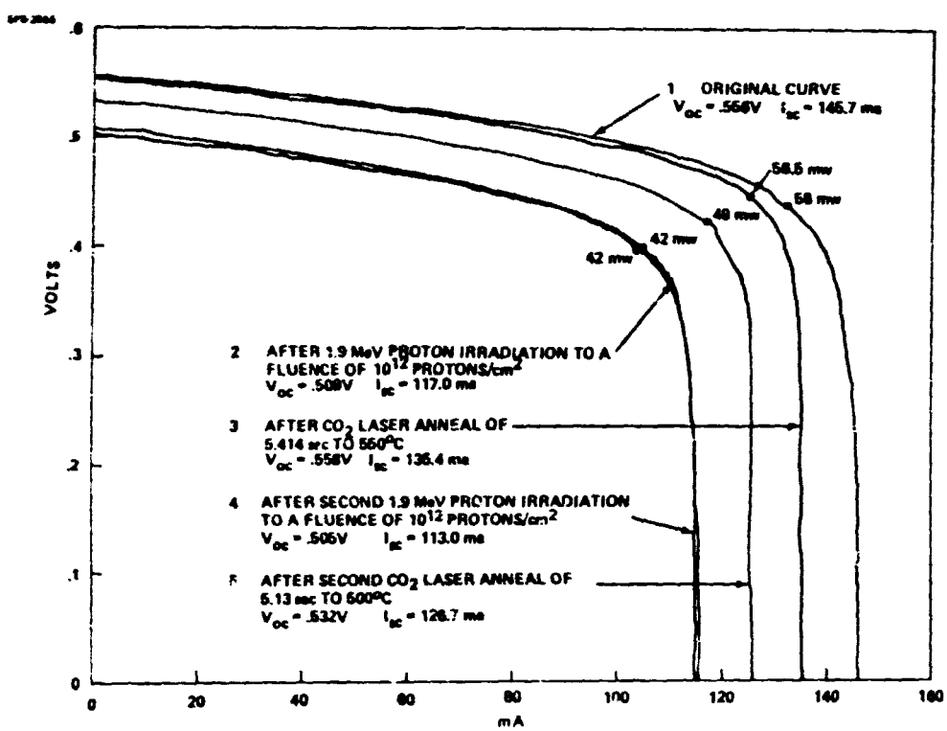

Figure 53; CO_2 Laser Annealed Solar Cell Without Coverglass, Solarex Cell No. 13

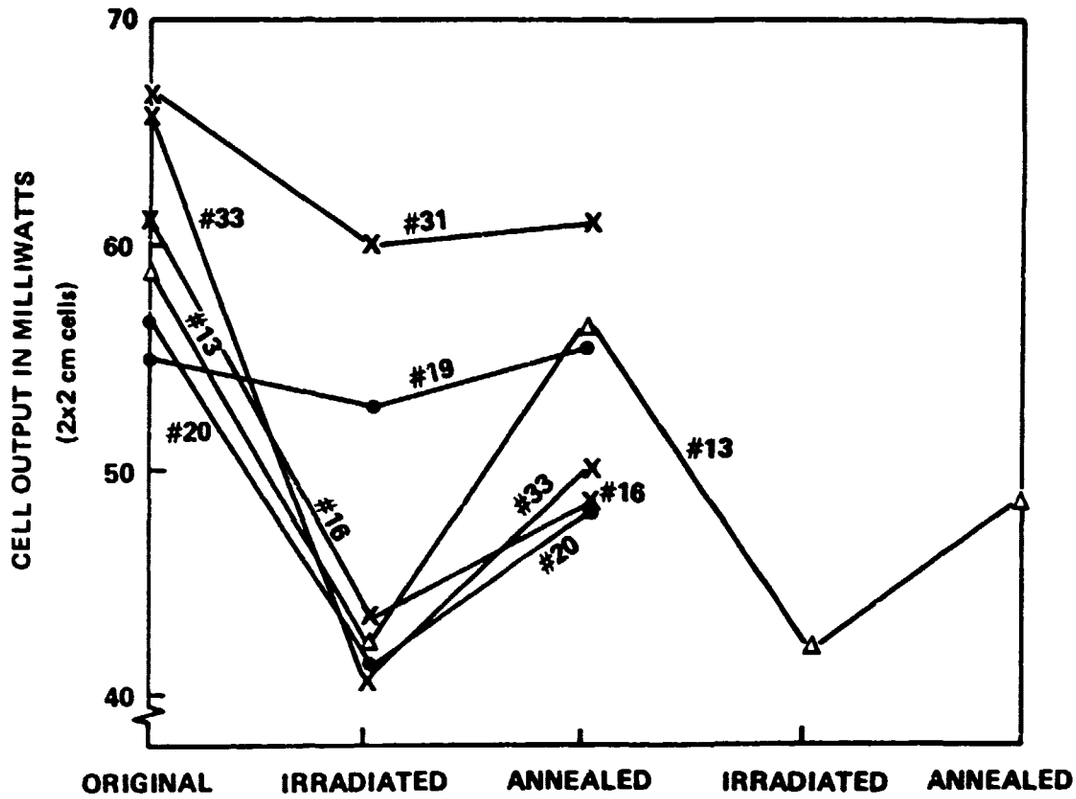

Figure 54; Degradation and Recovery of Maximum Power for Laser Annealed Solar Cells

8.0 CONCLUSIONS

Available application techniques for those glasses that are thermally compatible to silicon at annealing temperatures (500°C) are slow or require glass in a form not presently available. Deposition rates for glass range from 2 μm/hr for ion-beam sputtering to 100 μm/hr for electron-beam evaporation. Although the E-beam process is faster, the quality of the deposited glass layer is poor having a high bubble content.

Mechanically the 50 μm-thick solar cell and equivalent thickness glass cover must be stress free to prevent distortion or breakage due to thermal shock during laser exposure. Electrostatic bonding of glass to the 50 μm-thick solar cell requires a stress free thin cell to prevent cell breakage as pressure is applied during bonding.

Corning 7070 glass has thermal expansion characteristics that are very closely matched to silicon such that this glass is an acceptable silicon cell cover at annealing temperatures. Corning 7070 glass is not commercially available at this time in 50 μm to 75 μm thickness to be electrostatically bonded to a 50 μm thick solar cell.

These preliminary laser beam annealing tests showed an average 50% recovery from charged particle irradiation damage with 5-10 seconds exposure. Thermal bulk annealing in an oven for 20 minutes has shown 90-100% recovery. This difference in recovery suggests a time dependance for more complete annealing.

9.0 RECOMMENDATIONS

To further the development of an integral glass cover for the 50 μm-thick solar cell requires the development of a fast glass deposition process or a thin glass sheet with associated bonding process such as electrostatic bonding.

The primary obstacle in testing 50 μm-thick cells is the high test sample loss due to breakage. To reduce these losses, handling techniques need to be developed such that the individual cell is protected from excessive external stress. Also, some cell distortion or breakage is due to internal stresses released when the cell temperature is raised to above 200°C. The cell, metalization and glass structure must be studied to reduce internal stresses in these thin cells. More study is necessary to determine the differences between short term (1-10 sec.) annealing effects and long term (20 minutes) annealing effects. Also, if thin cell breakage can be reduced, repeated annealing characteristics of 20-30 anneal cycles may disclose accumulative effects inherent in the annealing process especially when lasers are used at the annealing energy source.

Future tests should:

1. Explore a wider range of time, temperature, and degradation conditions with a statistically significant number of samples. This testing could be done on base (unglassed) cells.

2. Perform tests on glassed cells as soon as a suitable glassing technique has been developed. Ideally, cells fully encapsulated with covers, substrate, and interconnects should be tested.

BIBLIOGRAPHY

1. SPIRE Corporation subcontract to Boeing Aerospace Company.

2. Kirkpatrick, A.R., "internally Bonded Covers for Silicon Solar Cells", Eleventh Photovoltaic Specialists Conference Proceedings, pp 169, May 1975.

3. G. Brackley, K. Lawson, D. W. Satchell, "Integral Covers for Silicon Solar Cells", Ninth Photovoltaic Specialists Conference Proceedings, pp 174, May 1972.

4. Bruce Faraday, Richard Statler and Regina Tauke, "Thermal Annealing of Proton - Irradiated Silicon Solar Cells', Sixth Photovoltaic Specialists Conference Proceedings, pp 15, March 1967.

D180-25037-4

APPENDIX A

TEST PLAN FOR LASER ANNEALING OF ULTRA-THIN SOLAR CELLS

CONTRACT NAS9 15631 ECP 001

FOR: BOEING SOLAR POWER SATELLITE PROGRAM

SEPTEMBER 1978

FRANK WALKER, TECHNICAL LEADER
SIDNEY W. SILVERMAN, PROGRAM MANAGER

BOEING AEROSPACE COMPANY
SEATTLE, WA 98124

TABLE OF CONTENTS

TABLE OF CONTENTS (CONTINUED)

TEST PLAN

LASER ANNEALING OF RADIATED DAMAGED, ULTRA-THIN SOLAR CELLS

A.1.0 SCOPE

A.1.1 BACKGROUND

Little work has been done in the area of thermal annealing of solar cell radiation damage using laser energy. Thermal properties of advanced solar cell designs have not been tested at high temperature (500°C) and breakage of the ultra-thin (50μm) solar cells due to thermal shock is a serious concern in present developmental tests. As the state-of-the-art development of solar cells progresses, it is important that a good quantitative understanding of the physical properties of these cells be maintained as a basis for further development and accurate solar cell modeling.

A.1.2 OBJECTIVE

The test will define those solar cell and laser parameters that are pertinent to thermal annealing of 50μm silicon solar cells covered with 50μm to 75μm of borosilicate glass. Those parameters such as laser beam intensity, exposure time, beam uniformity, and the cell structure thermal stability will be examined and developed as much as the contract period and funding will allow. This test is an initial development task in which test parameters for future work are to be determined.

A.1.3 TECHNICAL APPROACH

This effort requires testing of laser annealed solar cells and analysis of test results. The contract allows for only minimal pre-test analysis.

Initial test parameters will be taken from earlier laser annealing tests performed on glass covered, 250μm thick solar cells and from a steady state thermodynamic model of the test cell structure. Pre-test parameters will be adjusted from post-test results in an iterative process that leads to the most effective annealing technique for the materials and laser being tested. In this manner, test analysis will establish the optimum exposure times and intensities of the laser beam for achieving annealing within the constraints of the allowable thermal stresses in the silicon-glass structure.

A.1.4 STATEMENT OF WORK

The proposed task will be performed by completing the following items:

(1) Establish initial test parameters for deposition of laser energy into the radiation damaged region of the silicon.

(2) Test laser effects on uncovered test cells and analyze the results to determine if thermal stresses cause observable damage to the silicon cell. Adjust the test parameters to optimize thermal annealing and minimize structural damage to the cell.

(3) Apply laser pulses to solar-cell-and-cover assemblies to confirm the ability of the covered cells to withstand the thermal stresses of laser annealing.

(4) Irradiate 7 glass covered cells with 1 MeV electrons to a fluence level of 2×10^{15} electrons/cm^2 and irradiate 3 glass covered solar cells with 11 MeV proton irradiation to a fluence level of 3×10^{12} protons/cm^2.

(5) Laser anneal the 10 specimens, measuring performance before and after.

(6) Perform repeated annealing on four of the 10 solar cell specimens. The number of repeat cycles will be determined.

(7) Write a report describing the work and summarizing the results.

A.1.5 DATA ANALYSIS

To determine the effect of particle irradiation and laser annealing on each solar cell, pre- and post-test electrical parameters will be compared. In addition, thermal measurements made on the cell during laser beam exposure will be used to adjust laser beam intensity and duration to prevent mechanical damage to the cell. A solar cell will be judged mechanically damaged when such damage is observable with the aid of a X10 power microscope.

A.2.0 ELECTRICAL PERFORMANCE TEST

A.2.1 PURPOSE

The objective of this test is to measure electrical performance characteristics for each cell at standard conditions while illuminated by a solar simulator.

A.2.2 TEST CONDITIONS

A. Illumination: 1.0 solar constant $\pm$ 0.75% ($\pm$ 0.25% goal).
B. Spectral distribution: AMO conditions.
C. Uniformity: $\pm$ 2.0%.
D. Stability: $\pm$ 1.0% ($\pm$ 0.25% goal). (As measured with a control cell).
E. Cell temperature: 25°C $\pm$ 1°C.
F. Environment: Air

A.2.3 TEST MEASUREMENT ACCURACY

A.2.3.1 Spectral

A. Illumination: 0.1%.
B. Spectral radiance: ± 3.0% (+9.0% in U.V. range).
C. Uniformity: ± 1.0%.

A.2.3.2 Thermal

A. Cell temperature ± 0.5°C.

A.2.3.3 Electrical

A. Short circuit current: ± 0.1%.
B. Open circuit voltage: ± 0.1%.
C. BFS cell accuracy: ± 0.1%.
D. I-V characteristic curve accuracy: As defined by Attachment B.

A.2.4 SAMPLE SIZE AS REQUIRED

A.2.5 TEST EQUIPMENT

A.2.5.1 Optical

A. X-25 Mark II Solar Simulator (Refer to Attachment A).
B. Beckman Spectroradiometer.

A.2.5.4 Thermal

A. Temperature control test block.

A.2.5.3 Electrical

A. Digital voltmeter.
B. Moseley Model 135 X-Y Plotter.
C. Spectrolab D-550 Electronic Load.
D. "Balloon Flight Standard".

A.2.6 ELECTRICAL PERFORMANCE TEST PROCEDURE

NOTE 1: A solar cell test group is comprised of 3 monitor cells and the test cell batch. The monitor cells are to be tested before and after the test cell batch, and at intervals no longer than 30 minutes during a test.

A. Turn on all equipment and allow 20 minute warm-up.
B. Calibrate the solar simulator with the BFS solar cell to the prescribed intensity level.
C. Measure and record the temperature and short-circuit current of the control cell for future recalibration of the solar simulator.
D. Mount a solar cell in the test fixture and make electrical connections.
E. Stabilize the solar cell in the test fixture and make electrical connections.

NOTE 2: Steps F through J are to be in accordance with Attachment B.

F. Measure and record the open-circuit voltage of the cell.
G. Plot the cell current-voltage characteristics by sweeping the load from open-circuit voltage to short-circuit current.
H. Measure and record the short-circuit current of the cell.
I. Measure and record the temperature of the cell.
J. Remove the solar cell from the test fixture.

NOTE 3: Repeat Steps D through J until the test group is finished. Repeat testing of the monitor cells in accordance with NOTE 1, as necessary.

K. Check the repeatability of each monitor cell performance to determine if it is in accordance with the requirements of this test plan.

L. Recalibrate the solar simulator every 30 minutes with the control cell after verifying its test temperature.

A.3.0 ELECTRON BOMBARDMENT TEST

A.3.1 PURPOSE

This test will establish the degradation characteristics of the glass covered 2 mil. solar cells to 1 MeV electron bombardment.

A.3.2 TEST CONDITIONS

A. Electron energy: 1 MeV $\pm$ 5%.
B. Beam flux: 10^9 to 5×10^{11} electronics/cm^2 - sec., $\pm$ 16%.
C. Fluence level: 2×10^{15} electrons/cm^2, $\pm$ 16%.
D. Solar Cell Temperature: $30^oC \pm 5^oC$.

A.3.3 TEST MEASUREMENT ACCURACY

A. Beam energy: $\pm$ 0.4%.
B Beam flux: $\pm$ 16% (See Attachment C).
C. Fluence level: $\pm$ 16% (See Attachment C).
D. Solar cell temperature: $\pm$ 1.3^oC.

A.3.4 SAMPLE SIZE

7 glass-covered, 2 mil, silicon solar cells.

A.3.5 TEST EQUIPMENT

A. Dynamitron.
B. Keithley 610 Electrometer.
C. Brookhaven Instruments Model 1000C Current Integrator.
D. Type-K Thermocouple Strip Chart Recorder.

A.3.6 ELECTRON BOMBARDMENT TEST PROCEDURE

A. Verify the uniformity, energy and flux of the charged particle beam.
B. Mount the test cells on the test block.
C. Record the temperature of the target.
D. Turn on the charged particle source and bombard the test cells until the correct fluence level is achieved.
E. Turn off the charged particle source.
F. Record the temperature of the target.
G. Remove cells from the test chamber.

A.4.0 PROTON BOMBARDMENT TEST

A.4.1 PURPOSE

This test will establish the degradation characteristics of the test solar cells to 1.5 MeV proton bombardment.

A.4.2 TEST CONDITIONS

A. Proton energy: 11 MeV $\pm$ 5%.
B. Beam flux: 10^7 to 10^9 protons/cm^2 - sec., $\pm$ 16%.
C. Fluence level: 3×10^{12} protons/cm^2, $\pm$ 16%.
D. Solar cell temperature: $25^oC \pm 10^oC$.

A.4.3 TEST MEASUREMENT ACCURACY

A. Beam energy: $\pm$ 0.4%.
B. Beam flux: $\pm$ 16% (See Attachment C).
C. Fluence level: $\pm$ 16% (See Attachment C).
D. Solar cell temperature: $\pm$ 1.3^{o}C.

A.4.4 SAMPLE SIZE

3 test cells.

A.4.5 TEST EQUIPMENT

A. Dynamitron.
B. Keithley 610 Electrometer.
C. Brookhaven Instruments Model 1000C Current Integrator.
D. Type-K Thermocouple Strip Chart Recorder.

A.4.6 PROTON BOMBARDMENT TEST PROCEDURE

A. Verify the uniformity, energy and flux of the charged particle beam.
B. Mount the test cells on the test block.
C. Record the temperature of the target.
D. Turn on the charged particle source and bombard the test cells until the correct fluence level is achieved.
E. Turn off the charged particle source.
F. Record the temperature of the target.
G. Remove cells from the test chamber.

A.5.0 LASER ANNEALING TEST

A.5.1 PURPOSE

This test will establish the recovery potential of thermal annealing using a CO_2 laser energy source.

A.5.2 TEST CONDITIONS

A. Maximum power: 250 watts.
B. Beam wavelength: 10.6 μm (CO_2).
C. Target area: $2\pi cm^2$.
D. Beam energy density: ~40 watts/cm^2.
E. Beam uniformity: multimode operation.
F. Exposure duration: variable from 0.1 sec. to 2 sec. with the use of a mechanical shutter.
G. Solar cell temperature: 25^oC to 500^oC during test.
H. Environment: Air.
I. Solar cell mounting: The cell structure is to be unrestrained and lain horizontally, face up, on a block of fused silica. The CO_2 laser beam is projected vertically, normal to the solar cell surface.

A.5.3 TEST MEASUREMENT ACCURACY

A. Beam energy: $\pm$ 10%.
B. Beam uniformity: The energy distribution at the target is mapped at the start of the test and whenever the beam path is altered by means of lenses or mirrors.
C. Solar cell temperature: $\pm$ 5^oC.

A.5.4 SAMPLE SIZE

As required.

A.5.5 TEST EQUIPMENT

A. 250 watt CO_2 laser manufactured by Coherant Radiation of Palo Alto, CA (Model 421).

B. Huggins Infra-Scope.

C. Type-K Thermocouple Strip Chart Recorder.

D. Mechanical shutter to provide accurate exposure times of from 0.1 sec. to 2 sec.

A.5.6 LASER ANNEALING TEST PROCEDURE

A. Place test cell on target block.

B. Connect thermocouple wires to Type-K thermocouple strip chart recorder.

C. Make continuous thermocouple measurements throughout test.

D. Record Huggins Infra-Scope measurements of solar cell temperature and compare with calibration value for room temperature.

E. Record infra-scope output throughout test.

F. Turn on CO_2 laser and allow warm-up as recommended by manufacturer.

G. Record beam energy level.

H. Actuate mechanical shutter to expose solar cell to laser beam for desired exposure period.

I. Turn off CO_2 laser.

J. Disconnect solar cell from test equipment and remove solar cell from target block.

K. Repeat steps A through J until all solar cell specimens have been tested.

ATTACHMENT A

SOLAR SIMULATOR DESCRIPTION

Solar cell performance will be measured while irradiating the cells with a Spectrolab X-25 Mark II solar simulator. This simulator is spectrally filtered to closely match the solar spectrum at air mass zero (AMO). The irradiance of the simulated solar beam will be set to 1.0 Earth-Suns (approximately 135.3 mw/cm^2) as measured with a calibrated balloon flight standard (BFS) solar cell provided by the Jet Propulsion Laboratory. The total irradiance will be measured with a TRW differential radiometer, and the spectral irradiance will be measured with a Beckman model 139323 spectroradiometer.

Calibration of all solar simulators will be performed before use on this program, and after each 100 hours of solar simulator operation. The following will be verified at each calibration.

Solar beam uniformity of irradiance.

Solar beam spectral energy distribution.

Solar beam irradiance stability.

The solar simulation accuracy and calibration procedures are defined in Boeing Document D180-15115-1.

ATTACHMENT 3

REQUIREMENTS FOR MEASURING CURRENT-VOLTAGE CHARACTERISTICS

The following technique shall be used in measuring the current-voltage characteristic (I-V curve) of each solar cell. The curve shall be plotted on bond graph paper having 10 divisions per 1/2 inch grid.

Verify electrical zero and mark on data sheet.

Measure the open-circuit voltage (V_{oc}) using a digital voltmeter with the electronic load at zero current. Mark and label this point on the data sheet. 1

Measure the short-circuit current (I_{sc}) using a digital voltmeter with the electronic load at zero voltage. Mark and label this point on the data sheet. 1

Record the cell temperature, calibration cell output, solar cell serial number, date, and solar simulator serial number on the data sheet.

Periodically check the X-Y plotter to determine that hysterisis does not exceed 4 percent in current at any voltage.

1 The I_{sc} and V_{oc} of the I-V curve plot shall be within 1/20 of an inch of the respective digital voltmeter readings.

ATTACHMENT C

PARTICLE IRRADIATION MEASUREMENT ERROR

The tolerance of the Faraday Cup used to measure particle flux is ± 15% and the tolerance of the Keithley 610 Electrometer that monitors the Faraday Cup is ± 3%, therefore, the probable error in the flux measurement is:

$$\sqrt{(0.5)^2 + (0.03)^2}$$

or ± 15.3%. The tolerance of the integrator used to determine total fluence is ± 2%, therefore, the probable error in fluence measurement is:

$$\sqrt{(0.5)^2 + (0.03)^2 + (0.02)^2}$$

or ± 15.4%.

APPENDIX B

TEST DATA

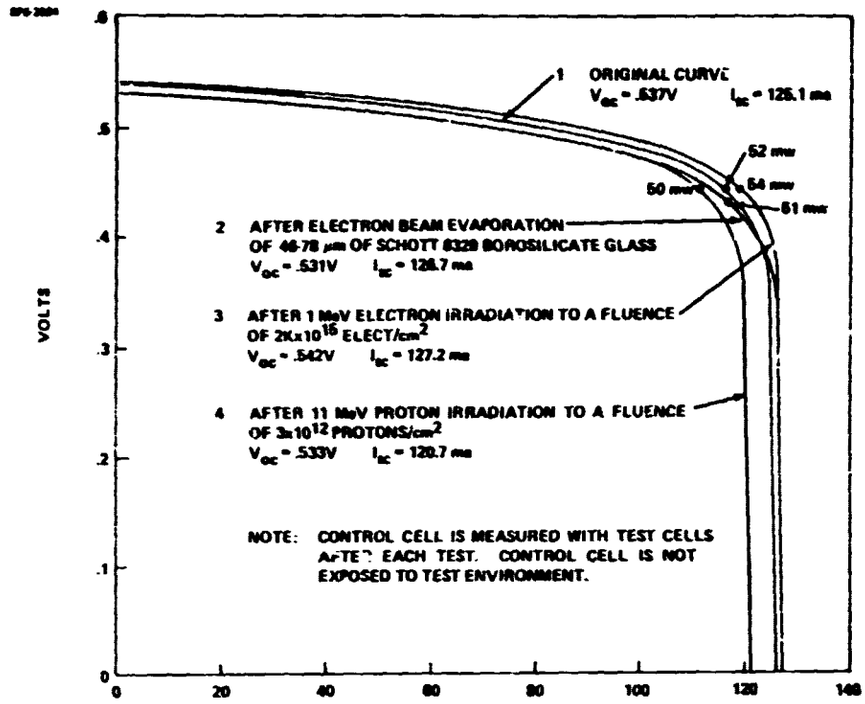

Control Cell for Laser Annealing Tests, Solarex Cell No. 14

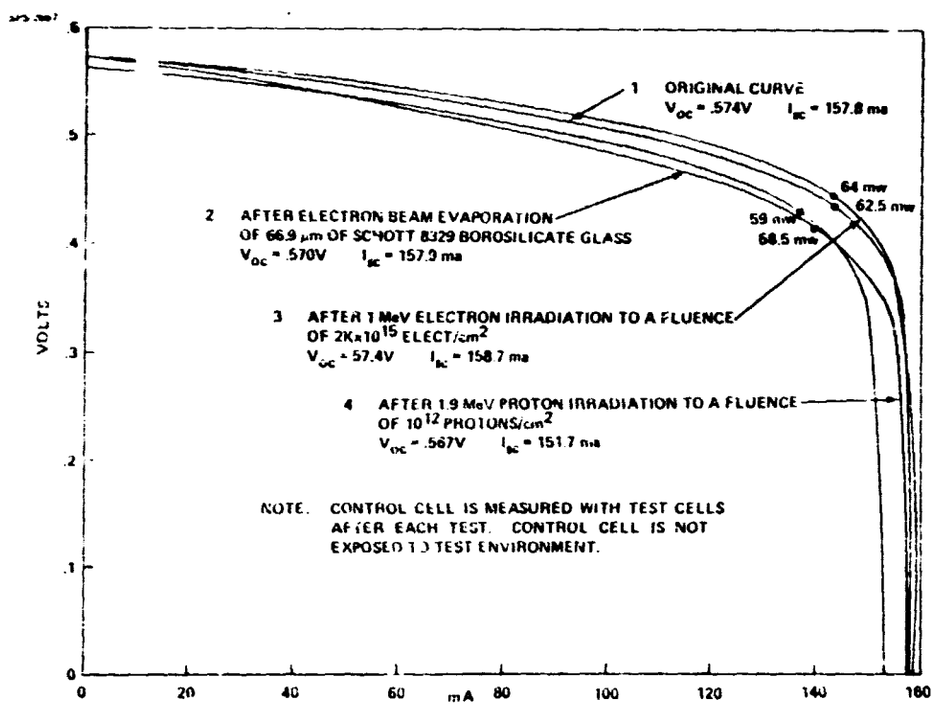

Control Cell for Laser Annealing Tests, O.C.L.I. Cell No. 22

SOLAREX CELLS WITH e-BEAM EVAPORATED, SCHOTT B329 GLASS COVERS

$$\%\Delta = \frac{\phi_{(AFTER)} - \phi_{(BEFORE)}}{\phi_{(BEFORE)}} \times 100$$

SOLAR CELL DESCRIPTION	TEST DESCRIPTION	1 V_{oc} (v)	2 $\%\Delta(V_{oc})$	3 $\%\delta(V_{oc})$	4 I_{sc} (ma)	5 $\%\Delta(I_{sc})$	6 $\%\delta(I_{sc})$	7 P_{max} (mw)
SOLAREX #1	ORIGINAL PARAMETERS	0.554			141.7			61
	AFTER COVERED WITH 46μ OF SCHOTT B329	0.545	-1.62	98.38	136.9	-3.39	96.61	57
	AFTER 1 MeV elect. IRRAD TO 2X10^15 e/cm²	0.520	-4.59	93.86	118.5	-13.44	83.63	47
SOLAREX #2	ORIGINAL PARAMETERS	0.555			141.4			60
	AFTER COVERED WITH 60μm OF SCHOTT B329	0.548	-1.26	98.74	137.4	-2.83	97.17	56
	AFTER 11 MeV PROTON IRRAD. TO 3X10^12 p/cm²	0.501	-9.58	90.27	97.1	-29.33	68.67	36
SOLAREX #3	ORIGINAL PARAMETERS	0.558			141.9			60.5
	AFTER COVERED WITH 60μm OF SCHOTT B329	0.549	-1.61	98.39	140.9	-0.70	99.30	57.5
SOLAREX #4	ORIGINAL PARAMETERS	0.560			141.7			61
	AFTER COVERED WITH 60μm OF SCHOTT B329	0.544	-2.86	97.14	140.3	-0.99	99.01	50
SOLAREX #5	ORIGINAL PARAMETERS	0.500			141.3			58
	AFTER COVERED WITH 70μm OF SCHOTT B329	0.541	+8.20	108.20	137.1	-2.97	97.03	54
	AFTER 1 MeV elect. IRRAD TO 2X10^15 e/cm²	0.525	-2.96	105.00	118.9	-13.27	84.15	43
SOLAREX #6	ORIGINAL PARAMETERS	0.534			125.6			49
	AFTER COVERED WITH 70μm OF SCHOTT B329	0.515	-3.56	96.44	120.7	-3.90	96.10	45
	AFTER 1 MeV elect. IRRAD. TO 2X10^15 e/cm²	0.502	-2.52	94.01	113.0	-6.38	89.97	42
SOLAREX #7	ORIGINAL PARAMETERS	0.529			124.1			50.5
	AFTER COVERED WITH 78μm OF SCHOTT B329	0.512	-3.21	96.79	119.5	-3.71	96.29	46
	AFTER 11 MeV PROTON IRRAD TO 3X10^12 p/cm²	0.496	-3.13	93.76	92.5	-22.59	74.54	34.5
SOLAREX #8	ORIGINAL PARAMETERS	0.538			128.0			51
	AFTER COVERED WITH 78μm OF SCHOTT B329	0.525	-2.42	97.58	123.8	-3.28	96.72	43
SOLAREX #9	ORIGINAL PARAMETERS	0.536			126.5			52
	AFTER COVERED WITH 78μm OF SCHOTT B329	0.521	-2.80	97.20	123.9	-2.06	97.94	47
	AFTER 1 MeV elect. IRRAD TO 2X10^15 e/cm²	0.512	-1.73	95.52	110.7	-10.65	87.51	43
SOLAREX #10	ORIGINAL PARAMETERS	0.526			125.1			48
	AFTER COVERED WITH 70μm OF SCHOTT B329	0.512	-2.66	97.34	121.4	-2.96	97.04	45
	AFTER 1 MeV elect. IRRAD TO 2X10^15 e/cm²	0.493	-3.71	96.73	112.2	-7.58	89.69	40
SOLAREX #11	ORIGINAL PARAMETERS	0.531			126.3			50.5
	AFTER COVERED WITH 70μm OF SCHOTT B329	0.516	-2.82	97.18	124.1	-1.74	98.26	46
SOLAREX #12	CONTROL CELL ORIGINAL PARAMETERS	0.537			125.1			52
	CONTROL FOR SCHOTT GLASS COVER MEAS.	0.531	-1.12	98.88	126.7	+1.28	101.28	51
	CONTROL FOR ELECT. IRRAD. MEAS.	0.542	+2.57	100.93	127.2	+0.39	101.68	54
	CONTROL FOR PROTON IRRAD MEAS	0.533	-1.66	99.26	120.7	-5.11	96.48	50

± 0.3% ± 2.60%

BOEING

SHT. NO.

REV LTR _____ APPROVAL _____ DATE _____

(AFSCM-AFLCM 310-1A REF 25-62-18.0)

FOLDOUT FRAME 1

$- \phi_{(BEFORE)} \times 100$

FORE)

$$\overline{\%\delta} = \left[1 + \left(\frac{\phi_{(AFTER)} - \phi_{(ORIGINAL)}}{\phi_{(ORIGINAL)}}\right)\right] \times 100$$

AMO - ISC

135.3 mw/cm²

	4	5	6	7	8	9	10	11	12	13	14	15	16
	I_{SC} (ma)	$\%\Delta(I_{sc})$	$\%\delta(I_{sc})$	P_{max} (mw)	$\%\Delta(P_m)$	$\%\delta(P_m)$	ff	$\%\Delta$(ff)	$\%\delta$(ff)	EFF	$\%\Delta$(EFF)	$\%\delta$(EFF)	
	141.7			61			0.78			11.26			
3	136.9	-3.39	96.61	57	-6.56	93.44	0.76	-2.56	97.44	10.52	-6.57	93.43	
6	118.5	-13.44	83.62	47	-17.54	77.05	0.76	0	97.44	8.68	-17.49	77.09	
	141.4			60			0.76			11.08			
4	137.4	-2.83	97.17	56	-6.67	93.33	0.74	-2.63	97.37	10.34	-6.68	93.32	
	97.1	-29.33	66.67	36	-35.71	60.00	0.74	0	97.37	6.65	-35.69	60.02	
	141.9			60.5			0.76			11.17			
	140.9	-0.70	99.30	57.5	-4.96	95.04	0.74	-2.63	97.37	10.62	-4.92	95.08	
	141.7			61			0.77			11.26			
	140.3	-0.99	99.01	50	-18.03	81.97	0.66	-14.29	85.71	9.23	-18.03	81.97	
	141.3			58			0.82			10.71			
	137.1	-2.97	97.03	54	-6.90	93.10	0.73	-10.98	89.02	9.97	-6.91	93.09	
	118.9	-13.27	84.15	43	-20.37	74.14	0.69	-5.48	84.15	7.94	-20.36	74.14	
	125.6			49			0.73			9.05			
	120.7	-3.90	96.10	45	-8.16	91.84	0.72	-1.37	98.63	8.31	-8.18	91.82	
	113.0	-6.38	89.97	42	-6.67	85.71	0.74	+2.78	101.37	7.75	-6.74	85.64	
	124.1			50.5			0.77			9.32			
	119.5	-3.71	96.29	46	-8.91	91.09	0.75	-2.60	97.40	8.49	-8.91	91.09	
	92.5	-22.59	74.54	34.5	-25.00	68.32	0.75	0	97.40	6.37	-24.97	68.35	
	128.0			51			0.74			9.42			
	123.8	-3.28	96.72	43	-15.69	84.31	0.66	-10.81	89.19	7.94	-15.71	84.29	
	126.5			52			0.77			9.60			
	123.9	-2.06	97.94	47	-9.62	90.38	0.73	-5.19	94.81	8.68	-9.58	90.42	
	110.7	-10.65	87.51	43	-8.51	82.69	0.76	+4.11	98.70	7.94	-8.53	82.71	
	125.1			48			0.73			8.86			
	121.4	-2.96	97.04	45	-6.25	93.75	0.72	-1.37	98.63	8.31	-6.21	93.79	
	112.2	-7.58	89.69	40	-11.11	83.33	0.72	0	98.63	7.39	-11.07	83.41	
	126.3			50.5			0.75			9.32			
	124.1	-1.74	98.26	46	-8.91	91.09	0.72	-4.00	96.00	8.49	-8.91	91.09	
	125.1			52			0.77			9.60			
	126.7	+1.28	101.28	51	-1.92	98.08	0.76	-1.30	98.70	9.42	-1.88	98.13	
	127.2	+0.39	101.68	54	+5.88	103.85	0.78	+2.63	101.30	9.97	+5.84	103.85	
	120.7	-5.11	96.48	50	-7.41	96.15	0.78	0	101.30	9.23	-7.42	96.15	
			±2.60%			±2.85%			±1.35%			±3.85	

% DEGRADATION OF POWER DUE TO SERVICING

DATE _____

O.C.L.1 CELLS WITH e-BEAM EVAPORATED, SCHOTT B329 GLASS COVERS

$$\%\Delta = \frac{\phi_{(AFTER)} - \phi_{(BEFORE)}}{\phi_{(BEFORE)}} \times 10$$

SOLAR CELL DESCRIPTION	TEST DESCRIPTION	1 V_{oc} (v)	2 $\%\Delta(V_{oc})$	3 $\%\delta(V_{oc})$	4 I_{sc} (ma)	5 $\%\Delta(I_{sc})$	6 $\%\delta(I_{sc})$
O.C.L.1 #21	ORIGINAL PARAMETERS	0.548			160.8		
	AFTER COVER WITH 78μm OF SCHOTT B329	0.540	-1.46	98.54	152.1	-5.41	94.5
O.C.L.1 #22	CONTROL CELL ORIGINAL PARAMETERS	0.574			157.8		
	CONTROL FOR SCHOTT GLASS COVER MEAS.	0.570	-0.70	99.30	157.9	+0.06	100.0
	CONTROL FOR ELECT. IRRAD MEAS	0.574	+0.70	100.00	158.7	+0.51	100.5
	CONTROL FOR PROTON IRRAD MEAS	0.567	-1.22	98.78	151.9	-4.28	96.2
O.C.L.1 #23	ORIGINAL PARAMETERS	0.560			154.0		
	AFTER COVER WITH 78μm OF SCHOTT B329	0.552	-1.43	98.57	142.1	-7.73	92.2
O.C.L.1 #24	ORIGINAL PARAMETERS	0.548			147.7		
	AFTER COVERED WITH 78μm OF SCHOTT B329	0.537	-2.01	97.99	141.2	-4.40	95.6
	AFTER 1MeV elect. IRRAD. TO 2×10^{15} e/cm²	0.498	-7.26	90.88	130.5	-7.58	88.3
O.C.L.1 #25	ORIGINAL PARAMETERS	0.476			153.4		
	AFTER COVERED WITH 70μm OF SCHOTT B329	0.458	-3.78	96.22	144.2	-6.00	94.0
O.C.L.1 #26	ORIGINAL PARAMETERS	0.555			155.1		
	AFTER COVERED WITH 60μm OF SCHOTT B329	0.558	+0.54	100.54	143.9	-7.22	92.7
	AFTER 1MeV elect. IRRAD TO 2×10^{15} e/cm²	0.503	-9.86	90.63	130.5	-9.31	84.1
O.C.L.1 #27	ORIGINAL PARAMETERS	0.571			156.7		
	AFTER COVERED WITH 60μm OF SCHOTT B329	0.559	-2.13	97.90	148.1	-5.49	94.5
	AFTER 1MeV elect. IRRAD TO 2×10^{15} e/cm²	0.485	-13.24	84.94	130.7	-11.75	83.4
O.C.L.1 #28	ORIGINAL PARAMETERS	0.536			154.6		
	AFTER COVERED WITH 46μm OF SCHOTT B329	0.553	+3.17	103.17	146.1	-5.50	94.5
	AFTER 1MeV PROTON IRRAD TO 3×10^{12} P/cm²	0.466	-15.73	86.94	110.4	-24.46	71.4
				±0.61%			±2.15%

BOEING NO.

REV LTR _____ APPROVAL _____ DATE _____

(AFSCM/AFLCM 310-1A REF 3-62-18.1)

ORIGINAL PAGE IS OF POOR QUALITY

FOLDOUT FRAME 1

PRECEDING PAGE BLANK NOT FILMED

ϕ(BEFORE) X 100
ϕ)

$$\%\delta = \left[1 + \left(\frac{\phi_{(AFTER)} - \phi_{(ORIGINAL)}}{\phi_{(ORIGINAL)}}\right)\right] \times 100$$

AMO - ISC
135.3 $\frac{mw}{cm^2}$

4	5	6	7	8	9	10	11	12	13	14	15	16
(ma)	$\%\Delta(I_{sc})$	$\%\delta(I_{sc})$	P_{max} (mw)	$\%\Delta(P_m)$	$\%\delta(P_m)$	FF	$\%\Delta$(FF)	$\%\delta$(FF)	EFF	$\%\Delta$(EFF)	$\%\delta$(EFF)	
0.8			53			0.60			9.79			
2.1	-5.41	94.59	47	-11.32	88.68	0.57	-5.0	95.00	8.68	-11.34	88.66	
7.8			62.5			0.69			11.54			
7.9	+0.06	100.06	58.5	-6.40	93.60	0.65	-5.80	94.20	10.80	-6.41	93.59	
8.7	+0.51	100.57	64	+9.40	102.40	0.70	+7.69	101.45	11.82	+9.44	102.43	
4.5	-4.28	96.26	59	-7.81	94.40	0.69	-1.43	100.00	10.89	-7.87	94.37	
4.0			63			0.73			11.63			
2.1	-7.73	92.27	41	-34.92	65.08	0.52	-28.77	71.23	7.57	-34.91	65.09	
7.7			53			0.65			9.79			
4.2	-4.40	95.60	49	-7.55	92.45	0.65	0	100.00	9.05	-7.56	92.44	
8.5	-7.58	88.35	43	-12.24	81.13	0.66	+1.54	101.54	7.94	-12.27	81.10	
3.4			29.5			0.40			5.45			
4.2	-6.00	94.00	26	-11.86	88.14	0.39	-2.50	97.50	4.80	-11.93	88.07	
5.1			61			0.71			11.26			
3.9	-7.22	92.78	57.5	-5.74	94.26	0.72	+1.41	101.41	10.62	-5.68	94.32	
2.5	-9.31	84.14	49	-19.78	80.33	0.75	+4.17	105.63	9.05	-14.78	80.37	
6.7			63			0.70			11.63			
8.1	-5.49	94.51	57.5	-8.73	91.27	0.69	-1.43	98.57	10.62	-8.61	91.32	
0.7	-11.75	83.41	46	-20.00	73.02	0.73	+5.80	104.29	8.49	-20.06	73.00	
4.6			58			0.70			10.71			
6.1	-5.50	94.50	54.5	-6.03	93.97	0.67	-4.29	95.71	10.06	-6.07	93.93	
1.4	-24.46	71.41	36	-33.94	62.07	0.70	+4.48	100.00	6.65	-33.90	62.09	

±2.15% ±4.40% ±2.62 ±4.42%

FOLDOUT FRAME 2

THERMALLY ANNEALED SOLAR CELLS

$$\%\Delta = \frac{\phi(\text{AFTER}) - \phi(\text{BEFORE})}{\phi(\text{BEFORE})} \times 100$$

TEST PA

SOLAR CELL DESCRIPTION	TEST DESCRIPTION	1 V_{oc} (v)	2 $\%\Delta(V_{oc})$	3 $\%\delta(V_{oc})$	4 I_{sc} (ma)	5 $\%\Delta(I_{sc})$	6 $\%\delta(I_{sc})$	7 P_{Max} (mw)	8 $\%\Delta(P_{M}$
SOLAREX #13	ORIGINAL PARAMETERS	0.540			114.8			46	
	AFTER 1.9MeV PROTON IRRAD. TO 1x10^12 P/cm²	0.498	-7.78	92.22	104.2	-9.23	90.77	35	-23.91
	AFTER 20 min ANNEAL AT 450°C	0.529	+6.22	97.96	122.4	+17.47	106.62	41	+17.14
	AFTER 1.9MeV PROTON IRRAD TO 1x10^12 P/cm²	0.509	-3.78	94.26	103.8	-15.20	90.42	37	-9.76
	AFTER 20 MIN ANNEAL AT 450°C	0.533	+4.72	98.70	120.5	+16.09	104.97	46	+24.32
SOLAREX #19	ORIGINAL PARAMETERS	0.532			114.1			46	
	AFTER 1.9MeV PROTON IRRAD TO 1x10^12 P/cm²	0.503	-5.45	94.55	106.5	-6.66	93.34	41	-10.87
	AFTER 20 min ANNEAL AT 500°C	0.530	+5.37	99.62	122.1	+14.65	107.01	49	+19.51
	AFTER 1.9MeV PROTON IRRAD TO 1x10^12 P/cm²	0.506	-4.53	95.11	103.6	-15.15	90.80	39	-20.41
	AFTER 20 min. ANNEAL AT 500°C	0.525	+3.75	98.68	120.0	+15.83	105.17	47	+20.51
SOLAREX #20	ORIGINAL PARAMETERS	0.530			114.7			43	
	AFTER 1.9MeV PROTON IRRAD TO 1x10^12 P/cm²	0.495	-6.60	93.40	106.4	-7.24	92.76	37	-13.95
	AFTER 20 min ANNEAL AT 500°C	0.527	+6.46	99.43	122.9	+15.51	107.15	46	+24.32
	AFTER 1.9MeV PROTON IRRAD. TO 1x10^12 P/cm²	0.495	-6.07	93.40	98.4	-19.93	85.79	35	-23.91
	AFTER 20 min ANNEAL AT 500°C	0.520	+5.05	98.11	120.2	+22.15	104.80	40	+14.29
SOLAREX #13 L	ORIGINAL PARAMETERS	0.556			145.7			58	
	AFTER 1.9MeV PROTON IRRAD TO 1x10^12 P/cm²	0.509	-8.45	91.55	117.0	-19.70	80.30	42	-27.59
	AFTER 5 sec CO_2 LASER ANNEAL TO 500°C	0.558	+9.63	100.36	137.4	+17.44	94.30	56.5	+34.52
	AFTER 1.9MeV PROTON IRRAD TO 1x10^12 P/cm²	0.505	-9.50	90.83	113.0	-17.76	77.56	42	-25.66
	AFTER 5 sec CO_2 LASER ANNEAL TO 500°C	0.532	+5.35	95.68	126.7	+12.12	86.96	49	+16.67
SOLAREX #16 L	ORIGINAL PARAMETERS	0.562			148.0			61	
	AFTER 1.9MeV PROTON IRRAD TO 1x10^12 P/cm²	0.514	-8.54	91.46	118.6	-19.86	80.14	44.5	-27.05
	AFTER 1.02 & 1.183 sec CO_2 LASER ANNEAL TO 403 & 558°C	0.529	+2.92	94.13	131.2	+10.62	88.65	50.0	+12.36
SOLAREX #18 L	ORIGINAL PARAMETERS	0.564			148.0			58	
	AFTER 1.9MeV PROTON IRRAD TO 1x10^12 P/cm²	0.560	-0.71	99.29	142.2	-3.92	96.08	56	-3.45
	AFTER 8.2 sec CO_2 LASER ANNEAL TO 500°C	0.560	0	99.29	123.1	-13.43	83.18	48	+3.57
SOLAREX #19 L	ORIGINAL PARAMETERS	0.550			147.0			55	
	AFTER 1.9MeV PROTON IRRAD TO 1x10^12 P/cm²	0.549	-0.18	99.82	142.0	-3.40	96.60	53	-3.64
	AFTER 11.2 sec CO_2 LASER ANNEAL TO 500°C	0.550	+0.18	100.00	139.3	-1.90	94.76	55.5	+4.72
SOLAREX #20 L	ORIGINAL PARAMETERS	0.564			146.1			57	
	AFTER 1.9MeV PROTON IRRAD TO 1x10^12 P/cm²	0.515	-8.69	91.31	114.0	-21.97	78.03	41	-28.07
	AFTER 16.2 sec CO_2 LASER ANNEAL TO 500°C	0.548	+6.41	97.16	137.0	+20.18	93.77	48	+17.07
O.C.L.1 #31 L	ORIGINAL PARAMETERS	0.582			163.9			67	
	AFTER 1.9MeV PROTON IRRAD TO 1x10^12 P/cm²	0.567	-2.58	97.42	151.0	-7.87	92.13	60	-10.45
	AFTER 8.2 sec CO_2 LASER ANNEAL TO 500°C	0.568	+0.18	97.59	154.1	+2.05	94.02	61	+1.67
O.C.L.1 #32 L	ORIGINAL PARAMETERS	0.579			160.9			66	
	AFTER 1.9MeV PROTON IRRAD TO 1x10^12 P/cm²	0.565	-2.42	97.58	152.0	-5.53	94.47	60	-9.09
	AFTER 11.2 sec CO_2 LASER ANNEAL TO 500°C	0.542	+4.07	93.61	136.8	-10.00	85.02	51	-15.00
O.C.L.1 #33 L	ORIGINAL PARAMETERS	0.581			160.0			66	
	AFTER 1.9MeV PROTON IRRAD. TO 1x10^12 P/cm²	0.475	-18.24	81.76	123.0	-23.13	76.88	40.5	-38.64
	AFTER 16.2 sec CO_2 LASER ANNEAL TO 500°C	0.533	+12.21	91.74	149.1	+21.22	93.19	50	+23.46
SOLAREX #44 L	ORIGINAL PARAMETERS	0.540			132.2			52	
	AFTER 8.2 sec CO_2 LASER ANNEAL TO 500°C	0.536	-0.74	99.26	132.4	+0.15	100.15	51.5	-0.96
SOLAREX #45 L	ORIGINAL PARAMETERS	0.558			141.7			60	
	AFTER 16.2 sec CO_2 LASER ANNEAL TO 500°C	0.553	-0.90	99.10	140.4	-0.92	99.08	60	0

L after cell # indicates laser anneal, cells #13, 19 and 20 were annealed in an oven.

$\%\Delta = \left[\frac{\phi(\text{AFTER}) - \phi(\text{BEFORE})}{\phi(\text{BEFORE})}\right] \times 100$

$\%\delta = \left[1 + \left(\frac{\phi(\text{AFTER}) - \phi(\text{ORIGINAL})}{\phi(\text{ORIGINAL})}\right)\right] \times 100$

AMO - ISC 135.3 $\frac{mw}{cm^2}$

TEST PARAMETERS

5	6	7	8	9	10	11	12	13	14	15	16
$\%\Delta(I_{sc})$	$\%\delta(I_{sc})$	P_{max} (mw)	$\%\Delta(P_m)$	$\%\delta(P_m)$	ff	$\%\Delta(ff)$	$\%\delta(ff)$	EFF.	$\%\Delta(EFF.)$	$\%\delta(EFF.)$	
		46			0.74			8.49			
-9.23	90.77	35	-23.91	76.09	0.67	-9.46	90.54	6.46	-23.91	76.09	
+17.47	106.62	41	+17.14	89.13	0.63	-5.97	85.14	7.57	+17.18	89.16	
-15.20	90.42	37	-9.76	80.43	0.70	-11.11	94.59	6.83	-9.78	80.45	
+16.09	104.97	46	+24.32	100.00	0.72	+2.86	97.30	8.49	+24.30	100.00	
		46			0.76			8.49			
-6.66	93.34	41	-10.87	89.13	0.77	+1.32	101.32	7.57	-10.84	89.16	
+14.65	107.01	49	+9.51	106.52	0.76	-1.30	100.00	9.05	+9.55	106.60	
-15.15	90.80	39	-20.41	84.78	0.74	-2.63	97.37	7.20	-20.44	84.81	
+15.83	105.17	47	+20.51	102.17	0.75	+1.35	98.68	8.68	+20.56	102.24	
		43			0.71			7.94			
-7.24	92.76	37	-13.55	86.05	0.70	-1.41	98.59	6.83	-13.98	86.02	
+15.51	107.15	46	+24.32	106.98	0.71	+1.43	100.00	8.49	+24.30	106.93	
-19.93	85.79	35	-23.91	81.40	0.72	+1.41	101.41	6.46	-23.91	81.36	
+22.15	104.80	40	+14.29	93.02	0.64	-11.11	90.14	7.39	+14.40	93.07	
		58			0.72			10.71			
-19.70	80.30	42	-27.59	72.41	0.71	-1.39	98.61	7.75	-27.64	72.36	
+17.44	94.30	56.5	+34.52	97.41	0.74	+4.23	102.78	10.43	+34.58	97.39	
-17.76	77.56	42	-25.66	72.41	0.74	0	102.78	7.75	-25.70	72.36	
+12.12	96.96	49	+16.67	84.48	0.73	-1.35	101.39	9.05	+16.77	84.50	
		61			0.73			11.27			
-19.86	80.14	44.5	-27.05	72.95	0.73	0	100.00	8.22	-22.06	72.94	
+10.62	88.65	50.0	+12.36	81.97	0.72	-1.37	98.63	9.24	+12.41	81.99	
		58			0.69			10.71			
-3.92	96.08	56	-3.45	96.55	0.69	0	100.00	10.34	-3.45	96.55	
-13.43	83.18	48	+3.57	100.00	0.84	+21.74	121.74	10.71	+3.58	100.00	
		55			0.68			10.16			
-3.40	96.60	53	-3.64	96.36	0.68	0	100.00	9.79	-3.64	96.36	
-1.90	94.76	55.5	+4.72	100.91	0.72	+5.88	105.88	10.25	+4.70	100.89	
		57			0.69			10.52			
-21.97	78.03	41	-28.07	71.93	0.70	+1.45	101.45	7.57	-26.15	71.96	
+20.18	93.77	48	+17.07	84.21	0.64	-8.57	92.75	8.86	+17.04	84.22	
		67			0.70			12.37			
-7.87	92.13	60	-10.45	89.55	0.70	0	100.00	11.08	-10.43	89.57	
+2.05	94.02	61	+1.67	91.04	0.70	0	100.00	11.26	+1.62	91.03	
		66			0.71			12.19			
-5.53	94.47	60	-9.09	90.91	0.70	-1.41	98.59	11.08	-9.11	90.89	
-10.00	85.02	51	-15.00	77.27	0.69	-1.43	97.18	9.42	-14.98	[illegible]	
		66			0.71			12.19			
-23.13	76.88	40.5	-38.64	61.36	0.69	-2.82	97.18	7.48	-20.59	61.36	
+21.22	93.19	50	+23.46	75.76	0.63	-8.70	88.73	9.23	+23.40	75.72	
		52			0.73			9.60			
+2.15	100.15	51.5	-0.96	99.04	0.73	0	100.00	9.51	-0.94	99.06	
		60			0.76			11.08			
-0.92	99.08	60	0	100.00	0.77	+1.32	101.32	11.08	0	100.00	

* NOTE I_{sc} LOSS IN CELLS # 18L, 19L AND 22L AFTER LASER ANNEAL

* NOTE REDUCED DEGRADATION IN CELLS # 18L, 19L & [illegible] 22L FROM 1.9 MeV RADIATION TO A FLUENCE OF 1×10^{15} P/cm²

* NOTE EFFECT OF IRRAD. AND THERMAL ON FILL FACTOR

* NOTE CELL FILL DEGREDATION IN ALL PARAMETERS

led in an oven.

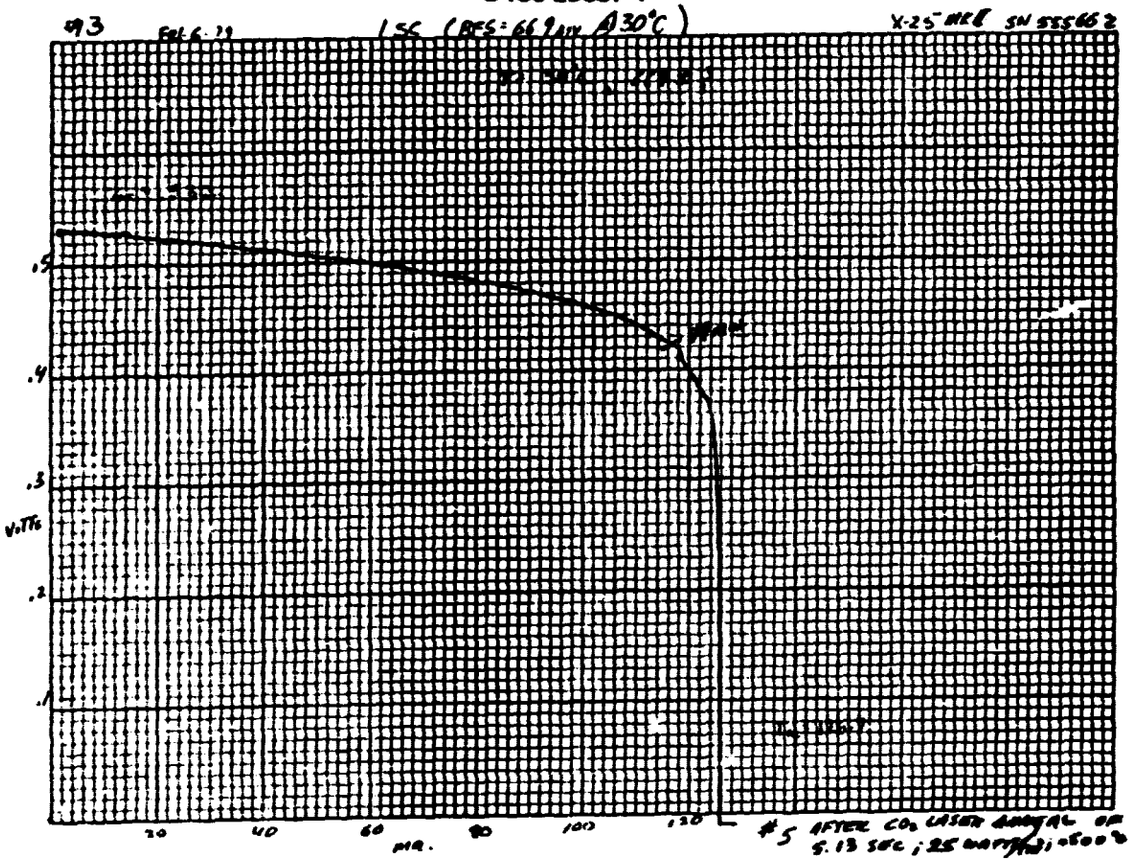

#5 AFTER CO_2 LASER ANNEAL OF 5.13 SEC; 25 WATTS; 600°C

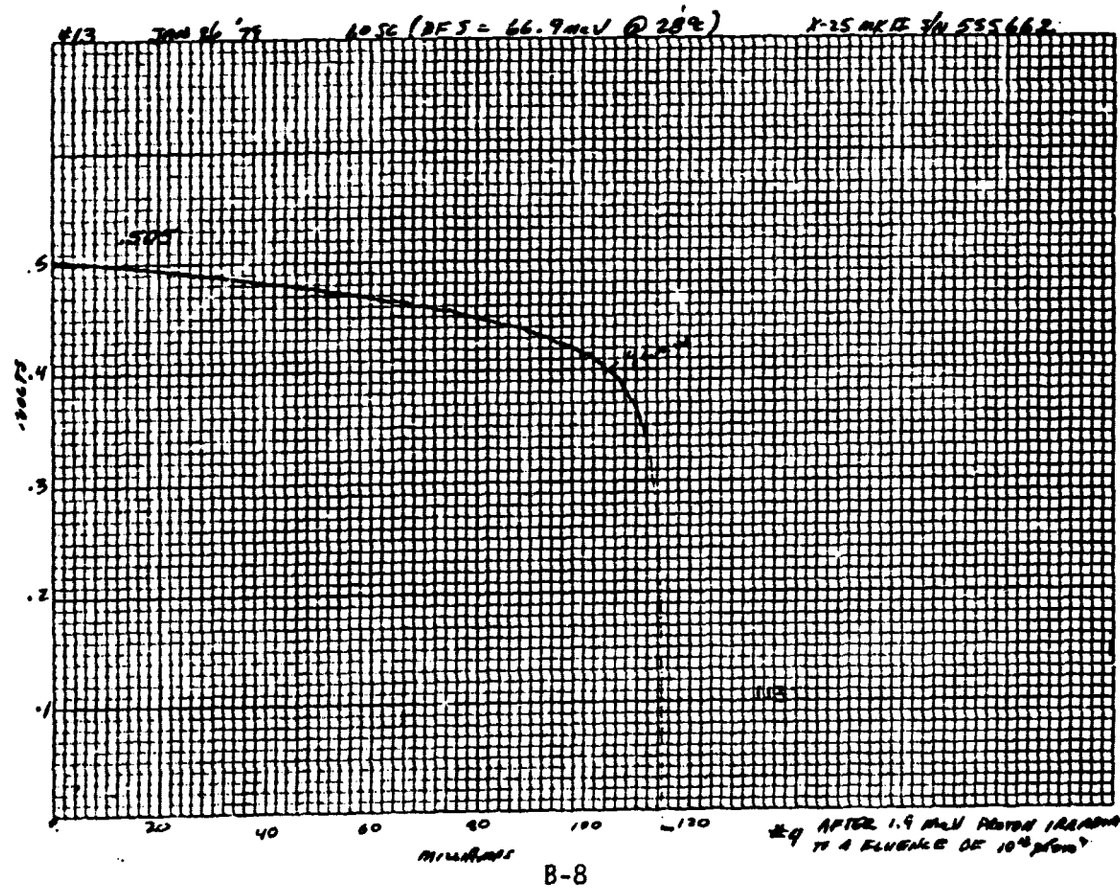

#9 AFTER 1.9 MeV PROTON IRRADIATION TO A FLUENCE OF 10^{13} p/cm²

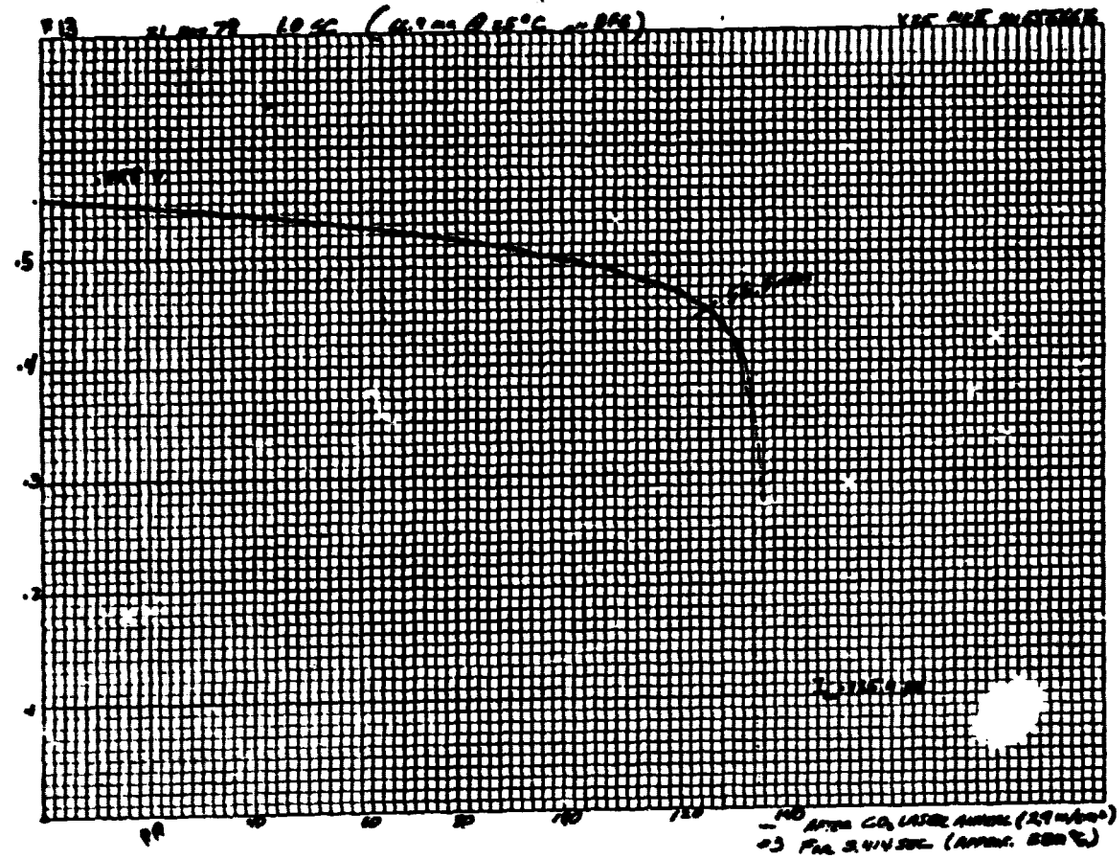

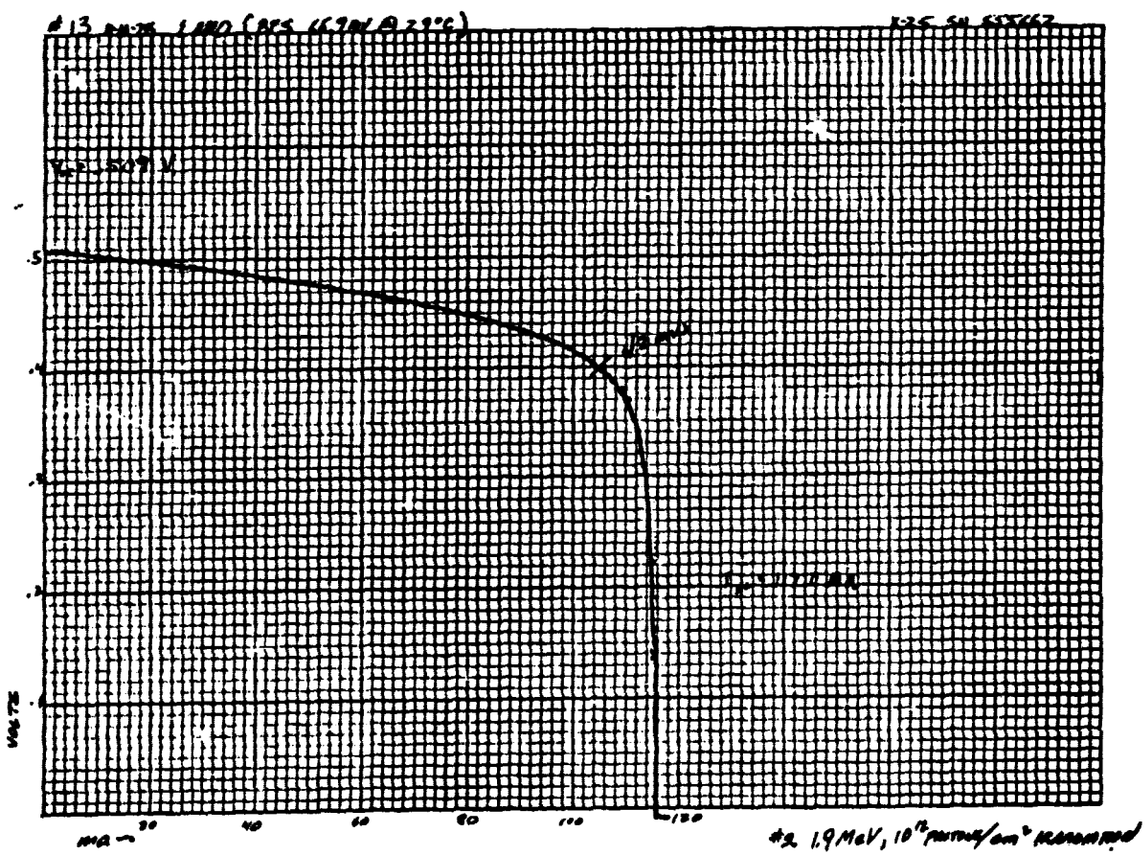

#2 1.9 MeV, 10^{17} protons/cm^2 irradiated

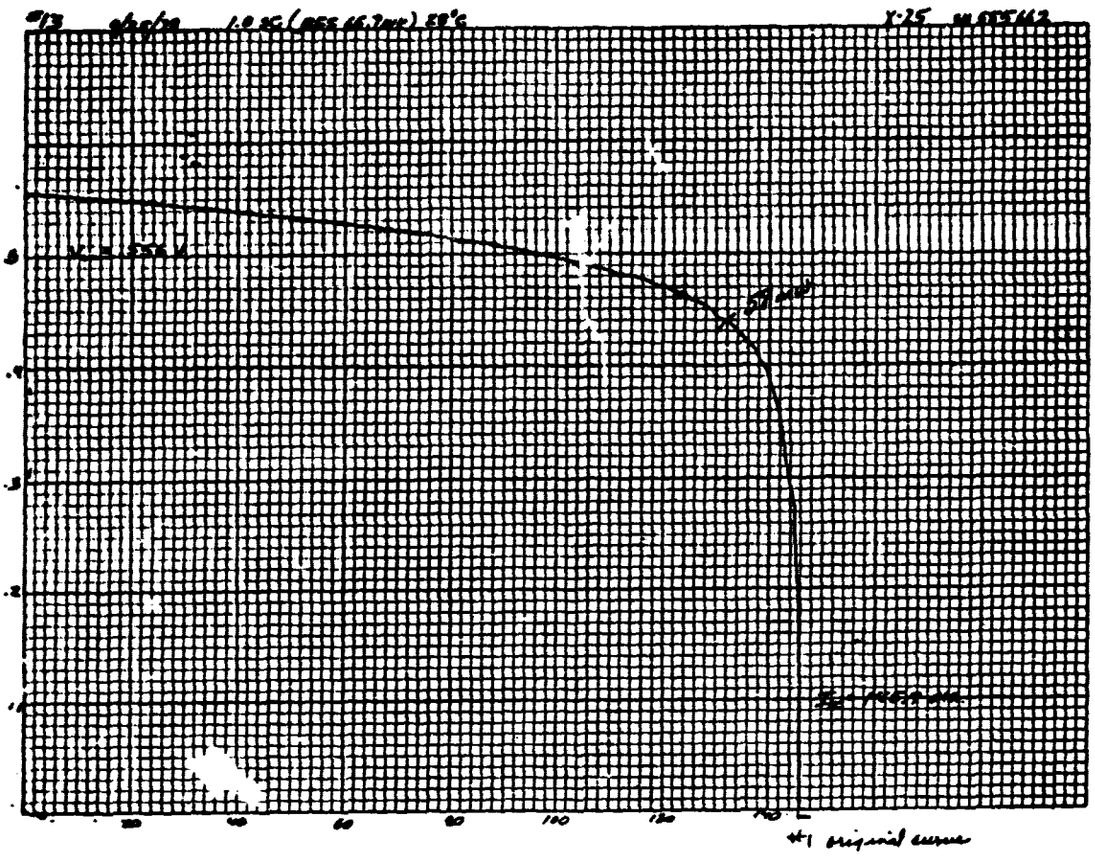
#13
X-25
.5
.4
.3
.2
.1
20
40
60
80
100
120
140
#1 original curve

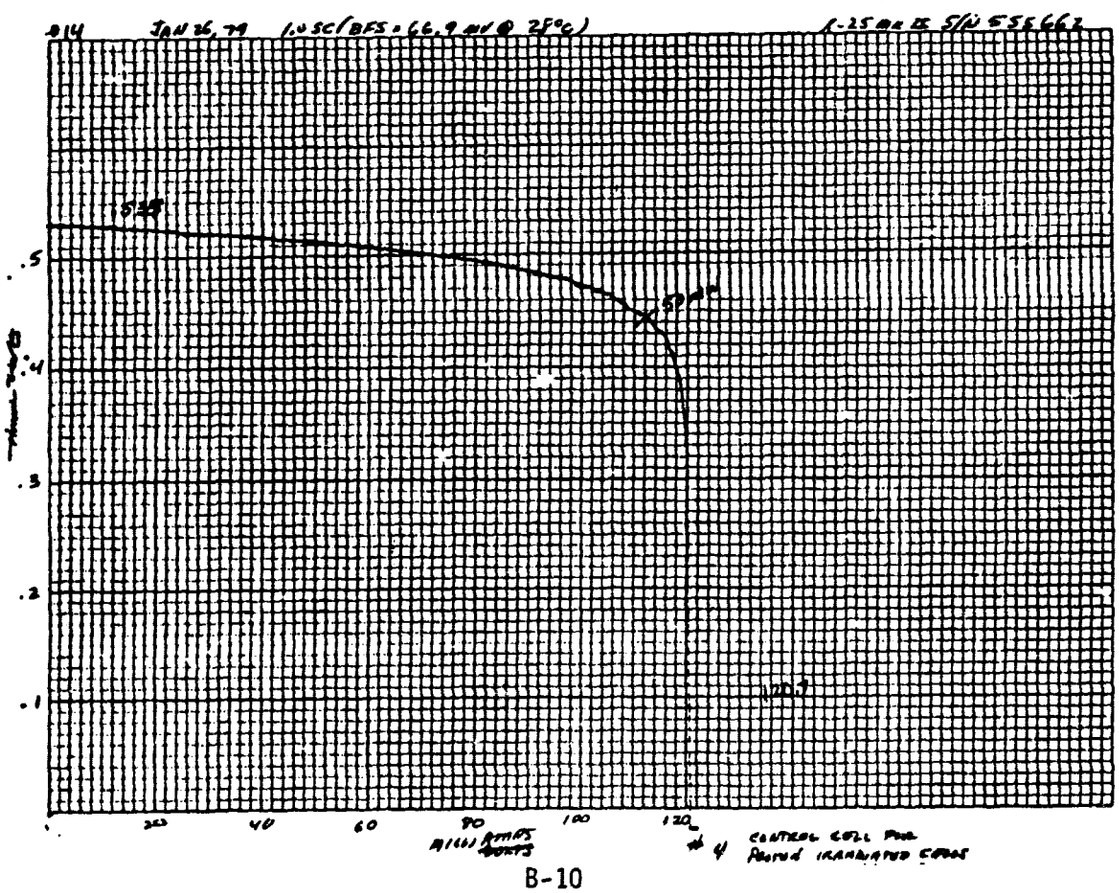
#14
JAN 26, 79
X-25
.5
.4
.3
.2
.1
20
40
60
80
100
120
MILLI AMPS
#4 CONTROL COIL FOR
PRIOR IRRADIATED CORES

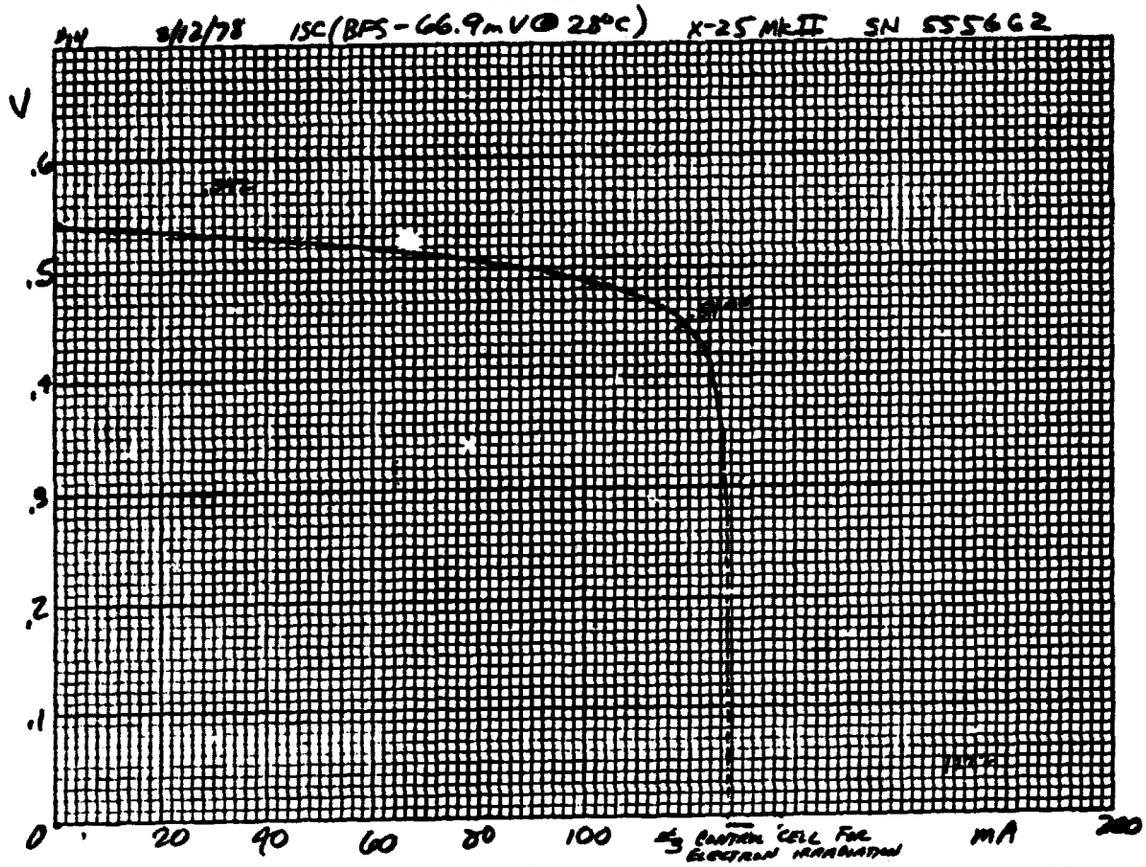

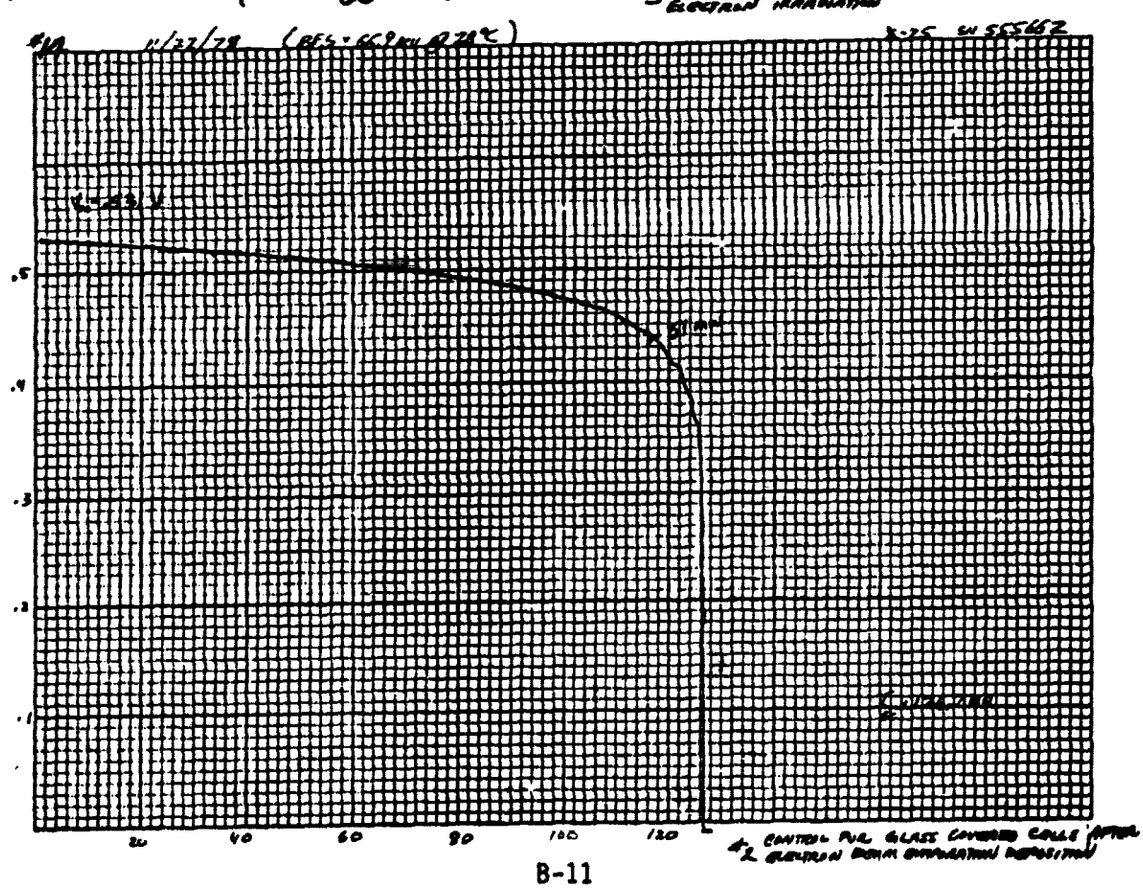

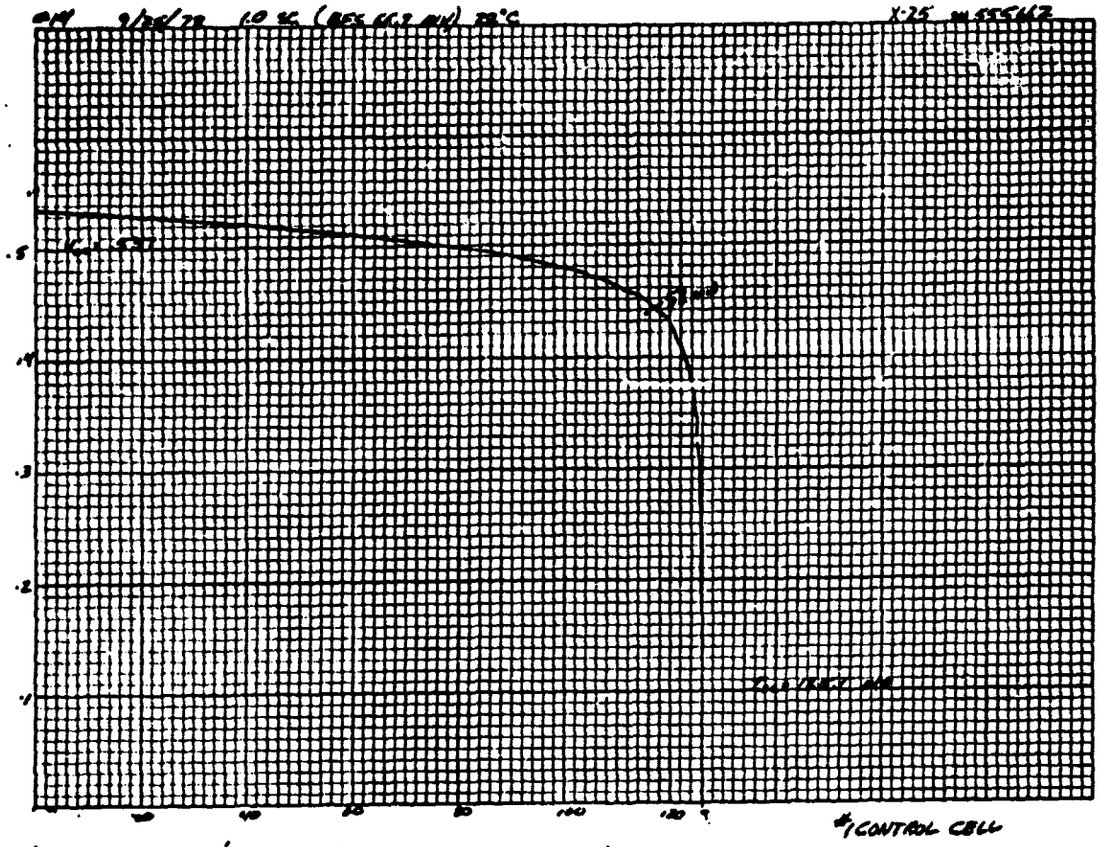
.5
.4
.3
.2
.1
40
60
100
#1 CONTROL CELL

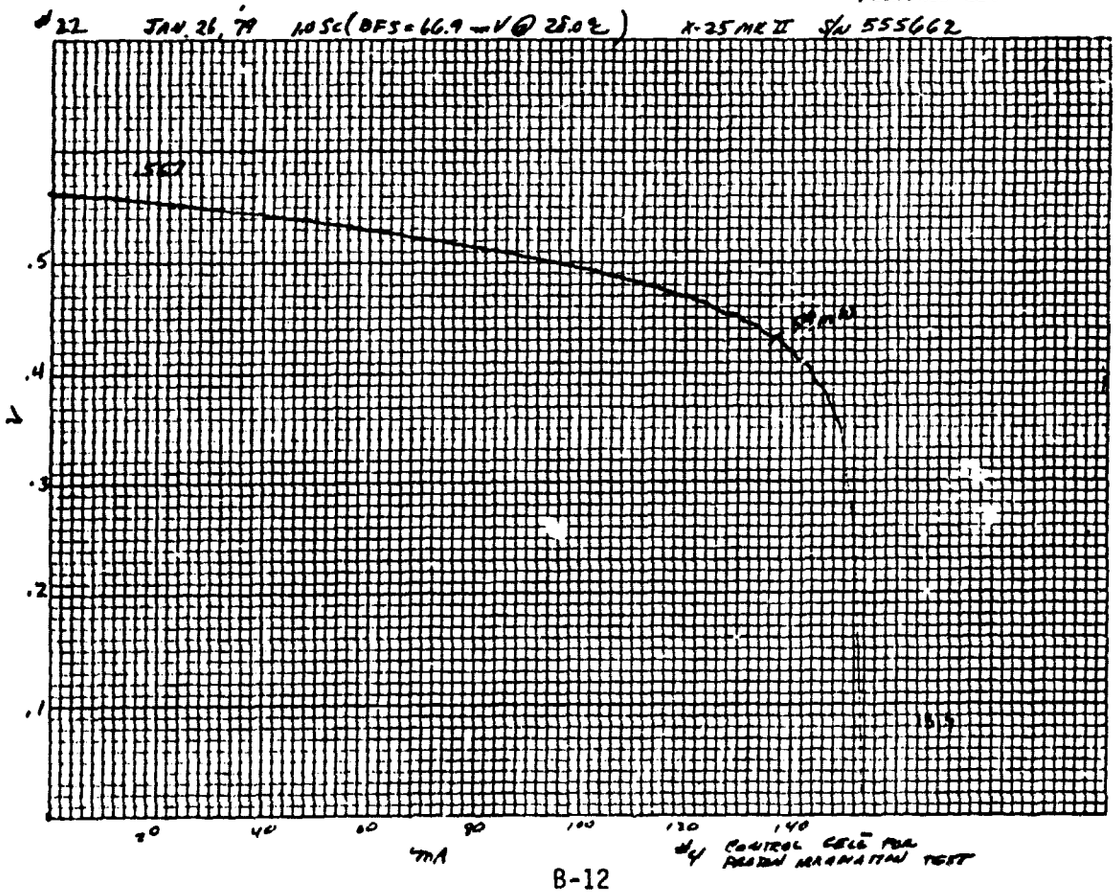
#22 JAN. 26, 79
X-25 MK II S/N 555662
.5
.4
.3
.2
.1
V
20
40
60
80
100
120
140
mA
#4 CONTROL CELL FOR RADIATION

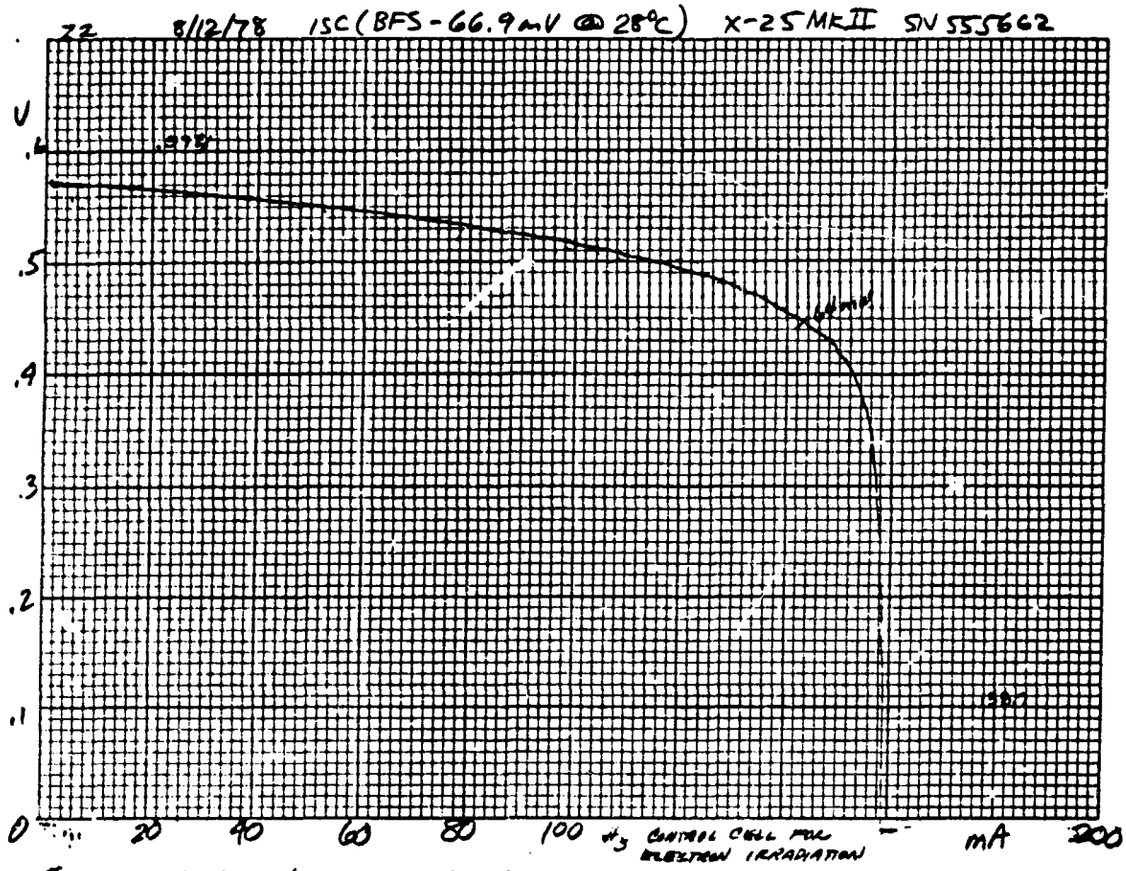
22 8/12/78 ISC (BFS - 66.9 mV @ 28°C) X-25 MKII SN 555662
V
.6
.5
.4
.3
.2
.1
0
20
40
60
80
100
mA
200
#3 CONTROL CELL FOR ELECTRON IRRADIATION

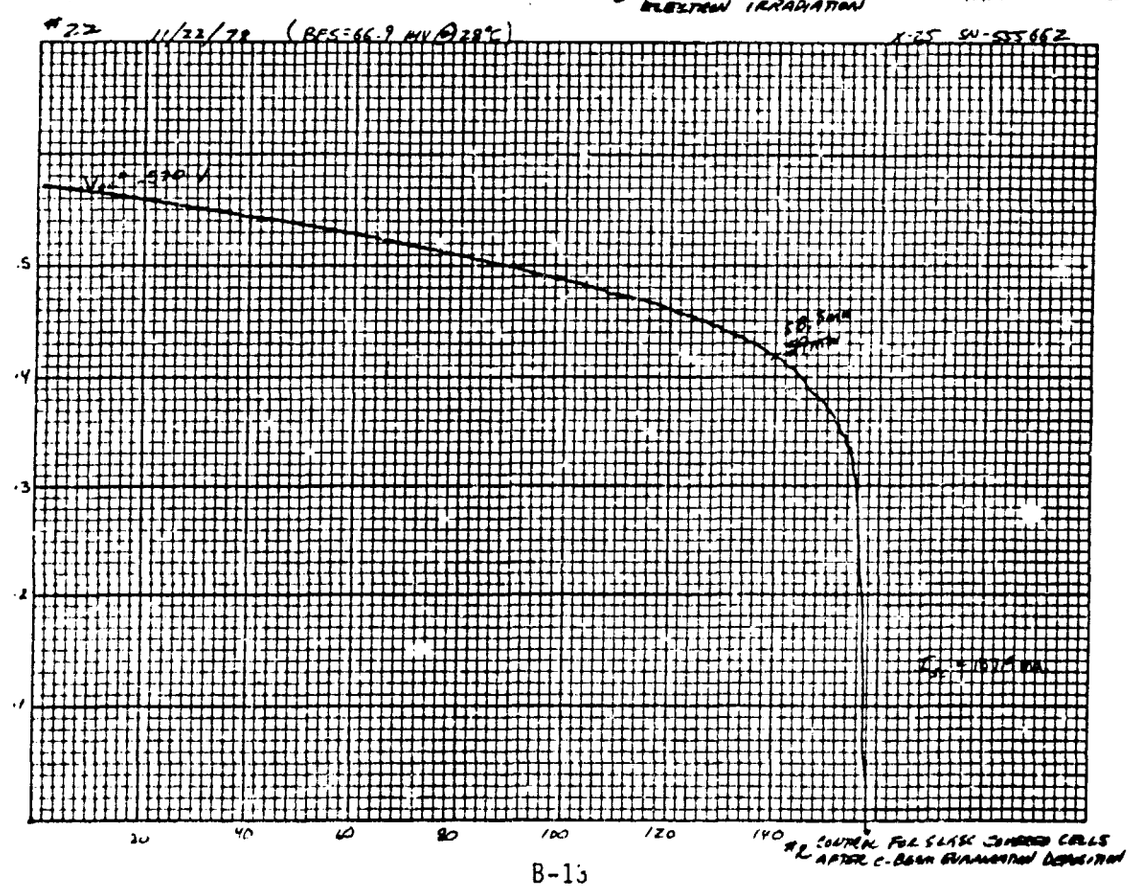
#22 11/22/78 (BFS=66.9 mV @ 28°C)
X-25 SN-555662
.5
.4
.3
.2
.1
20
40
60
80
100
120
140
#2 CONTROL FOR GLASS COVERED CELLS AFTER C-BEAM EVAPORATION DEPOSITION

U.C.L. 2cm x 2cm x 0.005cm silicon Solar Cell

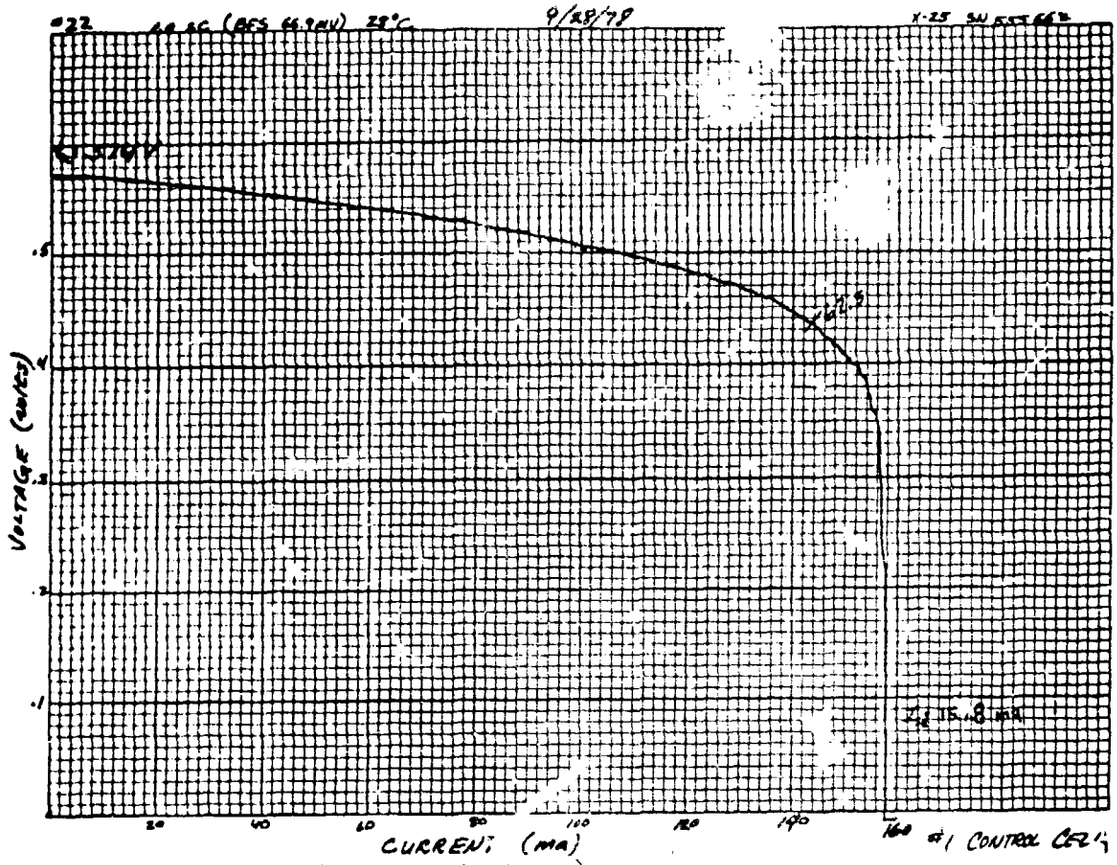

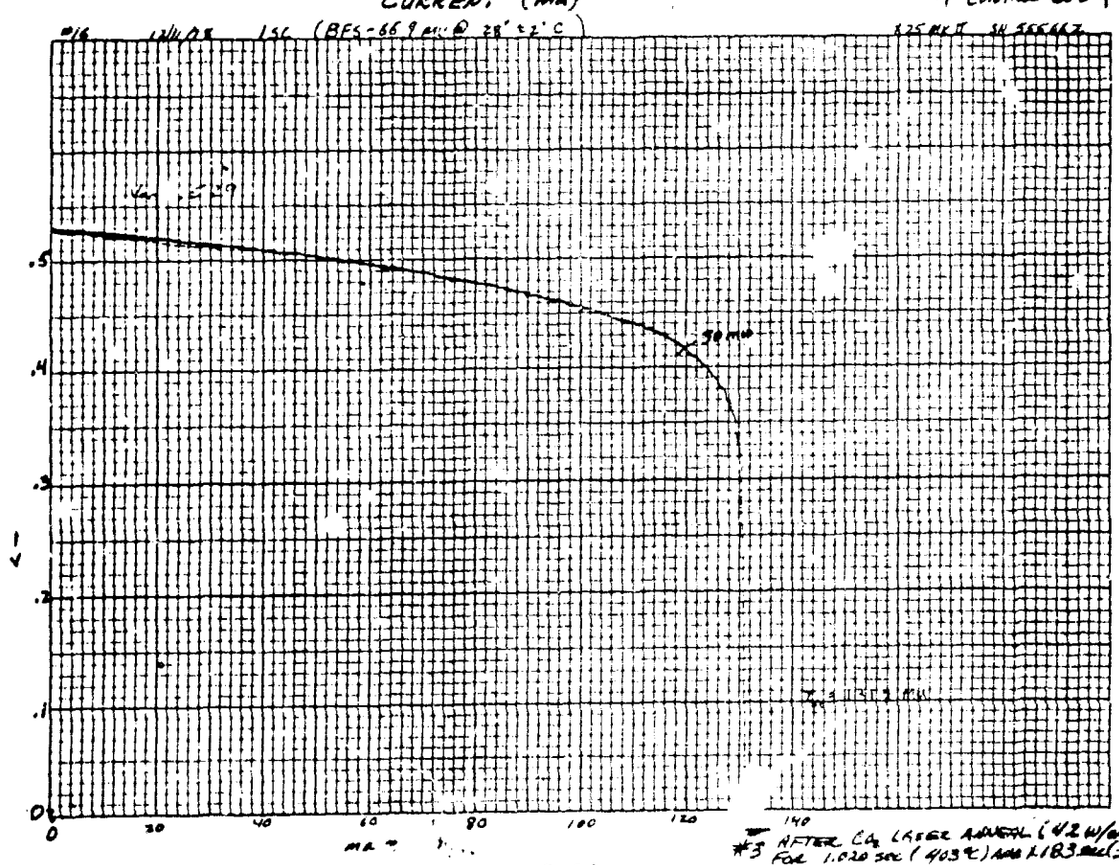

#3 AFTER CO_2 LASER ANNEAL (42 W/cm²) FOR 1,020 sec (403°C) AND 1,183 sec (550°C)

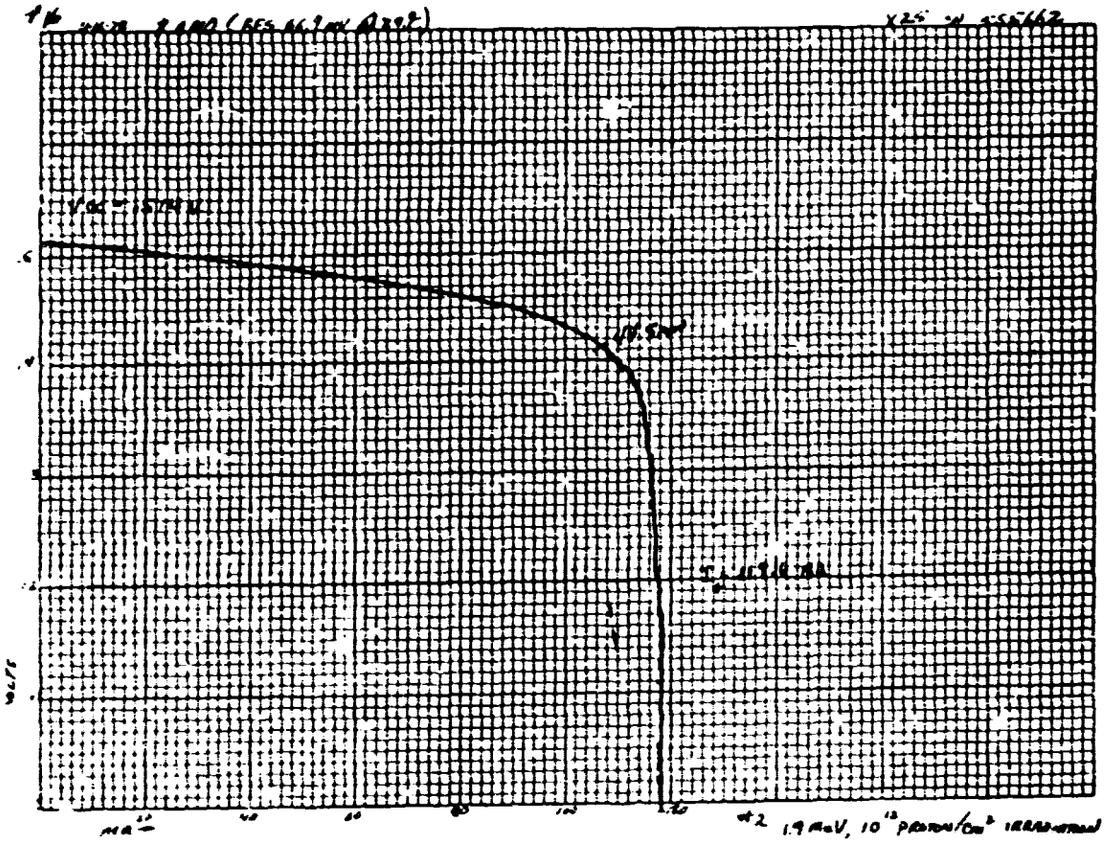

#2 1.9 MeV, 10^{12} proton/cm² irradiation

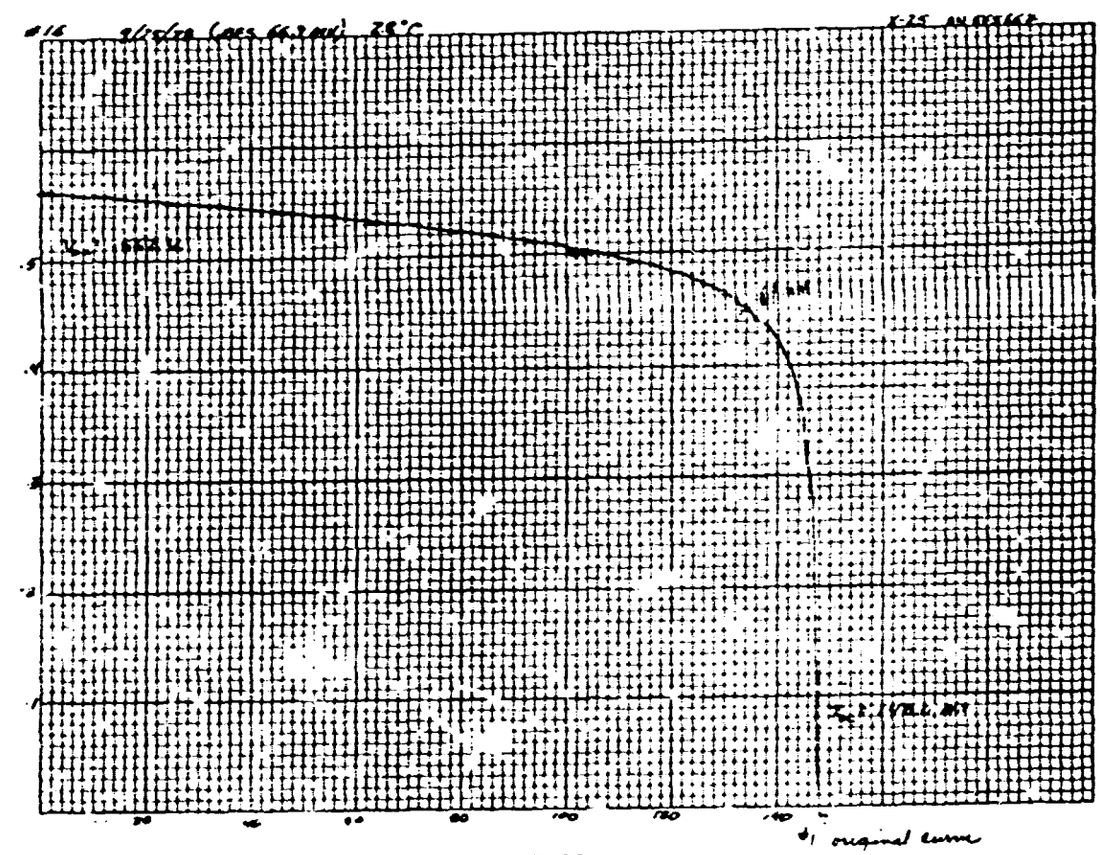

#1 original curve

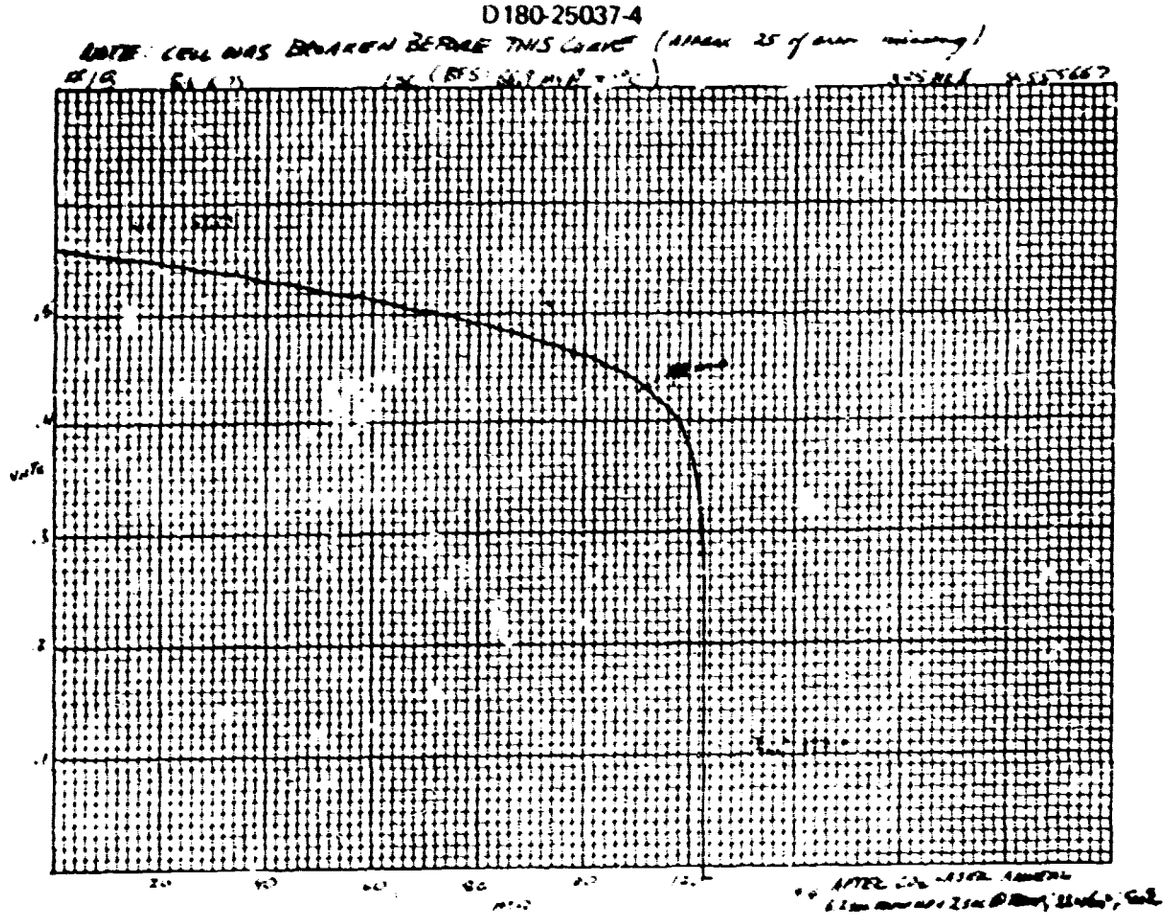

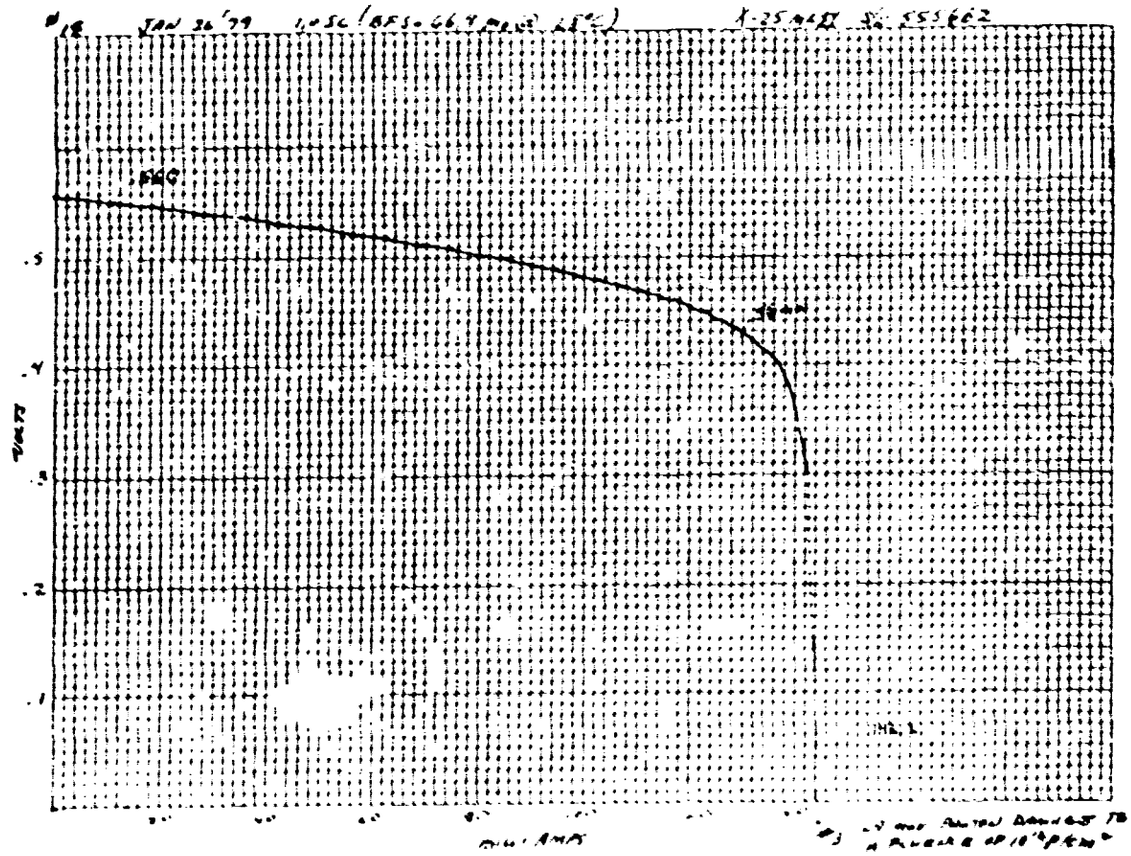

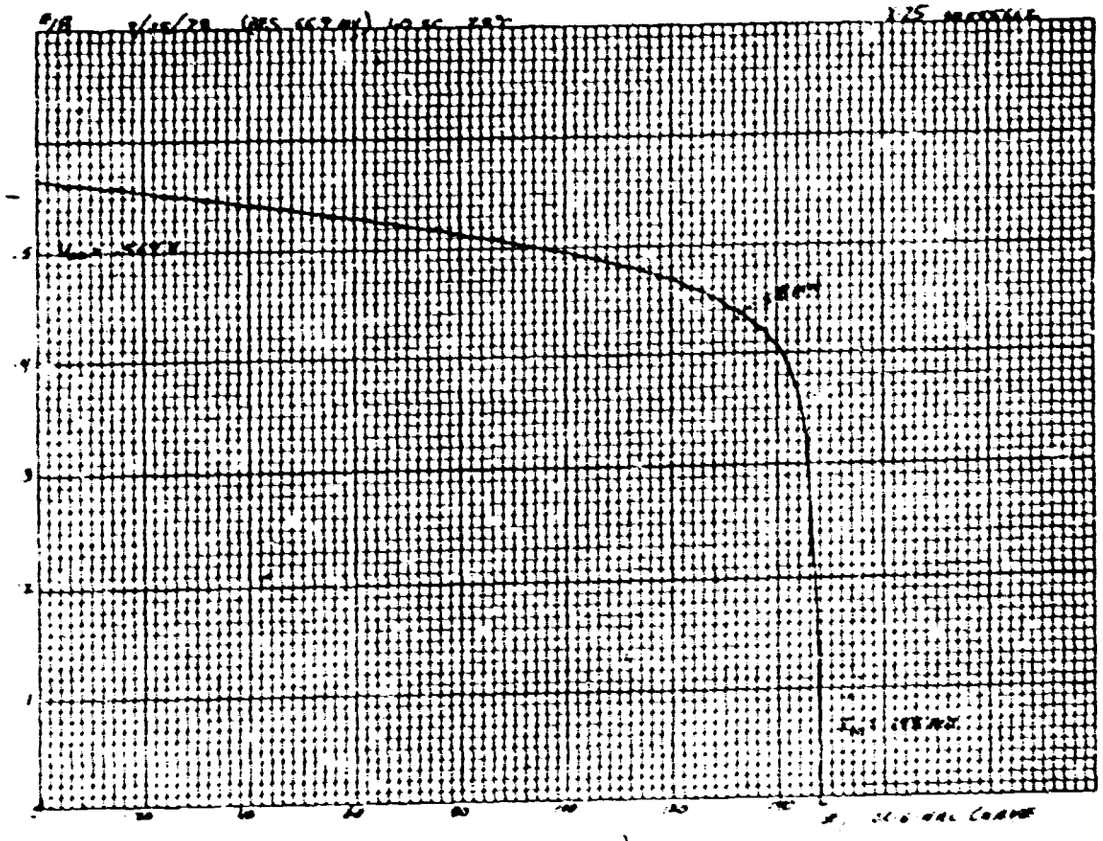

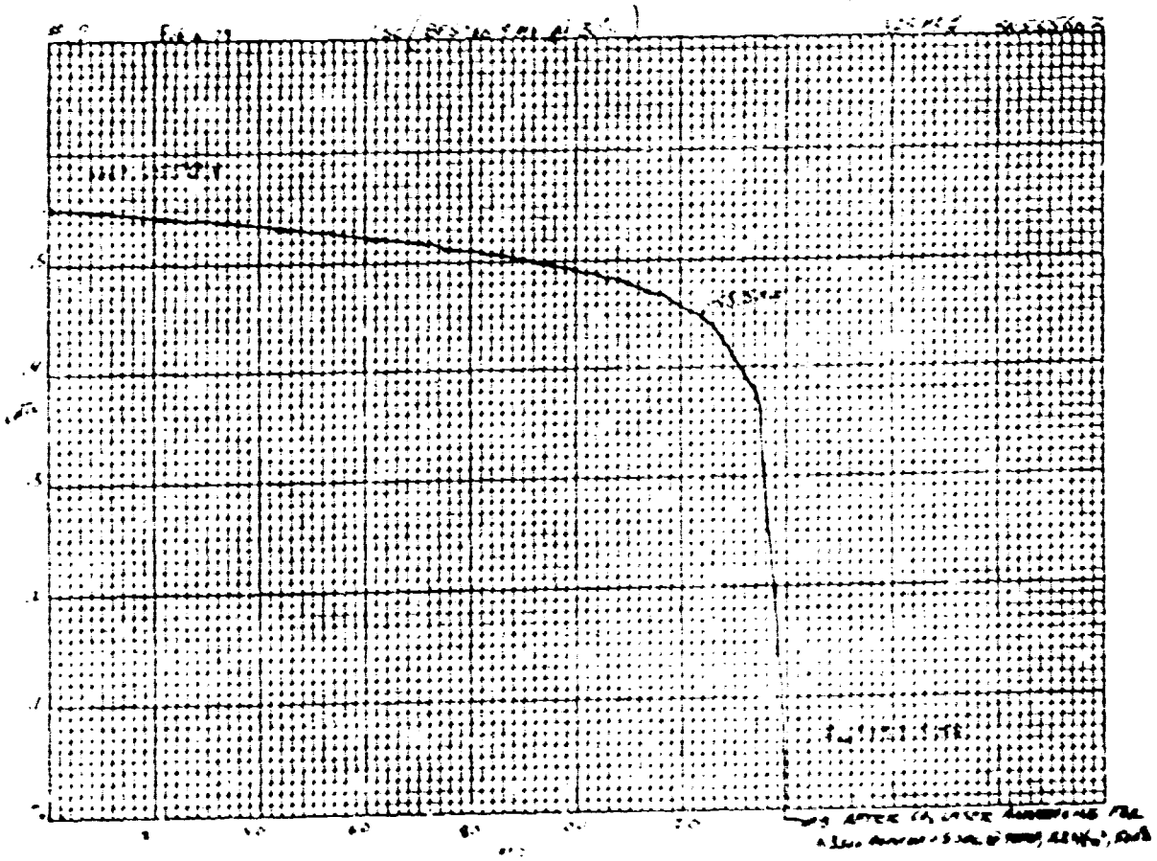

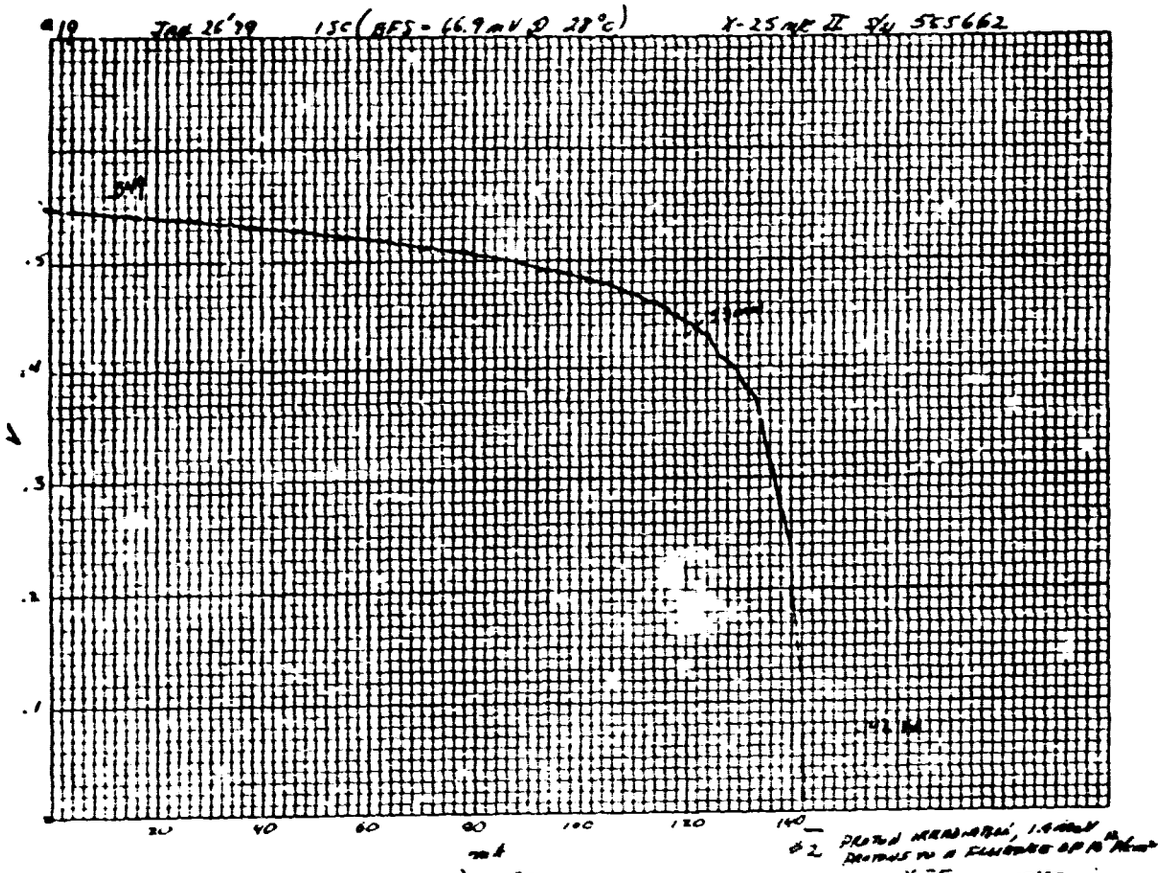
#19 JAN 26'79 15C (BFS - 66.9mV @ 28°C) X-25 mfg II S/N 585662
.5
.4
.3
.2
.1
20
40
60
80
100
120
140
mA

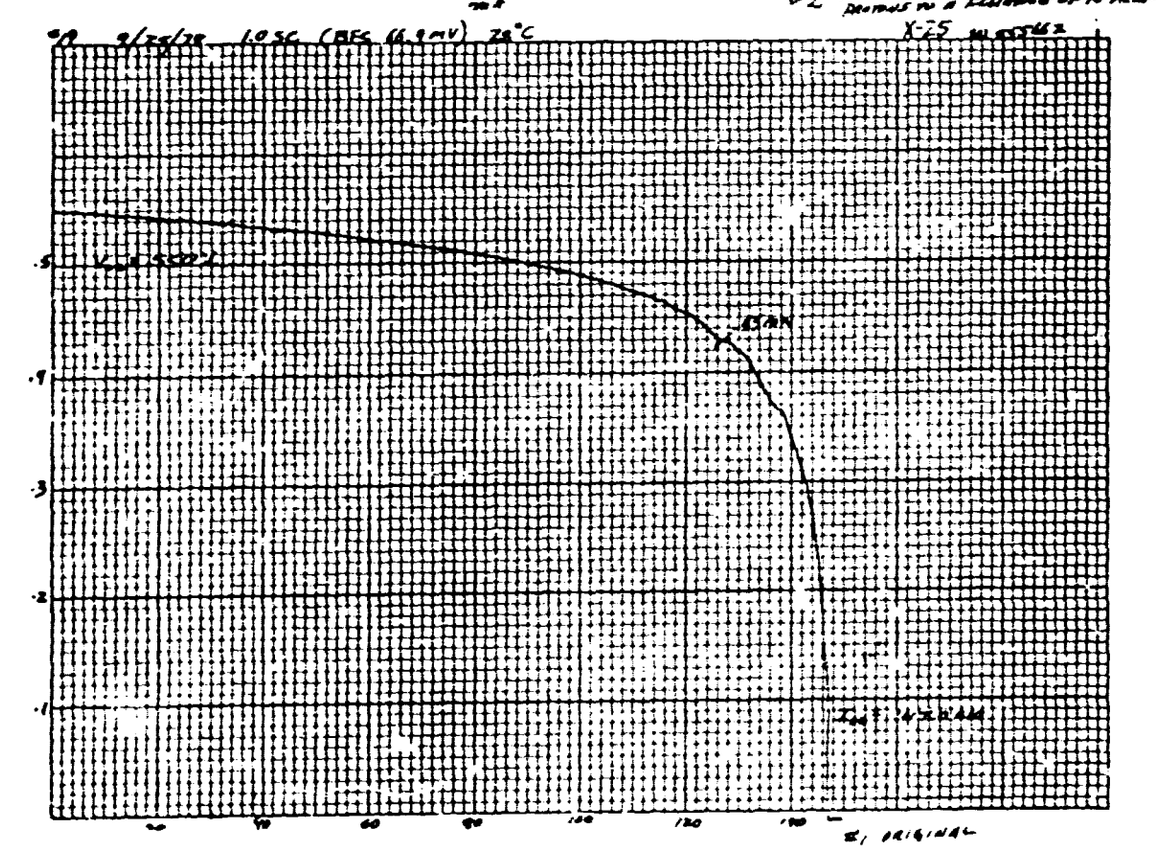
#18 9/25/78 1.0SC (BFS 66.9mV) 28°C X-25
.5
.4
.3
.2
.1
60
80
100
120
140
ORIGINAL

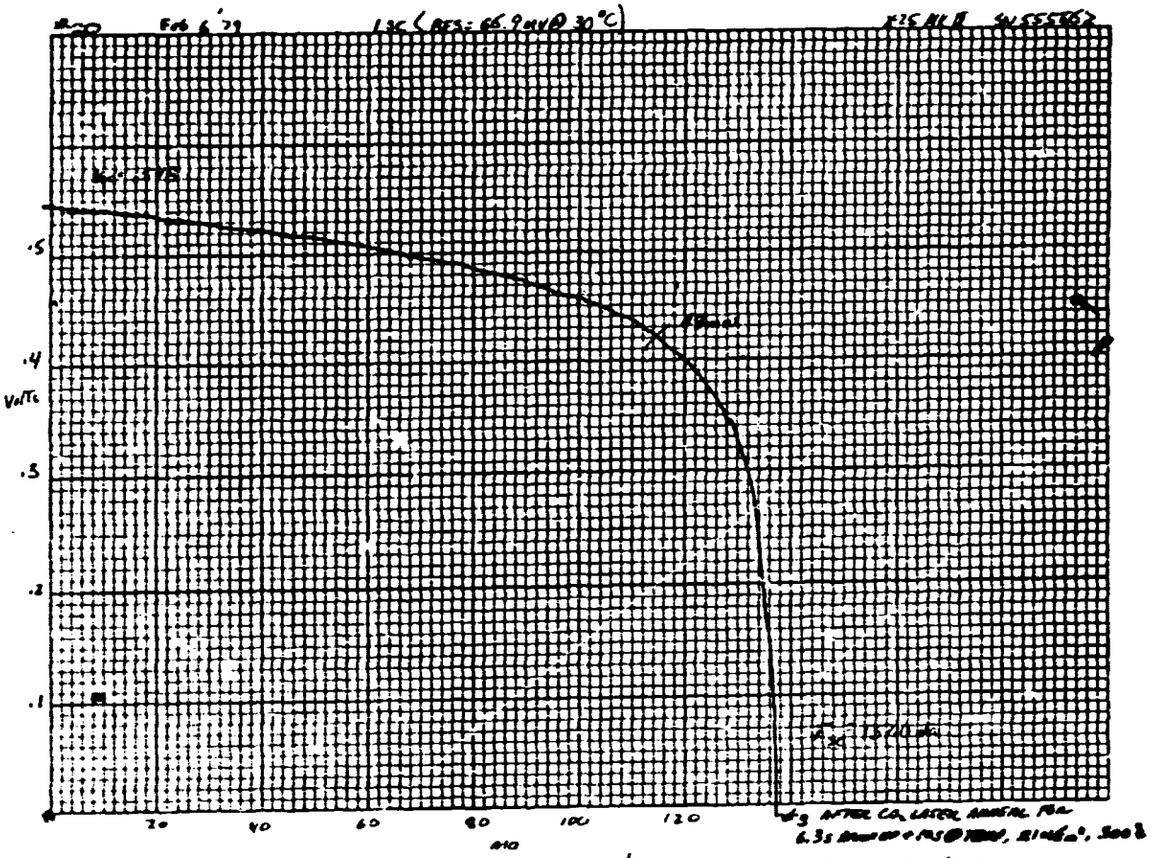
Feb 6 '79
1.5c (BFS: 66.9mV @ 30°C)
X-25 MK II
.5
.4
Voltage
.3
.2
.1
20
40
60
80
100
120
mA

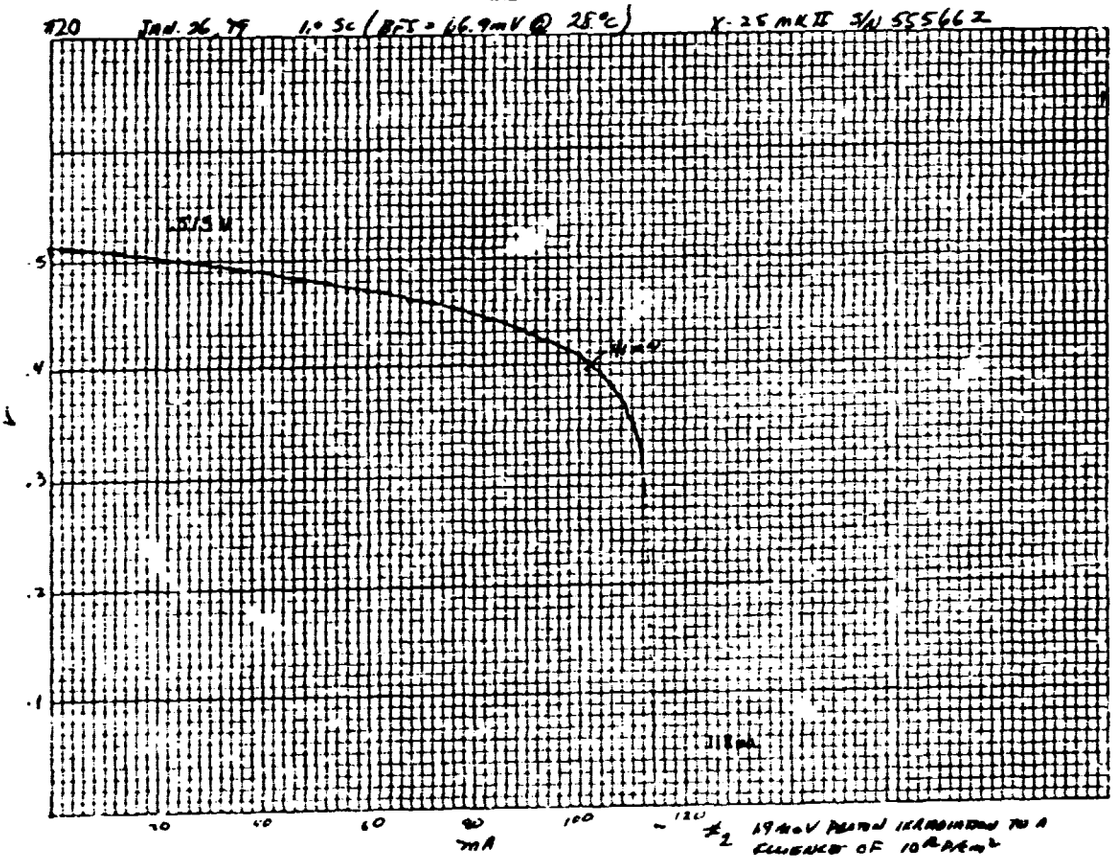
#20
Jan. 26, 79
1.0 Sc (BFS = 66.9mV @ 25°C)
X-25 MK II
.5
.4
.3
.2
.1
20
40
60
80
100
120
mA

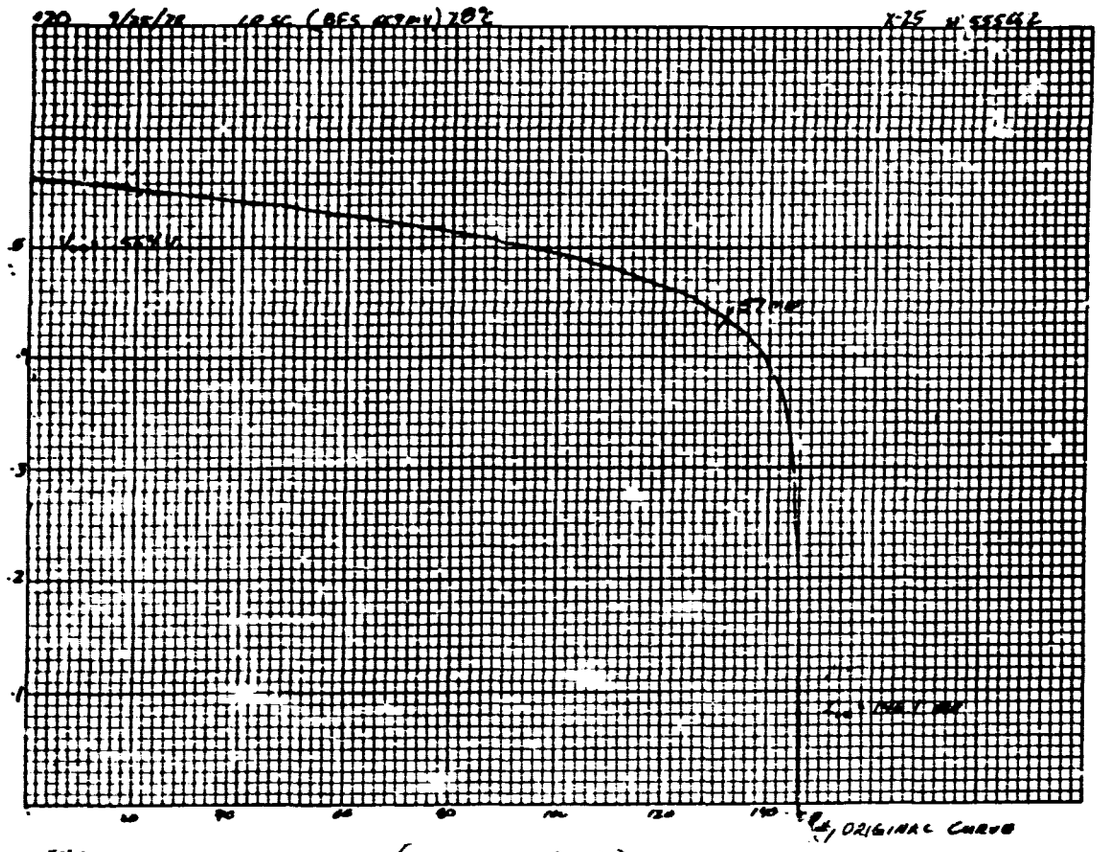
X-25
ORIGINAL CURVE

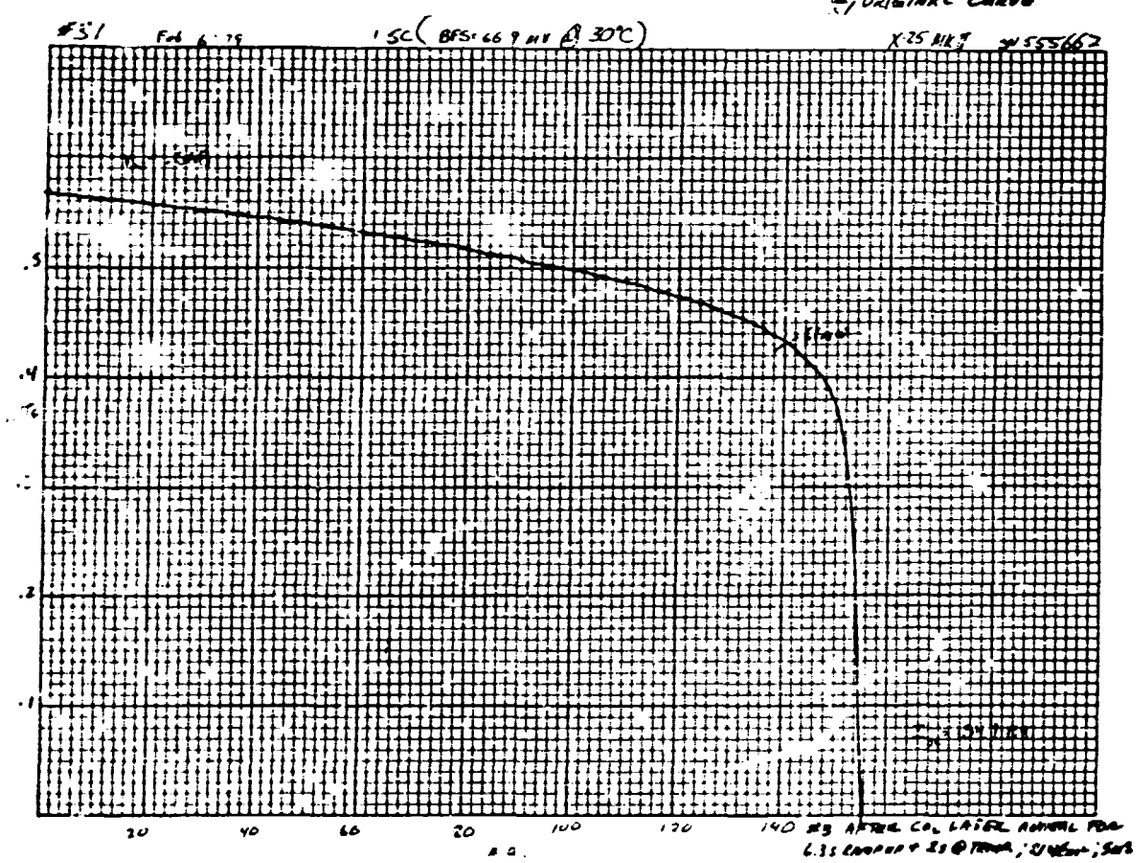
X-25
20
40
60
80
100
120
140

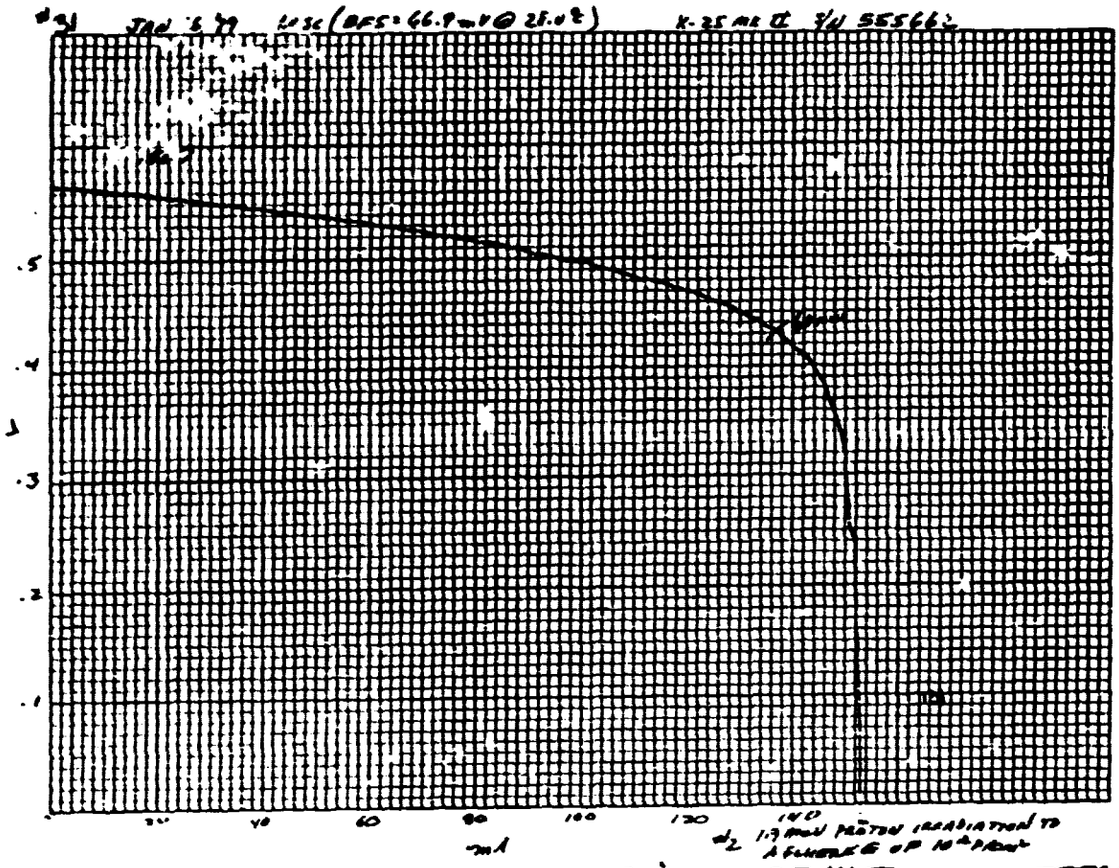

8/12/78 ISC (BFS-66.9 mV @ 28°C) X-25 Mk II SN 555662

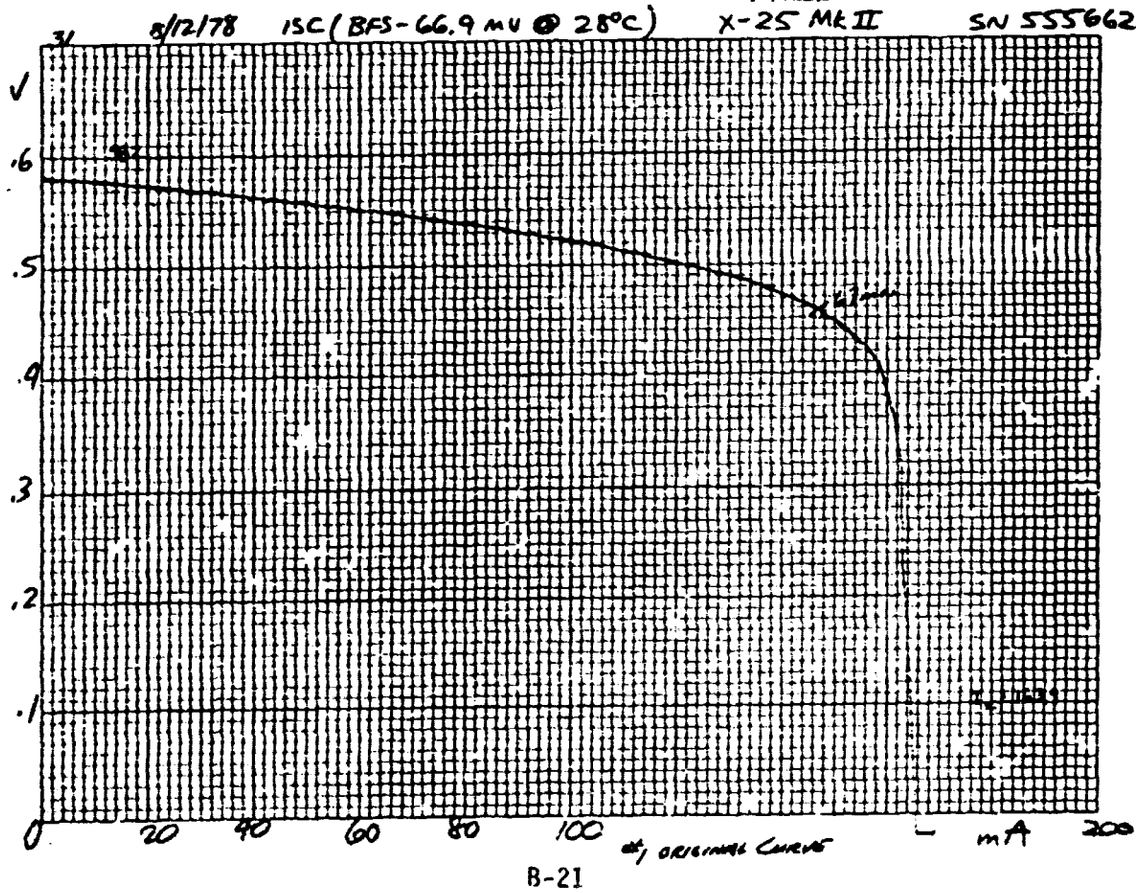

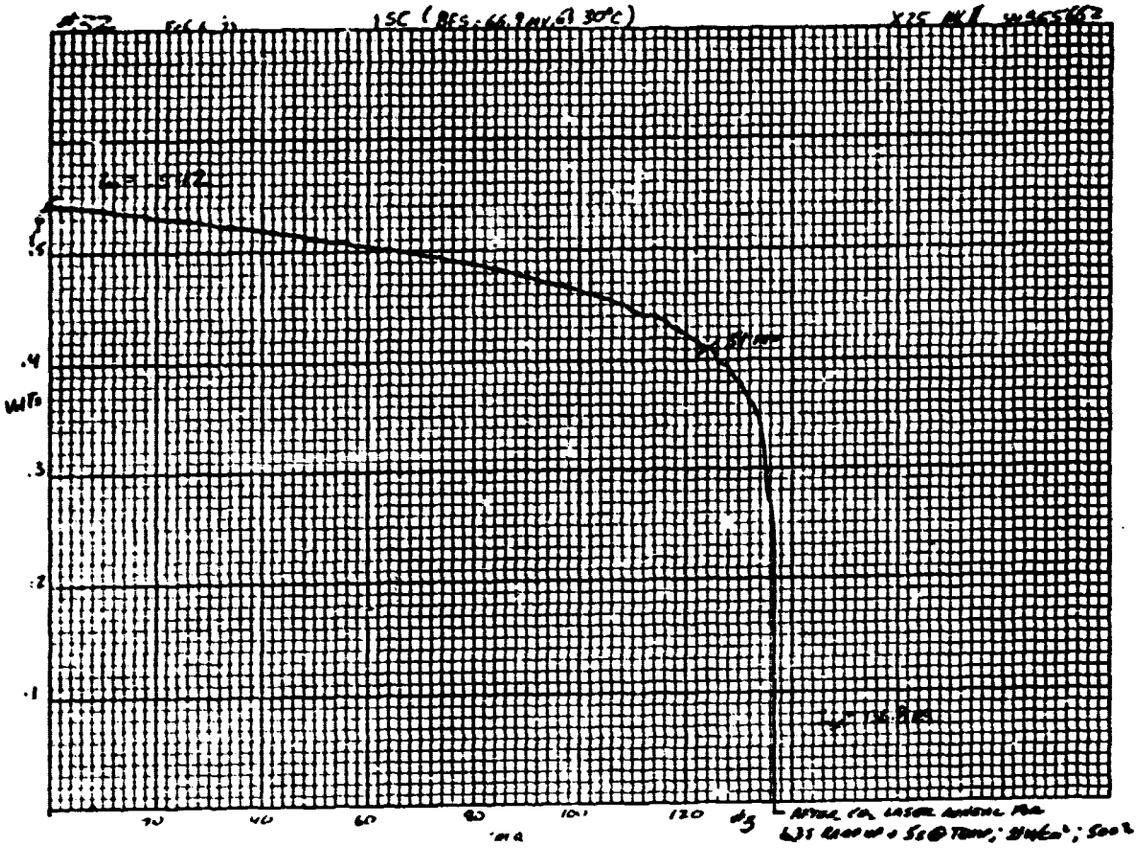
.4
.3
.2
.1
20
40
60
80
100
120
mA

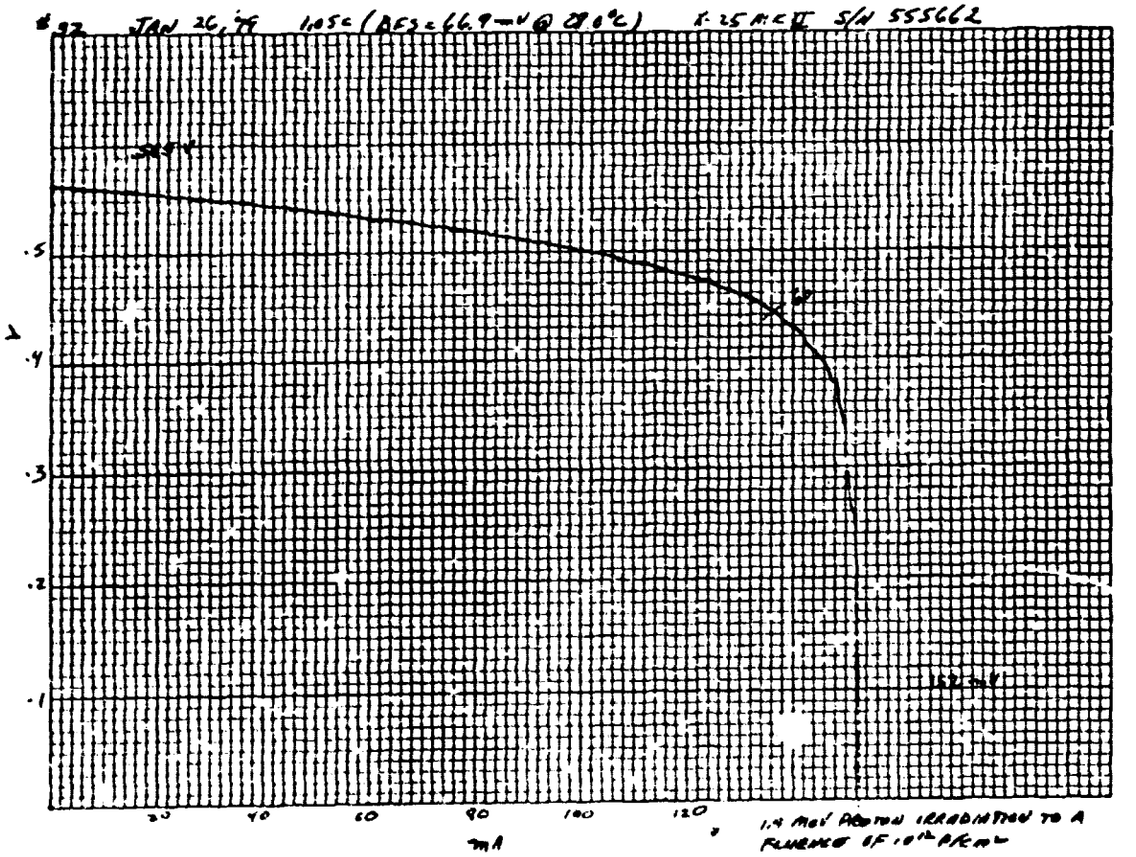
.5
.4
.3
.2
.1
20
40
60
80
100
120
mA

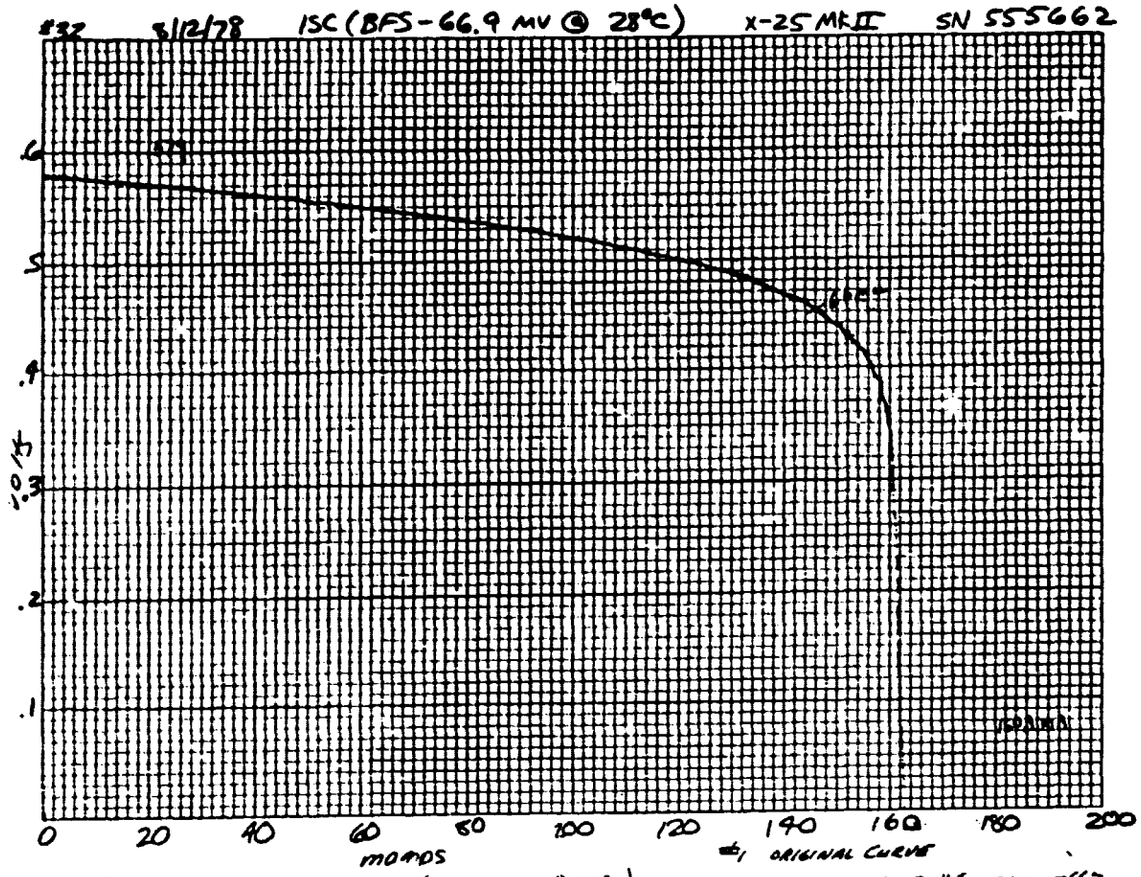
#32 8/12/78 ISC (BFS-66.9 MV @ 28°C) X-25 MK II SN 555662
.6
.5
.4
.3
.2
.1
0
20
40
60
80
100
120
140
160
180
200
MOMOS
#1 ORIGINAL CURVE

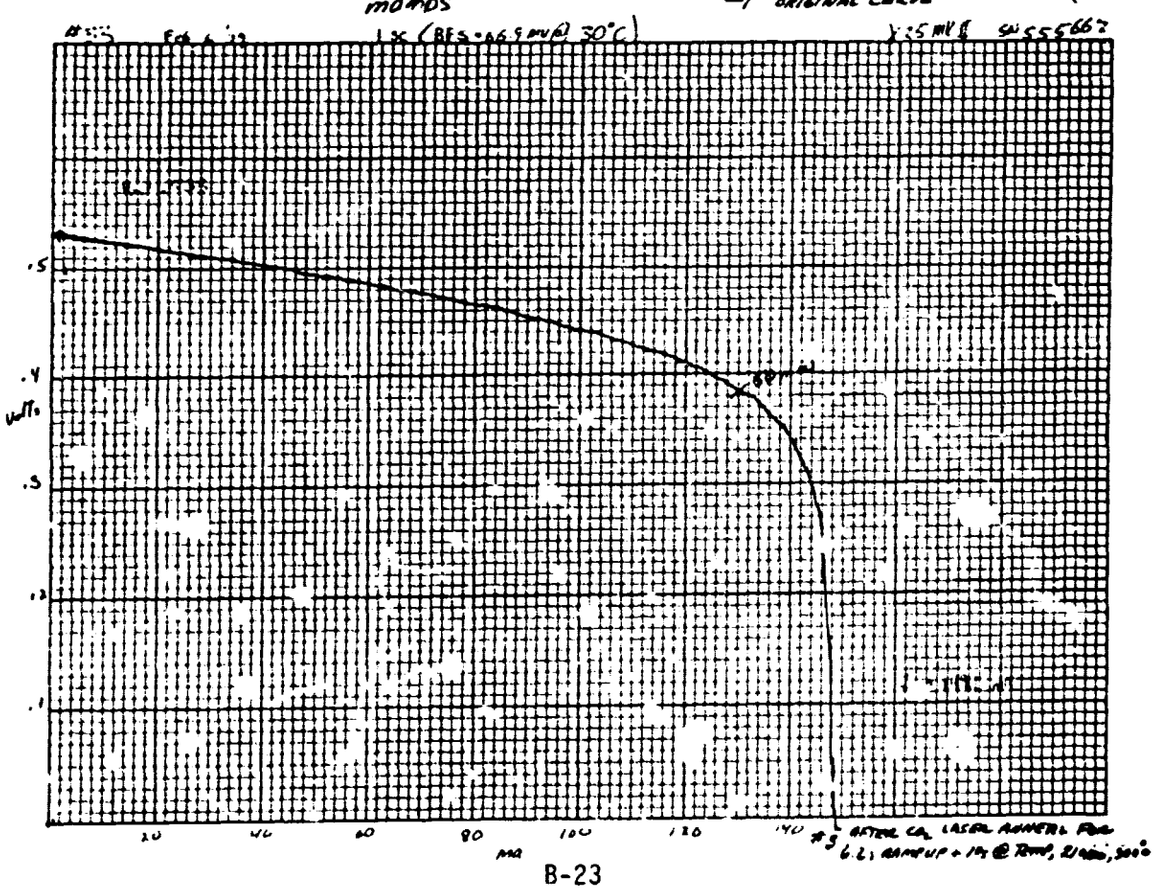
.5
.4
.3
.2
.1
20
40
60
80
100
120
140
MA
#5 AFTER CAL LASER ANNEAL FOR 6.2, RAMPUP + 1% @ TEMP, 21 min, 500°

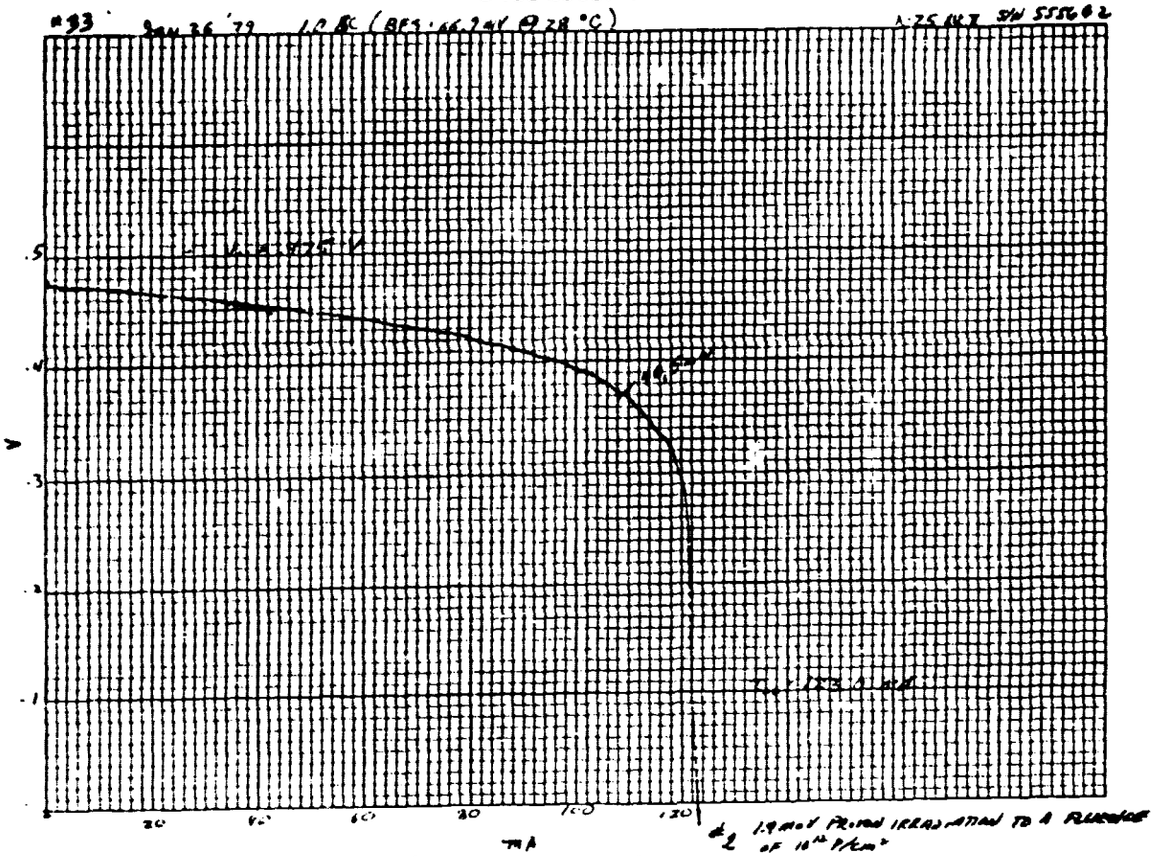
#33
JAN 26 '79
X-25 MK II
SN 555662
V
.5
.4
.3
.2
.1
20
40
60
80
100
120
mA
#2 1.9 MeV PROTON IRRADIATION TO A FLUENCE OF 10^11 P/cm^2

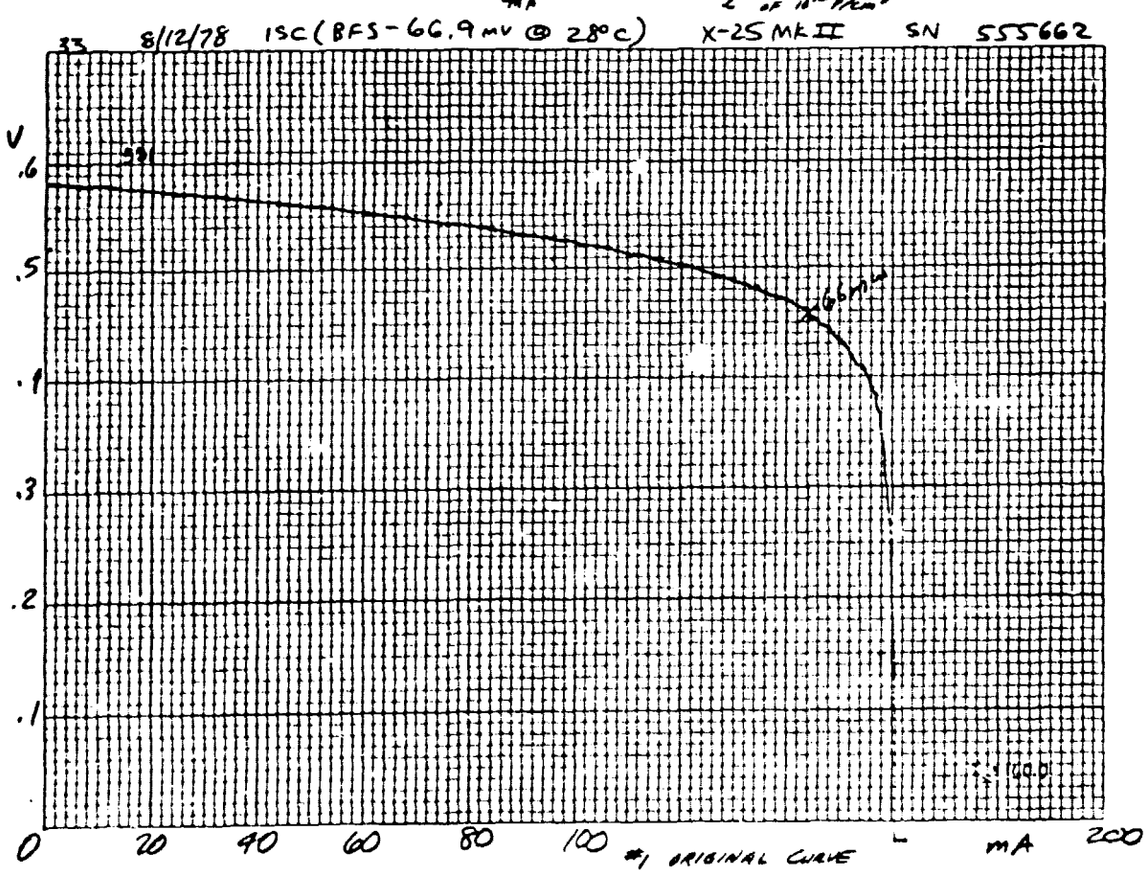
33
8/12/78
ISC (BFS-66.9 mV @ 28°C)
X-25 MK II
SN 555662
V
.6
.5
.4
.3
.2
.1
0
20
40
60
80
100
mA
200
#1 ORIGINAL CURVE